https://doi.org/10.15388/vu.thesis.268
https://orcid.org/0000-0001-8431-5437

VILNIUS UNIVERSITY

Raimonda
KUBILIŪTĖ

Diagnostic and prognostic DNA methylation biomarkers of renal clear cell carcinoma

DOCTORAL DISSERTATION

Natural Sciences,
Biology (N 010)

VILNIUS 2021

This dissertation was written between 2016 and 2020 at the Human Genome Research Laboratory, Institute of Biosciences, Life Sciences Center, Vilnius University. The research was supported by the Research Council of Lithuania and the scholarship from Vilnius University.

Academic supervisor:

Prof. dr. Sonata Jarmalaitė (Vilnius University, Natural Sciences, Biology, N 010).

https://doi.org/10.15388/vu.thesis.268
https://orcid.org/0000-0001-8431-5437

VILNIAUS UNIVERSITETAS

Raimonda
KUBILIŪTĖ

Šviesių ląstelių inkstų karcinomos diagnostiniai ir prognostiniai DNR metilinimo žymenys

DAKTARO DISERTACIJA

Gamtos mokslai,
Biologija (N 010)

VILNIUS 2021

Disertacija rengta 2016–2020 metais Žmogaus genomo tyrimų laboratorijoje, Biomokslų institute, Gyvybės mokslų centre, Vilniaus Universitete. Mokslinius tyrimus rėmė Lietuvos mokslo taryba ir Vilniaus universitetas.

Mokslinė vadovė:

Prof. dr. Sonata Jarmalaitė (Vilniaus universitetas, gamtos mokslai, biologija, N 010).

ACKNOWLEDGEMENTS

Firstly I would like to express my sincere gratitude to my scientific supervisor Prof. Sonata Jarmalaitė, for that conversation five years ago, that changed my life plans, for which I am eternally grateful, and which I do not regret in the slightest! Thank You for the opportunity to complete my doctoral studies in Your managed laboratory, thank You for the trust and belief in what I am doing, for the provided freedom and independence performing scientific research, valuable counsel, and support in the moments when it was most needed! I would like to sincerely thank Prof. Rimantas Daugelavičius separately, who helped me to discover this laboratory in the first place.

I am grateful to Kristina Stuopelytė (Šnipaitienė) for holding my hand and being alongside me at the very beginning of my doctoral studies, thank you for the honest and supporting conversations and the happy memories we created. I am grateful to Kristina Žukauskaitė not only for the enormous physical help she provided while conducting research but also for the additional motivation when I was lacking it the most, for the restored faith and patience, for the valuable and fun scientific discussions. Sincere gratitude goes to dr. Rasa Sabaliauskaitė and Algirdas Žalimas for warm conversations, support and benevolent help. I am grateful to dr. Kristina Daniūnaitė, and former students: Aušra Šumskaitė, Mark Bavriš, Rūta Matulevičiūtė and Eugenijus Ganža all of whom contributed to the carried out research in one way or another.

I would like to thank from the bottom of my heart my biology teacher Vidutė Tamošaitienė for the instilled love for biology that I have right now and it hurts me dearly that she had to finish her journey early battling an insidious disease.

I would like to thank separately all doctors from National Cancer Institute and Vilnius university hospital Santaros Klinikos that contributed to the collection of samples and clinical data, especially prof. dr. Feliksas Jankevičius, dr. Albertas Ulys and Algirdas Žalimas. Sincere gratitude goes to the patients and their relatives for the consent to participate in the scientific research.

I am extremely grateful to Benas, who provided me unconditional support from the very beginning, always was alongside me, was sad and happy together, had faith in me and encouraged me to move further.

I feel enormous gratitude for my parents for their unconditional love, faith in me and patience.

CONTENTS

LIST OF PUBLICATIONS AND PERSONAL CONTRIBUTION

Articles directly related to the topic of a doctoral dissertation, published in journals with a citation index (IF) in the Clarivate Analytics Web of Science platform:

1. **Kubiliute R**, Zukauskaite K, Zalimas A, Ulys A, Sabaliauskaite R, Bakavicius A, Zelvys A, Jankevicius F, Jarmalaite S. Clinical significance of novel DNA methylation biomarkers for renal clear cell carcinoma. *Journal of Cancer Research and Clinical Oncology* 2021 Oct 23. *Online ahead of print*. https://doi.org/10.1007/s00432-021-03837-7

   I have performed genome-wide DNA methylation profiling, selected gene validation in the renal tissue samples and independent cohort of the urine samples, analyzed the data, wrote the initial version of the manuscript, and corrected its drafts.

2. **Kubiliute R,** Zalimas A, Bakavicius A, Ulys A, Jankevicius F, Jarmalaite S. Clinical significance of *ADAMTS19*, *BMP7*, *SIM1* and *SFRP1* promoter methylation in renal clear cell carcinoma. *OncoTargets and Therapy* 2021 Oct 5;14:4979-4990. https://doi.org/10.2147/OTT.S330341

   I have performed global mRNA expression profiling, DNA methylation validation in the renal tissue samples, analyzed the data, wrote the initial version of the manuscript, and corrected its drafts.

3. **Kubiliute R,** Jarmalaite S. Epigenetic Biomarkers of Renal Cell Carcinoma for Liquid Biopsy Tests. *International Journal of Molecular Sciences* 2021 Aug 17;22(16):8846. https://doi10.3390/ijms22168846

   I have performed literature analysis on the epigenetic biomarkers for kidney cancer used in liquid biopsy tests, wrote the initial version of the manuscript, and corrected its drafts.

Patent Application

The patent application to the International Patent Office was prepared based on the results directly related to a doctoral dissertation topic.

Inventors: **Kubiliūtė R**, Jarmalaitė S;

Assigned Number: PCT/IB2021/052532;

Title: Clear cell renal cell carcinoma biomarkers and uses therefor.

I have performed genome-wide DNA methylation profiling, selected gene validation in the renal tissue samples and independent cohort of the urine samples, analyzed the data, wrote the patent application, and corrected its drafts.

Other publications, not directly related to the topic of a doctoral dissertation, in journals with a citation index in the Clarivate Analytics Web of Science platform:

1. **Kubiliute R**, Januskeviciene I, Urbanaviciute R, Daniunaite K, Drobniene M, Ostapenko V, Daugelavicius R, Jarmalaite S. Nongenotoxic ABCB1 activator tetraphenylphosphonium can contribute to doxorubicin resistance in MX-1 breast cancer cell line. *Scientific Reports* 2021;11(1):6556. https://doi.org/10.1038/s41598-021-86120-6

2. Daniunaite K, Sestokaite A, **Kubiliute R**, Stuopelyte K, Kettunen E, Husgafvel-Pursiainen K, Jarmalaite S. Frequent DNA methylation changes in cancerous and noncancerous lung tissues from smokers with non-small cell lung cancer. *Mutagenesis.* 2020;11:geaa022. http://doi.org/10.1093/mutage/geaa022 Online ahead of print.

3. **Kubiliūtė R**, Šulskytė I, Daniūnaitė K, Daugelavičius R, Jarmalaitė S. Molecular features of doxorubicin-resistance development in colorectal cancer CX-1 cell line. *Medicina (Kaunas)* 2016;52(5):298-306. http://doi.org/10.1016/j.medici.2016.09.003

LIST OF CONFERENCES

Presentations directly related to the topic of doctoral dissertation:

Poster presentations:

1. **Kubiliūtė R**, Žukauskaitė K, Žalimas A, Ulys A, Jankevičius F, Jarmalaitė S. DNA methylation biomarkers of clear cell renal carcinoma. ESMO „Molecular analysis for precision oncology virtual congress“. October 9-10, 2020; *Annals of Oncology* Supplements. https://doi.org/10.1016/j.annonc.2020.08.2184

2. Jarmalaite S, **Kubiliute R**, Nainys J, Zalimas A, Bakavicius A, Ulys A, Jankevicius F, Mazutis L. DNA Methylation Biomarkers of Clear Cell Renal Carcinoma. The 26th Meeting of the EAU Section of Urological Research (ESUR). Porto (Portugal), October 10-12, 2019;

3. **Kubiliūtė R**, Žalimas A, Bakavičius A, Ulys A, Jankevičius F, Jarmalaitė S. Novel DNA Methylation Biomarkers of Clear Cell Renal Carcinoma. EAU 6th Baltic Meeting. Tallinn (Estonia), May 24–25, 2019; *European Urology* Supplements. https://doi.org/10.1016/S1569-9056(19)32209-2

4. Šumskaitė A, **Kubiliūtė R**, Žalimas A, Ulys A, Jankevičius F, Jarmalaitė S. Promoter DNA Methylation Analysis of *BMP7*, *PCDH8* and *TFAP2B* Genes in Clear Cell Renal Carcinoma. The Coins'19 – 14th international conference of natural and life sciences. Vilnius (Lithuania), February 26-28, 2019;

5. **Kubiliūtė R**, Žalimas A, Ulys A, Jankevičius F, Jarmalaitė S. DNA Methylation Biomarkers of Clear Cell Renal Carcinoma. The Coins'19 – 14th international conference of natural and life sciences. Vilnius (Lithuania), February 26-28, 2019;

6. **Kubiliūtė R**, Žalimas A, Ulys A, Jankevičius F, Jarmalaitė S. Genome-wide DNA methylation profiling in Clear Cell Renal Carcinoma. XV International Conference of the Lithuanian Biochemical Society. Dubingiai (Lithuania). June 27-29, 2018;

7. **Kubiliūtė R**, Žalimas A, Ulys A, Jankevičius F, Jarmalaitė S. DNA Methylation Profile of Clear Cell Renal Carcinoma. EAU 5th Baltic Meeting. Riga (Latvia), May 25-26, 2018;

8. **Kubiliūtė R**, Daniūnaitė K, Žalimas A, Jankevičius F, Jarmalaitė S. Promoter Hypermethylation of Tumor Suppressor Genes in Renal Cell Carcinoma. EAU 4th Baltic Meeting. Vilnius (Lithuania), May 26-27, 2017.

Results also presented by oral presentations:

1. Žukauskaitė K, **Kubiliūtė R**, Žalimas A, Jarmalaitė S. Identification of novel urinary biomarkers for clear cell renal cell carcinoma diagnosis. „Health for All“, Kaunas (Lithuania). November 19-20, 2020. [award for best presentation];

2. Žukauskaitė K, **Kubiliūtė R**, Žalimas A, Jarmalaitė S. Analysis of novel urinary DNA-methylation-based biomarkers of clear cell renal cell carcinoma. 14th international young scientists conference „Biology: from a molecule up to the biosphere“. Kharkiv (Ukraine). November 27-29, 2019. [award for best presentation].

FINANCIAL SUPPORT

The present research was mainly supported by the Research Council of Lithuania (RCL) grant No. S-MIP-17/54 and partially funded by the European Social Fund according to the activity “Development of students’ ability to carry out R&D activities” under Measure No.09.03.3-LMT-K-712 “Development of Scientific Competences of Scientists, other Researchers and Students through Practical Research Activities” (grant No. 09.03.3-LMT-K-712-15-0214). The study was also partially supported by the 2014–2020 European Union Structural Funds according to the activity “Intelligence. Joint science-business projects” grant No. J05-LVPA-K-04-0029.

ABBREVIATIONS

RCC	Renal cell carcinoma
5mC	5-methylcytosine
ADAMTS19	*ADAM metallopeptidase with thrombospondin type 1 motif 19* gene
APC	*Adenomatous polyposis coli* gene
ASC	Asymptomatic control
ATP	Adenomatous polyposis coli gene
AUC	Area under the curve
BAP1	*BRCA1-associated protein 1* gene
BMP7	*Bone morphogenetic protein 7* gene
BMPs	Bone morphogenic proteins
CCND1	*Cyclin D1* gene
ccRCC	Clear cell RCC
CDH1	Cadherin 1 (E-cadherin)
CDKN2A	*Cyclin dependent kinase inhibitor 2A* gene
CGI	Cytosine-guanine dinucleotide-rich island, CpG island
chRCC	Chromophobe RCC
CI	Confidence intervals
CpG	Cytosine-guanine dinucleotide
Cq	Cycle of quantification
CT	Computed tomography
DAPK1	*Death-associated protein kinase 1* gene
DNMTs	DNA methyltransferases
(D)Se	(Diagnostic) sensitivity
(D)Sp	(Diagnostic) specificity
EAU	European Association of Urology
ECM	Extracellular matrix
EGF	Epidermal growth factor
EMT	Epithelial-mesenchymal transition
ERK1/2	Extracellular signal-regulated kinase 1/2
FBN2	*Fibrillin-2* gene
FH	Fumarate hydratase
FLRT2	*Fibronectin leucine-rich transmembrane protein 2* gene
GI	Genomic instability

GO	Gene ontology
GREM1	*Gremlin 1* gene
GSEA	Gene set enrichment analysis
GSK-β	Glycogen synthase kinase-β
GSTP1	*Glutathione S-Transferase Pi 1* gene
HIF1α	hypoxia-inducible factor α
HM27	Illumina HumanMethylation27 platform
HM450	Illumina HumanMethylation450K platform
HR	Hazard ratio
IGF	Insulin growth factor
ITH	Intratumor heterogeneity
JADE-1	Jade family protein 1
KDM5C	Lysine Demethylase 5C
M	Methylated gene status
MAPK	Mitogen-activated protein kinase
MC	Methylated control
MGMT	*O-6-Methylguanine-DNA Methyltransferase* gene
MMPs	Matrix metalloproteinases
MRT	Magnetic resonance tomography
MSP	Methylation-specific PCR
MTOR	*Mammalian target of rapamycin* gene
NF-κB	Nuclear factor-κB
NRT	Non-cancerous renal tissue
NTC	No template control
OS	Overall survival
p14	*CDKN2A transcript variant p14 (p14ARF)* gene
p16	*CDKN2A transcript variant p16 (p16INK4a)* gene
PBRM1	*Polybromo 1* gene
PBS	Phosphate-buffered saline
PCDH8	*Protocadherin-8* gene
PCR	Polymerase chain reaction
PDGF	Platelet-derived growth factor
PI3K	Phosphoinositide 3-kinase
pRCC	Papillary RCC
pT	Pathological tumor stage
PTEN	*Phosphatase and tensin homolog* gene

pVHL	Protein von-Hippel-Lindau
qMSP	Quantitative methylation-specific PCR
RARB	*Retinoic acid receptor β* gene
RASSF1A	*RAS association domain family member 1A* gene
ROC	Receiver operating characteristic curve
ROS	Reactive oxygen species
RT-qPCR	Reverse-transcription quantitative PCR
SCNAs	Somatic copy number alterations
SETD2	*SET domain-containing 2* gene
SFRP1	*Secreted frizzled-related protein 1* gene
SIM1	*Single-minded family bHLH transcription factor 1* gene
SNAI1	Snail Family Transcriptional Repressor 1
SWI/SNF	SWItch/Sucrose Non-Fermentable ATP-dependent chromatin remodeling complexes
TAC1	*Tachykinin-1* gene
TAN	Tumor-associated necrosis
TCA	Tricarboxylic acid
TCGA	The Cancer Genome Atlas
TFAP2B	*Transcription factor AP-2 beta* gene
TGF-β	Transforming growth factor β
TIMP3	*TIMP Metallopeptidase Inhibitor 3* gene
TNM	Tumore Node Metastasis staging system
TP53	*Tumor protein 53* gene
U	Unmethylated gene status
UC	Unmethylated control
US	Ultrasonography
VEGFA	Vascular endothelial growth factor-A
VEGFR2	Vascular endothelial growth factor receptor 2
VHL	*von-Hippel-Lindau* gene
WHO/ISUP	World health organization/International Society of Urological Pathology
WNT	Wingless and Int-1
ZEB2	Zinc Finger E-Box Binding Homeobox 2
ZNF677	*Zinc finger protein 677* gene

INTRODUCTION

Clear cell renal cell carcinoma (ccRCC) is the most common subtype of kidney tumors, accounting for most deaths from genitourinary cancers [1-3]. While most ccRCC cases are localized diseases, at least one-fifth of patients are present with metastasis at diagnosis [4]. This is attributed to the typical lack of symptoms of the primary ccRCC and nowadays, most kidney cancer cases are detected incidentally during abdominal imagining regarding unspecific symptoms [1,5]. The possibility to detect disease using liquid biopsy-based molecular biomarker tests followed by imaging could enhance early diagnosis and facilitate patients' follow-up and prognosis.

The potential disease biomarkers sources include tumor tissue (biopsy or surgical resection specimens) and bodily fluids, e.g., blood, urine. However, biopsies are less appropriate due to hazardous and painful procedures, subjective evaluation by a pathologist, the need for representative and sufficient quality tissue, and robust limitations on sampling frequency. The last two are extremely important for ccRCC characterized by high heterogeneity highly overlooked in the single biopsy studies [6-9]. While that heterogeneity may be captured better in body fluids, particularly urine, reflecting a broader spectrum of (epi)genetic alterations from various tumor foci and even micrometastatic spots. Most importantly, concerning the noninvasive nature of sample collection, urine can be obtained frequently and, due to the easily available repeatability and comparability, allow the detection of cancer at an early stage and follow the real-time state of the disease progression.

A recent study revealed that clonal expansion of ccRCC tumors is dilatory. A long time (up to 50 years) is required from the initial genetic alteration to the clinical manifestation of cancer [6]. While hardly any change is evident in corresponding histologically normal renal tissue, alterations in DNA methylation have already accumulated in such non-cancerous renal tissues [10], suggesting their suitability for early diagnosis of the disease. DNA methylation is the most widely studied epigenetic phenomenon, modulating gene expression and relating to various renal cancer clinical subgroups [11]. In addition, in comparison with genetic alterations, DNA methylation changes are more pronounced and frequent in kidney cancer [12]. Moreover, epigenetic marks can be easily detected in the body fluids such as urine by conventional and inexpensive PCR methods. Thus, it may serve as non-invasive biomarkers that could provide clinicians with rapid, objective, and accurate tools for the detection and follow-up of renal tumors.

Despite relatively high mortality rates from kidney cancer and the potential of DNA methylation as molecular marks of this disease, no diagnostic or prognostic RCC-specific epigenetic biomarkers have reached the clinic yet. Meanwhile, DNA methylation-based tests for other urological cancers (prostate, bladder) have been commercially available for a long time [13]. Currently, only seven studies shed an effort to analyze DNA methylation in urine samples of kidney cancer patients [14-20]. However, most previously published studies used a candidate gene approach and were tiny scale, thereby producing results with questionable clinical significance. Navigation toward clinical utility is challenging, requiring representative and large patient series, thorough screening, and sufficient validations to identify the most promising biomarkers. Yet DNA methylation is a perspective source of renal cancer biomarkers and is worth these efforts.

Aim and tasks

The present study aimed to establish aberrantly methylated genes in renal clear cell carcinoma tissues and evaluate their diagnostic and prognostic value and applicability as non-invasive urine-based disease biomarkers.

In order to achieve this aim, the following **tasks** have been carried out:

1. To establish genome-wide DNA methylation and global mRNA expression profile of cancerous ccRCC and paired non-cancerous renal tissues (NRT) to determine ccRCC-specific DNA methylation alterations and deregulated molecular pathways;

2. To evaluate methylation differences at the regulatory regions of selected protein-coding genes, namely *ZNF677, FBN2, PCDH8, TFAP2B, TAC1, FLRT2, ADAMTS19, BMP7, SIM1,* and *SFRP1* in the ccRCC and NRT samples to evaluate their diagnostic and prognostic value in the renal tissue samples;

3. To analyze the mRNA expression levels of the selected genes, particularly *ZNF677, FBN2, PCDH8, TFAP2B, TAC1,* and *FLRT2* in the ccRCC and NRT samples to evaluate associations with DNA methylation status and patients clinical-pathological parameters;

4. To validate methylation differences at the regulatory regions of selected genes, particularly *ZNF677, FBN2, PCDH8, TFAP2B,*

TAC1, and *FLRT2* in the urine samples of the patients diagnosed with ccRCC and asymptomatic controls, to evaluate the biomarkers applicability for non-invasive cancer detection and prognosis.

Scientific novelty and practical value of the study

The current study described for the first time the DNA methylation and gene expression profile in the Lithuania cohort of kidney cancer cases using either genome-wide and gene-targeted approaches. The obtained results deepened the understanding of DNA methylation role and deregulated signaling pathways in localized ccRCC tumors.

Genome-wide DNA methylation profiling utilizing microarrays allowed identifying a set of novel presumable DNA methylation biomarkers, having moderate to high diagnostic and/or prognostic potential. Moreover, identified DNA methylation alterations at the regulatory regions of selected genes appeared to be amenable for non-invasive detection in the urine samples of ccRCC patients. Thus, the results showed the promising potential of the chosen genes as candidates for further development of non-invasive tools for kidney cancer patients testing.

The methylation of most biomarkers investigated herein in the case of ccRCC has been analyzed for the first time in both tissue and urine samples and showed encouraging results due to their association with at least one clinical-pathological parameter. According to obtained results, the transcription factor encoding the zing finger protein 677 (ZNF677) gene is the most promising due to its significant association between promoter methylation and gene expression and correlation with numerous clinical-pathological factors parameters as well as patient survival. In addition, its combination with Protocadherin 8 (PCDH8) for the urine test showed a moderate diagnostic and magnificent prognostic value. Although additional validation is required, the obtained results seem to be rather promising. They may stimulate the further establishment of a new molecular test for kidney cancer detection and follow-up, improving the statistics of that malignancy.

Defending statements

1. Changes in the DNA methylation and mRNA expression of protein-coding genes are abundant in the case of ccRCC and dysregulate the particular biological and molecular processes directly related to cancer development and progression.

2. The methylation of protein-coding genes *ZNF677*, *FBN2*, *PCDH8*, *TFAP2B*, *TAC1*, *FLRT2*, *ADAMTS19*, *BMP7*, *SIM1,* and *SFRP1* are highly specific for ccRCC tissue, and a combination of *ZNF677*, *FBN2*, *PCDH8*, *TFAP2B*, *TAC1* & *SFRP1* produced high sensitivity for ccRCC and has potential to be used as a tool for cancer diagnostics.

3. The methylation of investigated genes, especially *ZNF677* and *PCDH8,* were significantly related to the most important prognostic factors of ccRCC (tumor size, stage, grade, necrosis) and recognized as potential prognostic ccRCC biomarkers. The methylation status of *ZNF677* and *FBN2* and many combinations of two-four genes in ccRCC tissue samples significantly predict patient's overall survival and has the potential to be used as a tool for disease prognosis.

4. The methylated status of *ZNF677* in the ccRCC tissues is directly related to the significantly lower expression, which itself associated with numerous adverse clinical-pathological parameters and shorter patient's overall survival, making *ZNF677* an extremely promising biomarker of ccRCC.

5. The methylation level of *ZNF677*, *FBN2*, *PCDH8*, *TFAP2B*, *TAC1,* and *FLRT2* are significantly higher in the urine samples of ccRCC patients compared to asymptomatic controls and multimarker panel consisting of *ZNF677 & PCDH8*, either with or without *FBN2* or *FLRT2* produced moderate sensitivity and specificity for ccRCC and has potential to be used as a tool for non-invasive cancer diagnostics.

6. The methylation status of *PCDH8* or panel consisting of *ZNF677 & PCDH8* in the urine samples independently predicts ccRCC patients' overall survival and has the potential to be used as a tool for non-invasive prediction of cancer prognosis.

1. LITERATURE OVERVIEW

1.1. Kidney cancer

Kidney (or renal) cancer takes 14th place according to the incidence in both sexes worldwide and is among the top ten most common cancers in males [according to 2020 data from Cancer Today, Global Cancer Observatory, International Agency for Research on Cancer; https://gco.iarc.fr/]. In the year 2020, 431 288 new kidney cancer cases were diagnosed, accounting for about 2.2% of all cancers. The highest incidence rate of kidney cancer is determined in Australia, South America, and Central and Eastern Europe (**Fig. 1.1**). In Lithuania, 814 new kidney cancer cases were diagnosed in 2020, accounting for ~5% of all cancers.

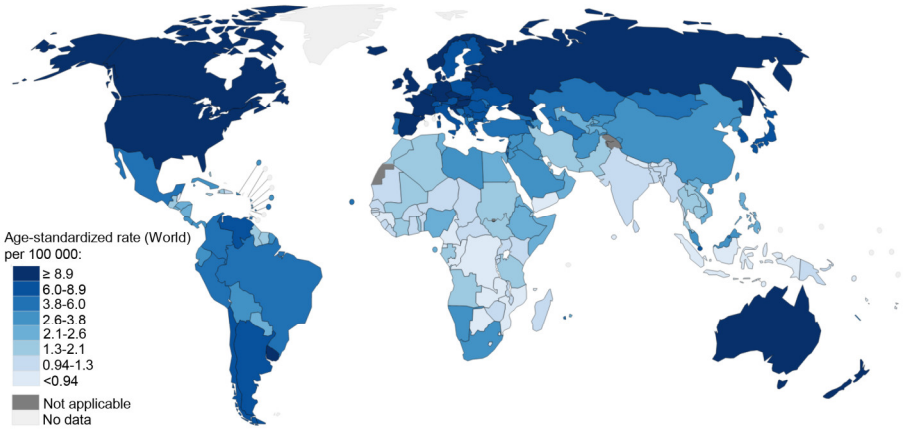

Fig 1.1. In 2020, estimated age-standardized incidence rates (World) of kidney cancer in both sexes.

Lithuania characterizes the highest incidence rate globally and takes 5th place according to the mortality rate (**Fig. 1.2**) [according to 2020 data from Cancer Today, Global Cancer Observatory, International Agency for Research on Cancer; https://gco.iarc.fr/]. However, the annually established (during 2006-2015) number of new cases and deaths is relatively stable and confirms the tendency of higher morbidity in men (**Fig. 1.3**) [according to Cancer Registry, National Cancer Institute, Lithuania; http://www.nvi.lt]. Furthermore, while most of these patients will present with localized disease, 25–40% of those treated with curative intent will develop the distant disease, and 20–25% of patients will present with metastatic disease at diagnosis [4]. This caused the significant health burden of that malignancy and raised the urgent need to diagnose the condition early and accurately and predict its further course.

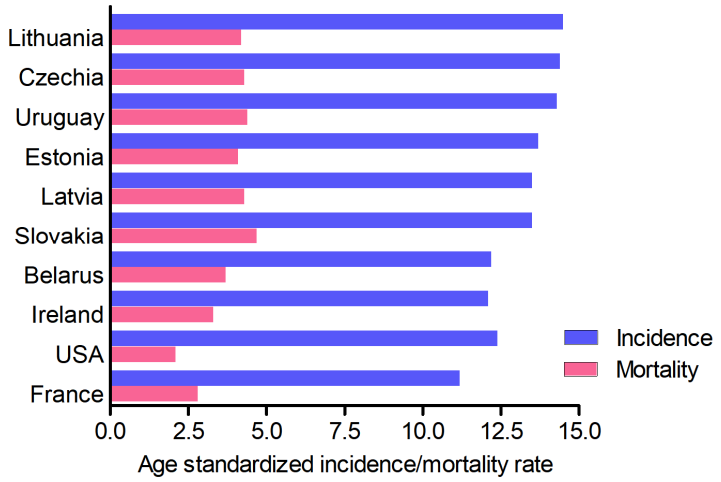

Fig 1.2. The top ten countries according to age-standardized incidence rates (World) of kidney cancer estimated in 2020. Data compiled from International Agency for Research on Cancer; https://gco.iarc.fr/].

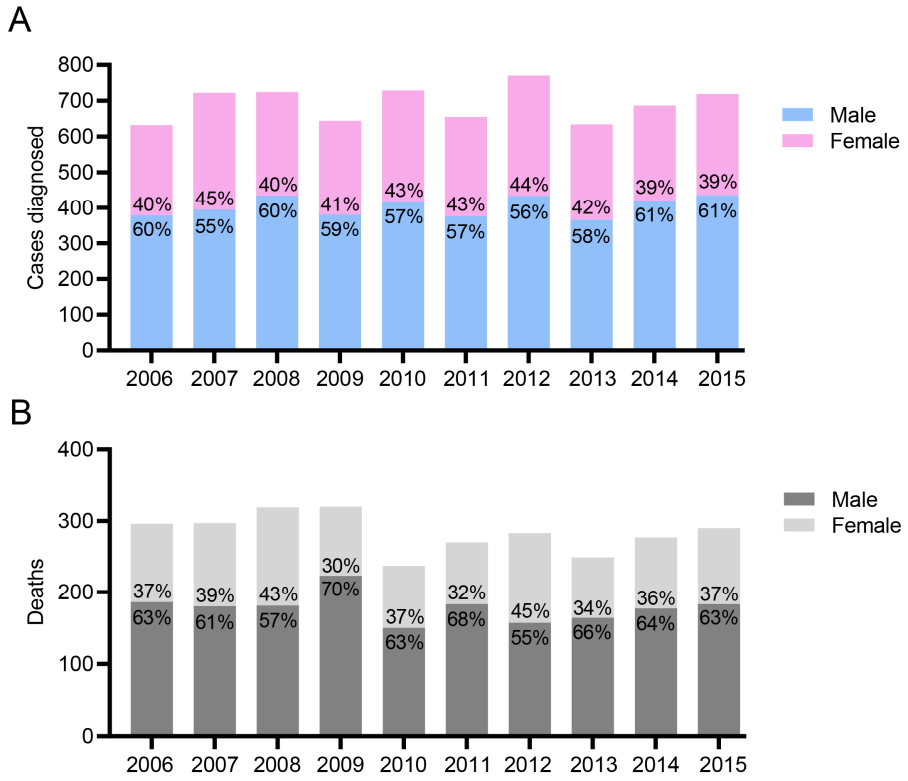

Fig 1.3. Trends of kidney cancer incidence (A) and mortality (B) amounts in Lithuania during 2006-2015. Data compiled from Cancer Registry, National Cancer Institute (Lithuania; http://www.nvi.lt).

1.1.1. Kidney anatomy and function

The kidney is a paired bean-shaped organ lying in the abdominal cavity behind the peritoneum. In adults, each kidney weighs about 100-200 g and has dimensions equal to 10.9-11.2 cm in length and 3.2-3.4 cm in thickness, with the left kidney being slightly larger than the right one [21]. On the medial surface of the kidney is the hilum through which the renal artery, vein, lymphatics, nerves, and ureter join to the inner regions of the kidney. From the outside, the kidney is enveloped with a tough fibrous layer called the renal capsule, surrounded by a mass of fatty tissue called the perirenal fat, mitigating excess movement of the kidneys and an additional coat called *Gerota fascia* [22].

The inner structure of the kidney is composed of two main areas: the outer cortex and the inner medulla, which comprises outer and inner zones. The medulla consists of several renal pyramids that arise from the cortical/medullary border and form the renal papilla at the apex. The renal pyramids are the primary functional unit of the kidney where concentrated urine is produced. Each renal papilla is associated with a minor calyx which collects urine from the pyramids. Several minor calyces merge to form a major calyx which passes to the renal pelvis. The renal pelvis is a funnel-shaped structure draining urine into the ureter connecting the kidney to the bladder where the urine is stored.

The urine is formed in the nephrons, which are the kidneys' basic structural and functional units. Each kidney contains about 1 million nephrons, each of which starts with the Bowman's capsule consisting of squamous epithelial cells surrounding the glomerular capillaries and located at the renal cortex. The blood arrived by the afferent arteriole is filtered at the glomerulus, and the formed filtrate immediately enters the proximal tubule, extended from the Bowman's capsule. The proximal tubule is lined with cuboidal epithelial cells, characterized by the well-developed villi and microvilli at the apical membrane and abundance of the mitochondria, providing the high-capacity reabsorption (**Fig. 1.4**). About 60-70% of the fluid, containing sodium ions, glucose, amino acids, and anions, is passively reabsorbed from the proximal tubule and back to the blood circulation [22]. The proximal tubule consists of the convoluted segment located in the cortex and the straight segment leading into the medulla. At this segment, epithelial cells lose their microvilli and are characterized by the lower density of mitochondria. Further proximal tubule transit to the loop of Henle lined with the more squamous epithelial cells, absorbing about 20-25% of the total filtrate. Once the tubule returns to the cortex, it becomes the distal convoluted tubule, having few microvilli and

slightly lower amounts of mitochondria. Approximately 5–7% of the total filtrate is further reabsorbed at these tubules. All distal tubules converge and form collecting tubules, opening into the calyces, where concentrated urine is drained [21].

The area among the nephron capsule, tubules, and vascular network in the kidney is called the renal interstitium, which is filled with the extracellular matrix, interstitial fluids, and various types of cells, including dendritic cells, macrophages, lymphocytes, lymphatic endothelial cells, and miscellaneous fibroblasts [23,24]. The renal interstitium is distributed unevenly along the kidney and accounts for approximately 8% of the total parenchyma in the cortex, while up to 40% in the inner medulla [25,26]. Renal interstitium not only supports the tubular epithelium but also performs the physiologic endocrine function by producing erythropoietin and renin [27]. Erythropoietin is indispensable for hematopoiesis, and even 90% of this hormone in adults is produced by renal interstitial fibroblasts [28]. Renin is an enzyme produced by juxtaglomerular epithelioid appearance cells located near afferent arteriole. This protein is a key regulator of the renin-angiotensin-aldosterone hormone system, essential for the body's blood pressure and fluid balance regulation [29].

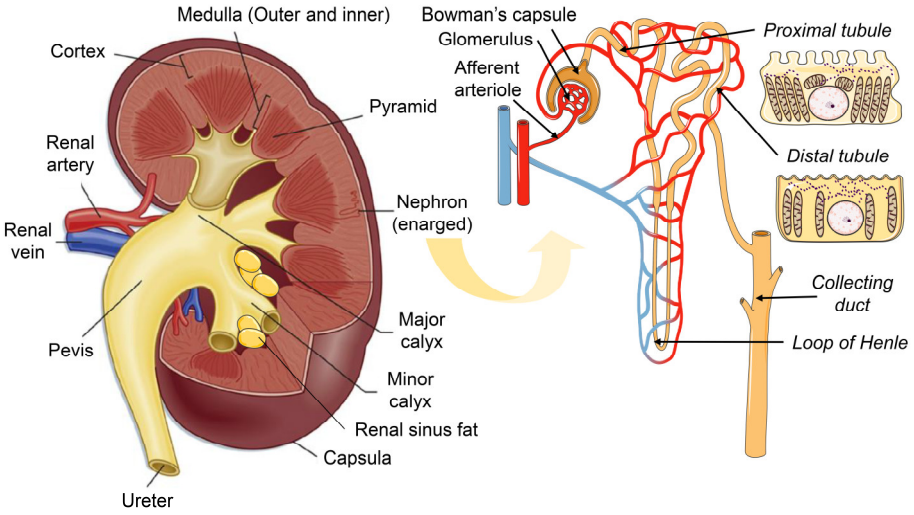

Fig 1.4. The simplified schematic structure of the human kidney. (Adapted from [30]).

1.1.2. Renal tissue carcinogenesis

About 25 different cell types in total are found in the renal parenchyma [31], reflecting the intricacy of kidney structure and function and leading to

the great diversity of renal cancers. Thus, renal cancer is not a single disease but comprises various cancer types developed in the kidney. Each cancer type is caused by different mutations, leading to different histology and the clinical course of the disease [5]. Renal cell carcinoma (RCC) originating from the epithelium of nephron tubules is the most common type of kidney cancer, accounting for 90% of all cases, and is the most lethal cancer of the urinary system [1,2].

According to the tissue histology and type of renal cells getting affected, the World Health Organization (WHO) classification describes the 16 different subtypes of RCC [32]. The three major subtypes of RCC are clear cell (also named as conventional) RCC (ccRCC), representing the most common form (70–80%), papillary RCC (pRCC) accounting for 10–15%, and chromophobe RCC (chRCC) accounting for 5% of RCC. In contrast, the remaining subtypes are very rare (each with ≤1% total incidence) [3]. Papillary and chromophobe subtypes are also called non-clear cell RCC. They strongly differ in tumor progression and behavior compared with ccRCC because of distinct genetic mutations and alterations in various signaling pathways [33]. Clinically, the most notable difference is disease prognosis, which is the worst for ccRCC with a 5-years survival rate of about 55-60%, compared to 70-90% for pRCC and 80-95% for chRCC [12].

Despite the rapidly improving molecular characterization of normal kidney cells and renal malignancies, the particular cell type from which each RCC subtypes arise remains elusive. However, it is well known that chRCC comes from the cells of the distal convoluted tubule of the nephron; meanwhile, both pRCC and ccRCC originate in the epithelium of the proximal convoluted tubule (**Fig. 1.5 A**) [34,35]. Although derived from the same part of the nephron, it is believed that pRCC arises from kidney progenitor cells, while ccRCC is from the mature renal tubular cells [36, 37].

The nephron epithelial cells are usually mitotically quiescent, but in the case of kidney injury, they show a remarkable potential to regenerate and re-establish a functional epithelial barrier [35]. Although it is unclear whether this regenerative process is initiated by progenitor cells or by dedifferentiated epithelial cells, it is believed that the program used during epithelial regeneration may act in oncogenic transformation as well [35,37,38]. Additional support for the role of renal regeneration in tumor initiation, promotion, and progression stems from the observation that many of the established RCC risk factors put a strain on kidney function and might invoke kidney damage and repair programs [3].

According to the historical data, during the response to kidney injury, matured tubular epithelial cells can regress into mesenchymal one, the process

called epithelial-mesenchymal transition (EMT) [39-41]. During EMT, epithelial cells lose their intercellular junctions and barrier integrity, acquiring a mesenchymal phenotype characterized by increased motility [42,43]. However, kidney tubular epithelial cells rarely conduct an entire EMT program and, in most cases, express both epithelial and mesenchymal markers, known as partial EMT [44]. During such a process, epithelial cells obtain stem cell-like characteristics, playing a vital role in the initial steps toward renal cancerogenesis (**Fig. 1.5 A**) [43,45,46]. Furthermore, dramatic metabolic rearrangement, resulting in a decreased level of ATP synthesis due to dysregulated fatty acids oxidation, leading to intracellular lipid accumulation, is observed in these cells [44,47]. In addition, these cells secret various growth factors, cytokines, chemokines, followed by inflammatory cells' recruitment, causing chronic inflammation and further EMT progression [47,48]. Finally, such epithelial cells may enter the path of oncogenic transformation if they harbor relevant genetic predisposition and accumulate additional genetic alterations, causing uncontrolled cell growth and tumor development.

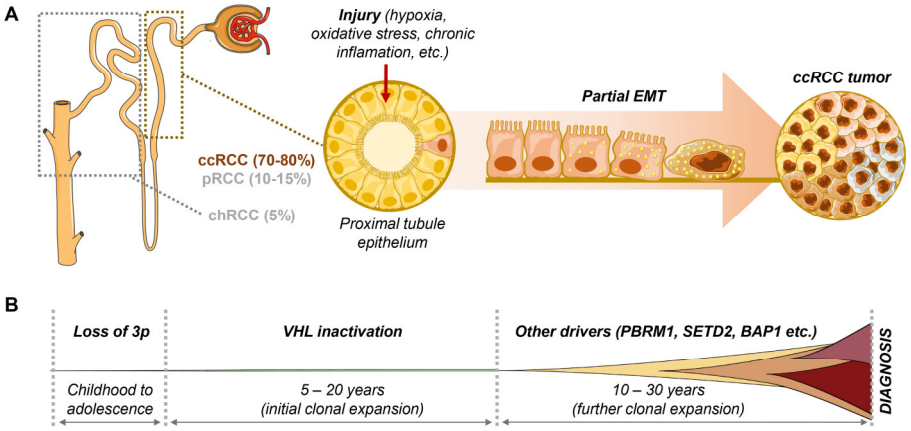

Fig 1.5. The putative origin of ccRCC. A – ccRCC originate from proximal tubule epithelial cells which after injury undergo a partial EMT, possibly playing a key role in the initial steps toward renal tissue fibrosis and development of ccRCC (partly adapted according to [35,44]); B – putative nature and timing of key oncogenic events in ccRCC, depicting the evolutionary trajectories of tumors in patients (adapted according to [6]).

The recent studies indicate that sporadic ccRCC is initiated by loss of 3p, harboring von Hippel–Lindau (*VHL*) tumor suppressor gene (in detail described later), seemingly arising in childhood or adolescence. Decades later, the point mutation in the remaining *VHL* copy occurred; however, cancer still remains undetectable for another 10-30 years (**Fig. 1.5 B**) [6]. Then, additional

mutations of other drivers, such as *PBRM1*, *SETD2*, *BAP1, TERT, PI3K,* and many others, occur. Given the greater diversity of genes, these additional driver mutations are considerably less rate-limiting, and once happens, a substantial clonal expansion is induced, and at this stage, the developing tumor has a sufficient population size to be diagnosed.

While various organs have well-defined premalignant lesions, the corresponding histological alterations in the renal tissue are poorly described. This is mainly due to the lack of practical screening approaches for renal tumors [49]. Nevertheless, in the two studies examining kidney tissue for the dysplastic changes, preneoplastic alterations were identified mainly in the cortex, which was similar to RCC [50,51]. The dysplastic changes in the tubular epithelium encompass increased nuclear size and pleomorphic vesicular nucleus along with interstitium fibrosis, erythrocyte extravasation, and lymphoplasmacytic infiltration. However, to demonstrate the progression of renal dysplasia into invasive carcinoma histologically is complicated due to the intricated biopsy sampling of the tubular system. Still, it was shown in the experimental models [52], and it appears that dysplasia is also a premalignant lesion in the human kidney.

Clear cell RCC is usually a unifocal and unilateral tumor, while multifocality and bilaterality are observed in only 2-7% and 1-2% of sporadic cases, respectively [53]. The tumors of ccRCC are usually golden yellow due to the accumulation of lipids and glycogen in the cancer cells, emphasizing the metabolic rearrangement of this tumor subtype [35,54]. In addition, the areas of hemorrhage, fibrosis, necrosis, and cystic degeneration are also observed and give a variegated appearance of the tumor [54]. Histologically ccRCC is characterized by epithelial cells with clear cytoplasm and well-demarcated cell membrane, scattered within a highly vascularized stroma. These tumors may also contain cells with granular eosinophilic cytoplasm, still displaying high levels of lipids and glycogen [54]. Ultrastructurally, ccRCC cells show tubular differentiation with long microvilli seen in renal proximal tubule epithelial cells as well.

1.1.3. Renal cell carcinoma diagnosis, staging, and prognosis

Many renal masses remain asymptomatic until the late disease stages, and most diagnoses result from incidental findings due to extensive use of non-invasive imaging investigating various non-specific symptoms [55,56]. Clinically renal cell carcinoma is associated with a classic triad of flank pain, hematuria, and palpable abdominal mass. Still, these signs are rare (6-10%) and correlate with aggressive histology and advanced disease [57, 58].

Diagnosis is usually strongly suspected by imaging studies, such as ultrasonography (US), abdominal computed tomography (CT), or magnetic resonance tomography (MRT), performed for other medical reasons [55,56,59]. However, due to the high diagnostic accuracy of abdominal imaging, renal tumor biopsy is unnecessary in patients with a contrast-enhancing renal mass for prescribed partial or radical nephrectomy. Thus, the risk of patients' overtreating remains, especially in renal masses smaller than 1 cm (26%), while the sensitivity of US is extremely low in that condition [60]. Furthermore, although the sensitivity and specificity of CT and MRT reach 100% and ≥ 90%, respectively, none of these methods can distinguish benign renal lesions from neoplastic [61,62].

The exact treatment strategy must be appointed when the renal cancer is confirmed, depending on tumor histology and stage [63,64]. The use of the current Tumour Node Metastasis (TNM) classification is recommended for tumor staging and treatment decisions making [65,66]. The TNM classification system is based on three major parameters: T (tumor) describes the size of the primary tumor; N (node) refers to the degree of tumor invasion into regional tissues (venous, renal capsule, adrenal gland); M (metastasis) shows the status of distant metastasis (**Table 1.1**).

Without tumor histology and stage, tumor grade contributes to RCC prognosis as well. In 1982 Fuhrman *et al.* proposed a four-grade system based upon the simultaneous assessment of cancerous cells' nuclear size, shape, and nucleolar prominence [67]. Although the Fuhrman grading system has been in international use for many years and has proven prognostic utility, it has numerous limitations. For example, grading in the *Fuhrman* system is based upon the highest-grade area, even if focal, where minute foci of higher-grade tumor or tumor adjacent to the necrotic zone would be taken into account [68]. These problems likely contribute to intra- and inter-observer variability in the evaluation of tumor grade [69-73]. Due to these limitations, today's *Fuhrman* grading system becomes inapplicable.

The new WHO/ISUP (International Society of Urologic Pathologists) grading system has been introduced following the conclusions of the 2012 ISUP Vancouver conference and is recommended for use by the WHO [74-76]. It is also a four-grade system considered according to nucleolar prominence (used to determine grades 1-3) and the presence of highly atypical "pleomorphic" cells and/or sarcomatoid or rhabdoid morphology (defining grade 4) (**Table 1.2**). Compared to the Fuhrman system, WHO/ISUP is easier to apply and provides superior prognostic information in cases of ccRCC [77].

Table 1.1. Currently used Tumor, Node, Metastasis staging system (TNM) for classification and staging of renal cancer (adapted from [65,78]).

T – primary tumor			
TX	Primary tumor cannot be evaluated		
T0	No indications of the primary tumor		
T1	Tumour ≤ 7 cm or less in greatest dimension, limited to the kidney		
T1a	Tumour ≤ 4 cm or less		
T1b	Tumour > 4 cm but ≤ 7 cm		
T2	Tumor > 7 cm in greatest dimension, limited to the kidney		
T2a	Tumour > 7 cm but < 10 cm		
T2b	Tumours > 10 cm, limited to the kidney		
T3	Tumour extends into major veins or perinephric tissues but not into the ipsilateral adrenal gland and not beyond *Gerota* fascia		
T3a	Tumor extends into the renal vein or its segmental branches, or tumor invades perirenal and/or renal sinus fat (peripelvic fat) or pelvicalyceal system but not beyond *Gerota* fascia		
T3b	Tumor grossly extends into the *vena cava* below the diaphragm		
T3c	Tumor grossly extends into *vena cava* above the diaphragm or invades the wall of the *vena cava*		
T4	Tumour invades beyond *Gerota* fascia (including contiguous extension into the ipsilateral adrenal gland)		
T – regional lymph nodes			
NX	Regional lymph nodes cannot be evaluated		
N0	No regional lymph node metastasis		
N1	Metastasis in regional lymph node(s)		
M – distant metastasis			
M0	No distant metastasis		
M1	Distant metastasis		
pTNM staging			
	T	**N**	**M**
Stage I	1	0	0
Stage II	2	0	0
Stage III	3	0	0
	1 or 2 or 3	1	0
Stage IV	4	0 or 1	0
	1 or 2 or 3 or 4	0 or 1	1

Recently it has been proposed that tumor-associated necrosis (TAN) should be involved in the WHO/ISUP grading system. Some studies have shown that the presence or absence of necrosis influences outcome predictions [79-81]. TAN is usually microscopic well-demarcated foci within a tumor [81]. There are several different interpretations of TAN pathogenesis, and

suggested mechanisms include an immune reaction, tumor outgrowth of blood supply, vascular immaturity, hypoxia, or increased density of small vessels [33,75,79,82,83]. As tumor necrosis has prognostic significance for ccRCC, independent of tumor stage and grade [33,75,83], its evaluation is valuable.

Table 1.2. The WHO/ISUP grading system for renal cell carcinoma (ccRCC and pRCC subtypes) (adapted from [68]).

Grade	Description
1	Tumor cell nucleoli absent or undistinguished and basophilic
2	Tumor cell nucleoli conspicuous, eosinophilic at 400x magnification and visible but not prominent at 100x magnification
3	Tumor cell nucleoli conspicuous and eosinophilic at 100x magnification
4	Tumors showing extreme nuclear pleomorphism, tumour giant cells and/or the presence of any proportion of tumour showing sarcomatoid and/or rhabdoid dedifferentiation.

Other factor associated with disease prognosis includes RCC subtype. Clear cell RCC has a worse prognosis than papillary or chromophobe RCC and is more likely to present at an advanced stage or with existing metastases [84-86]. Furthermore, the presence of sarcomatoid or rhabdoid appearance cells is associated with a poor outcome and distant metastasis [75,87,88]. This appearance may be presented at any RCC tumors but is most commonly seen in ccRCC and is classified as WHO/ISUP grade 4 [74,89]. Although such differentiation is rare and observed in approximately 5% of cases, they are related to very aggressive tumors [75,90,91].

As prognostic factors are not accurate when used alone, parameters have been combined in multivariable prognostic models and recommended by EAU guidelines for postoperative follow-up [78]. Such prognostic models for localized RCC encompass tumor stage, size, grade and necrosis (SSIGN) [92] or tumor stage, grade and Eastern Cooperative Oncology Group (ECOG) Performance Status score as in the University of California Integrated Staging System (UISS) [93] as well as several other models. However, despite the inclusion into guidelines, their use in routine clinical practice is not recommended [94].

1.1.4. Renal cell carcinoma progression and treatment

The clinical course of renal cell carcinoma is heterogeneous, ranging from indolent tumors (or cystic lesions) requiring no interventions to highly

aggressive metastatic RCC required medical management. The gold standard for patients with surgically resectable RCC is surgical excision by either partial or radical nephrectomy without adjuvant therapy. Meanwhile, for metastatic RCC, systemic treatment with targeted agents or immune checkpoints inhibitors is applied [3].

Surgical treatment of localized RCC depends on the clinical stage of the tumor and the general conditions (performance status) of the patients. For patients with T1 stage tumors and/or in the case of conditions impairing renal function (kidney stones, hypertension, diabetes Mellitus, von Hippel-Lindau syndrome, and others), partial nephrectomy, offering lower renal functional impairment compared to radical one, is assigned [95,96]. The five-year survival rate for these patients reached 95% [22]. For the larger tumors with higher stage or in the case of multiple small renal tumors, radical nephrectomy can be considered [3]. The five-year survival rate of such cases varies from approximately 60% to 90% [3].

Active surveillance is an acceptable option in the presence of slow-growing and less than 2 cm tumors or in the case of elderly patients with comorbidities for whom surgical resection is inapplicable [78,97,98]. Active surveillance is defined as the initial monitoring of tumor size by serial abdominal imaging (US, CT, or MRI) with delayed intervention reserved for tumors showing clinical progression (growth to >3-4 cm or by >0.4-0.5 cm per year [99]) during follow-up. Results from the multi-institutional study observed that active surveillance is not inferior to primary intervention [100]. Other treatment options for inoperable tumors are ablative therapy (destruction of viable tumor tissue with no disturbance of healthy area), including most commonly applied cryoablation and radiofrequency ablation [3,78].

Approximately 20-30% of RCC patients have metastases at diagnosis, while an additional 20-30% will develop the metastatic disease during follow-up, even if radical surgery has been initially performed [101]. The treatment of metastatic RCC is more complicated because of the cancer cells' resistance to conventional chemotherapy and radiotherapy [102]. Available interventions encompass tyrosine kinase inhibitors targeting VEGF signaling axis, mTOR, cytokines such as interferon-α, interleukin-2, and immune checkpoints (PD-1, PDL-1, or CTLA4) inhibitors [103-110]. In the case of an operable tumor along with systemic therapy, cytoreductive nephrectomy (removal of the primary tumor) can be applied as well and demonstrates better outcomes [111]. Although all these interventions may improve overall survival, complete remission is rare [112].

The deaths are typically the result of metastatic RCC with a five-year survival rate of approximately 20% [3,112]. Among patients to whom metastatic disease develops after partial or radical nephrectomy, it occurs within five years in about 90% of cases [101]. Local recurrence is relatively rare, while sites for distant metastases (M1) most frequently include the lung parenchyma (50–60%), bone (30–40%), liver (30–40%), and brain (5%) [113]. Considering the moderate frequency of the disease recurrence and the changing treatment of such cases, prognostic biomarkers that could lead the way for personalized treatment decisions are needed.

1.1.5. Etiology of renal cell carcinoma

Renal cell carcinoma is a complicated and aggressive malignancy generally developing as a sporadic disease but may be caused by familial factors as well. The evaluation of RCC risk factors is complex because incidental cancer detection by imagining performed for the other reasons might artificially influence the association between RCC and specific risk factors [114]. The potential risk factors comprise of both unmodifiable, like age, gender, genetic predisposition, and modifiable lifestyle factors, mainly smoking, alcohol consumption, and metabolic syndrome-related properties, including obesity and hypertension (reviewed in [115, 116]).

Age. Age at diagnosis of cancer is a well-recognized prognostic factor. Sporadic RCC is generally a disease of older adults, and most cases are diagnosed between age 65 and 74 years old [117]. The incidence rate rises steadily from around age 40 to 44 and more steeply from around age 65-69 years old [https://www.cancerresearchuk.org]. Only 3.4–7.5% of these tumors occur in adults <40 years of age and are characterized by a better prognosis [118]. However, the superior prognosis may be influenced by the better tolerance of treatment and the fact that papillary RCC, characterized by the less aggressive course of the disease, is more common in these age groups than older individuals [118].

Gender. Like most neoplasms, renal cell carcinoma is more common in men, accounting for about two-third of global cases and deaths [119]. The incidence ratio 2:1 is stable by age over time, and a part of this tendency may be explained by the greater rate of modifiable risk factors, such as smoking, hypertension, and obesity among men [115]. Moreover, the worse clinical feature and prognosis of the course of the disease was observed among the males [120]. This part can be explained by the fact that men are being diagnosed at a more advanced stage of the disease than women (56% diagnosed at stage pT2-4 compared to 29% of women) [121,122]. In

Lithuania, 48% of men and 38% of women were diagnosed with pT2-4 stage renal cancer in 2015 (Cancer Registry, National Cancer Institute; http://www.nvi.lt). Besides, males tend to have a larger tumor size, higher tumor grade, and higher incidence of regional or metastatic spread [121,122]. However, while comparing the same stage and grade tumors, the male still has the poorer prognosis [123] what suggests that there is an influence of sex hormones on RCC development and progression and a positive correlation between the expression of androgen receptors and the poorer prognosis was described [124,125].

Smoking and alcohol consumption. Smoking is largely the most significant modifiable risk factor of RCC. Tabacco smoke includes a mix of carcinogens, such as polycyclic aromatic hydrocarbons, β-naphthylamine, and nicotine, which are metabolized during filtration in the nephrons. The formed metabolites promote inflammation and DNA damage paving the way for carcinogenesis [115]. According to extensive retrospective analysis, former and current smokers had a ≥1.5-fold increased risk for RCC [126]. Moreover, cigarette smoking after disease diagnosis has been related to poorer prognosis (shorter overall and disease-free survival) as well [127]. Interestingly, some studies observed that moderate alcohol consumption is associated with reducing RCC risk [128-130]. Although the mechanism is not well understood, one of the hypotheses is that alcohol consumption would prevent insulin resistance [131], the main feature of obesity – another risk factor of RCC.

Obesity. A consistent association between increased body mass index and risk of RCC was found in several studies [132,133]. While the precise pathogenesis is unclear, it is well known that obesity contributes to tumor development at least in several respects. Specifically, obesity promotes the insensitivity to insulin and insulin-like growth factors; promote the production of inflammatory cytokines (e.g., tumor necrosis factor-α, interleukins-6/8/10); and reduce the level of adiponectin, which in harmony facilitate cell proliferation, over-production of DNA damaging free radicals and uncontrolled tumor growth [115,116,134]. For example, one study found that adding roughly 5 kg in body weight increases RCC risk by 25% in men and 35% in women [135]. Interestingly despite the contribution to increased RCC risk, obesity seems to be a favorable prognostic factor that might be partially explained by its mediated suppression of cachexia [116,136]. Besides, according to the meta-analysis, regular physical activity reduced RCC risk by 22% [137].

Hypertension. There is evidence that hypertension is an independent risk factor of RCC [132,135,138]. Hypertension damages the renal glomerulus and

tubular apparatus, possibly through chronic hypoxia and ROS-mediated lipid peroxidation, making the kidney more susceptible to carcinogens [115,116,139]. Besides, some angiogenic and other growth factors involved in hypertension may also participate in renal carcinogenesis by promoting cell proliferation and progression [116]. A history of hypertension was associated with a 67% increased risk of RCC [138]. In addition, it is observed that the risk of RCC further increased with time after hypertension diagnosis and poorly controlled hypertension [140]. However, hypertensive patients may also be more likely to get cross-sectional imagining and identify incidental renal tumors [114]. Thus, further studies are needed to unravel the association between hypertension and renal cancer.

Genetic susceptibility. While most renal cancer cases are sporadic, an inherited predisposition exists as well. The general features of inherited renal cell carcinoma are early-onset (<40 years of age), family history of renal cancer, and bilateral and/or multifocal renal tumors [141]. The most widely described genetic predisposition is Von Hippel-Lindau (VHL) disease caused by a mutation in gene *VHL* (in detail described below). VHL is an autosomal dominant inherited multisystem disorder characterized by developing various tumors, including ccRCC [141]. Renal cancer develops in 25-45% of VHL patients occurring in 20-40 years of age with a penetrance of 70% by the age of 60 [142]. It has been estimated that up to 600 tumors may develop in a single kidney of a VHL patient [143]. Some reports have described *BAP1* (described below) mutation in the germline of individuals with early-onset, bilateral and multifocal ccRCC as well [144,145]. Other conditions related to the RCC development includes hereditary papillary renal carcinoma (caused by *MET* proto-oncogene mutation) [146], Birt-Hogg-Dube syndrome (caused by *FLCN* mutation) [147], hereditary leiomyomatosis and renal cell carcinoma (caused by a mutation in Krebs cycle enzyme FH) [148] and succinate dehydrogenase (SDH)-deficient renal cancer (caused by a mutation in another Krebs cycle enzyme SDH) [149]. The clinician needs to recognize whether a patient has an inherited or sporadic form of renal cancer, which will impact patient management [141].

Various other modifiable environmental and occupational risk factors have also been implicated, but mechanisms underlying the link of these factors and RCC development in most cases remain unclear. Without the above mention hypertension, various other comorbidities, including kidney stones [150], type 2 diabetes [151], and liver (viral hepatitis) as well as chronic kidney diseases [135,152], have an impact on cancer development as well. Besides, epidemiological data suggest that analgesic use increases the risk of RCC [153]. Renal cell carcinoma is generally not considered an occupational

disease; however, the elevated risk has been linked to some agents, and the most notable is industrial solvent trichloroethylene [154].

Further studies are required in order to understand the mechanisms behind certain risk factors of renal cancer. However, overall evidence confirms that the best way to reduce the risk is to maintain a healthy weight and avoid smoking [155]. Besides, cancer prevention strategies are indispensable to sensitize public awareness for potentially preventable risk factors.

1.2. Genetic features of renal clear cell carcinoma

While a small part of ccRCC is inherited, most cases are sporadic, and more than 90% have characteristic cytogenetic abnormalities that involve conventional loss of genetic material from the chromosome arm 3p, along with loss of 14q (46%) and gains of 5q (60%) and 7q (40%) [156-159]. Although frequent somatic copy number alterations comprising other large chromosomal regions [156,157] are also observed in these tumors, their role in ccRCC is less elucidated. Meanwhile, the loss of 3p is the most widely studied and nearly universal phenomenon, constituting an early genetic event in ccRCC [160,161].

1.2.1. The role of 3p loss in renal clear cell carcinoma

The chromosome arm 3p harbor four genes commonly mutated in the case of ccRCC, particularly *VHL* (von-Hippel-Lindau), *SETD2* (SET domain-containing 2), *BAP1* (BRCA1-associated protein 1), and *PBRM1* (Polybromo 1) [156,162-164]. A mutation of *PBRM1* is observed in ≥ 40% of ccRCC cases, while *BAP1*, and *SETD2*, are mutated in roughly 10-15% of ccRCC. In contrast, the biallelic inactivation by mutation, homozygous deletion, or DNA methylation of *VHL* is determined in at least 90% of ccRCC [156,165-167]. Therefore, it is considered as a critical driver (epi)genetic alteration in ccRCC.

Function loss of *VHL* disturbed the key regulatory system used in cells under low oxygen conditions (hypoxia). *VHL* encoding protein pVHL is a member of a ubiquitin ligase complex, containing four additional proteins (elongins B, and C, Cul2, and Rbx1) [168]. In the case of well-oxygenated conditions (normoxia), this complex binds directly to the constitutively expressed hypoxia-inducible factor HIFα and targets it for proteasomal degradation through dioxygenase EGLN-mediated hydroxylation [35,168]. However, under low oxygen conditions, HIFα is no longer hydroxylated and thus is not targeted for degradation by pVHL. Instate of this, HIFα dimerizes to HIFβ and forms a transcriptional complex, activating the expression of 100-

200 genes. These genes promote cell adaptation to hypoxia through metabolic reprogramming (acute response) and angiogenesis (long-term response) [169,170]. In the ccRCC tumors lacking functional pVHL, the HIFα is constantly active even under normoxia, resulting in tumor angiogenesis, metabolic reprogramming, cell proliferation, EMT induction, and so on (**Fig. 1.6**) [3,35,46].

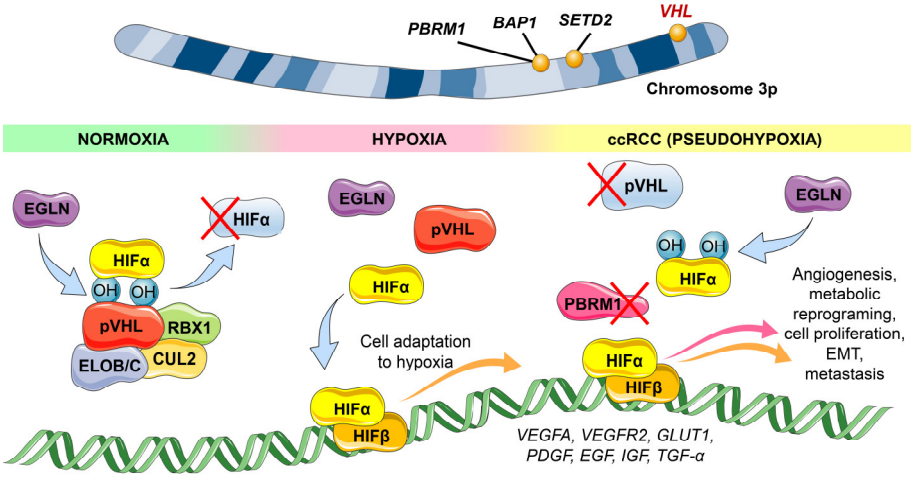

Fig. 1.6. The arrangement of frequently in ccRCC mutated gene on chromosome 3p and VHL-HIFα signaling cascade. At normoxia, the EGLN catalyzes the hydroxylation of HIFα transcription factors. Hydroxylated HIFα is recognized by the pVHL, conducting ubiquitination of HIFα leading to proteasomal degradation. Under hypoxia, HIFα is no longer hydroxylated and form the complex with HIFβ in the nucleus to induce the expression of genes required for cell adaptation to hypoxia. In ccRCCs, lacking VHL, hydroxylated HIFα is no longer destined for proteasomal degradation and translocate to the nucleus, initiating expression angiogenesis, cell proliferation, transformation, and metastasis-related genes. In the case of mutated *PBRM1*, this hypoxic response is even enhanced. (Adapted from [35]).

Among the HIFα induced genes, the endothelial growth factor (VEGF) family genes are the most widely studied. The VEGF-A protein, a member of the VEGF family, activates the VEGF receptor 2 (VEGFR2), located on the endothelial cells, which causes the process of angiogenesis, ensuring the supply of oxygen and nutrients to the tumor cells explaining the highly vascular ccRCC tumors phenotype [171,172]. The VEGFR2 is expressed on the cancer cells as well, and its activation leads to the induction of ERK1/2, AKT, MAPK, and Src kinases, which through a cascade of phosphorylation events, drive further tumor development and metastasis [171]. Besides, HIFα

induces expression of various other growth factors (PDGF, EGF, IGF, TGF-α), who thought interaction with appropriate tyrosine kinase receptors further enhance tumor growth and progression [173]. Moreover, HIFα may induce activation of nuclear factor kappa B (NF-κB) that regulate expression of EMT-related transcription factors, particularly ZEB2 and SNAI1, which thought repression of epithelial marker E-cadherin (CDH1), contribute to EMT initiation [174]. Furthermore, HIFα may directly induce these transcription factors and enhance EMT [175,176], playing an essential role in ccRCC development.

Activation of HIFα also leads to the rapid reorganization of the central metabolic pathways in ccRCC, including the reduction of oxidative phosphorylation and increment of aerobic glycolysis ("Warburg effect"), fatty acid, and glycogen synthesis leading to lipids and glycogen accumulation [177-179]. Such metabolic shifts are observed in many cancer cells and confer the capacity to meet bioenergetic demands such as uncontrolled proliferation and the acquisition of other hallmark traits of cancer, described by Hanahan and Weinberg [180,181]. However, renal cancer is one of the most studied and perhaps the exemplar of malignancies characterized by metabolic reprograming [182,183] and is labeled a metabolic disease [184-186]. Specifically, increased levels of HIFα lead to the induction of glucose transporters (GLUT-1) that even enhanced the Warburg effect in ccRCC cells [187]. In addition, altered levels of various enzymes directly or indirectly participating in the TCA (tricarboxylic acid) cycle are also observed in ccRCC [182,183,188,189]. Together these metabolic alterations promote the accumulation of various oncometabolite, which, mainly via epigenetic dysregulation, further enhance kidney tissue carcinogenesis [190-194].

Independently of HIFα, pVHL also assists the regulation of the WNT/β-catenin signaling pathway, playing an essential role in kidney development, injury repair, and tumorigenesis [195,196]. In the presence of WNT activating ligands, WNT binds to its receptor complex (Frizzled receptor and LRPs), which prevents β-catenin from degradation. This ensures β-catenin translocation to the nucleus, where its promotes transcription of various genes, including (proto)oncogenes *MYC* and *CCND1* (cyclin D), stimulating tumourigenesis [197]. Meanwhile, in the absence of WNT ligands, β-catenin is phosphorylated by glycogen synthase kinase-β (GSK-β) and targeted for degradation through further ubiquitylation by the complex of Jade family protein JADE-1 and pVHL [195]. Thus, in the absence of pVHL, β-catenin can't be targeted for degradation, which also promotes renal cancer progression.

Although mutated VHL deregulates various pathways related to the ccRCC development, VHL loss alone cannot induce renal epithelium cancerogenesis [198], and additional genetic or epigenetic events are needed. As it is mentioned previously, the most prevalent genetic event is the mutations in tumor suppressor genes, namely *PBRM1*, *SETD2*, and *BAP1*.

PBRM1 (encoding a component of the SWI/SNF-B chromatin remodeling complex) is a frequently mutated gene in ccRCC (40%), and it is likely to be a tumor suppressor through the involvement in the cellular senescence, genome stability, and coordination of DNA repair [199-201]. PBRM1 protein contributes to the controlling of DNA accessibility for transcription and regulates the expression of various genes, for example, encoding cell adhesion and cell signaling molecules [201-204]. Besides the role in transcriptional regulation, PBRM1 prevents tumorigenesis by promoting centromeric cohesion and genome stability [201]. Most *PBRM1* mutations are inactivating, and loss of its expression promotes ccRCC cell proliferation and migration [162] and enhances the HIFα-response [205]. Thus, PBRM1 is likely to play essential roles in frequently dysregulated cancer pathways and maintain genomic integrity, which is a barrier to tumorigenicity [206].

SETD2 encodes histone methyltransferase acting as tumor suppressor gene [207,208]. As in the case of PBRM1, SETD2 controls cellular senescence and participates in the maintenance of genome integrity through nucleosome stabilization, suppression of replication stress, and the coordination of DNA repair [209-213]. Specifically, SETD2 trimethylates the histone H3K36, leading to the open heterochromatin formation and reduction of DNA methylation [214-216]. Meanwhile, mutated *SETD2* is associated with increased genome instability, possibly through decreased DNA methylation at non-promoter regions [214-216].

BAP1 encodes the deubiquitinating enzyme associated with multiple protein complexes included BRCA1 (breast cancer type 1 susceptibility protein) and BRAD1 (BRCA1 associated RING domain protein 1), regulating DNA damage response, cell cycle, and apoptosis [217-219]. In addition, BAP1 also contributes to chromosome stability by binding the proteins essential for spindle assembly [220]. Interestingly, BAP1 does not promote tumorigenesis by accelerating cell growth but allows a slow and tolerant G1/S cell cycle checkpoint, leading to slower but uncontrolled tumor growth [163,221].

Almost all mutations involving *PBRM1*, *SETD2,* and *BAP1* are found in a subset of *VHL*-inactivated cells [157], and according to the recently proposed model, *PBRM1* is the second driver event in renal tumorigenesis after the loss of *VHL* [222]. Meanwhile, *SETD2* and *BAP1* mutations are likely to occur in

the pre-existing *VHL* and/or *PBRM1* mutated clones and contribute to tumor progression [157]. This is confirmed by the subsequent studies, demonstrating the association of mutated *SETD2* and *BAP1* but not *VHL* and *PBRM1* with worse survival of ccRCC patients, suggesting that *VHL* and *PBRM1* are implicated in the tumor initiation. At the same time, *SETD2* and *BAP1* contribute to further disease progression [223,224,225].

1.2.2. Other common genetic alterations and affected pathways

A comprehensive molecular analysis of primary ccRCC samples, as a part of The Cancer Genome Atlas (TCGA) project, revealed an infrequent number of somatic mutations in these tumors, with the nine most prevalent genes, including above mentioned *VHL*, *PBRM1*, *SETD2*, *BAP1* and five additional, namely *KDM5C*, *PTEN*, *MTOR*, *TP53* and *PIK3CA* [156]. While some later studies emphasized a few other genetic alterations in the genes related to chromatin remodeling complexes, PI3K-mTOR signaling, p53, and cell cycle signaling pathways [157, 223].

Clear cell renal carcinoma is exceptional from other cancers according to the widespread mutations in chromatin remodeling genes established in 69% of ccRCC with the predominance of SWI/SNF complex members [157,223]. Without previously described mutations in *PBRM1*, *SETD2,* and *BAP1*, inactivation of *KDM5C* and *KDM6A* encoding lysine-specific histone demethylases were also observed in 13% of ccRCC cases [223]. *KDM5C* is one of the HIFα target genes and is considered a tumor suppressor since its overexpression suppressed the global gene transcription and retarded tumor growth [226,227]. These lysin demethylases also contribute to heterochromatin maintenance. The ccRCC tumors harboring mutated *KDM5C* are characterized by heterochromatin disruption, genomic instability, and poor disease prognosis [228]. Considering the wide variety of other mutated chromatin remodeling genes (e.g., *ARID1A*, *SMARCA4*, *MLL3*, *ASXL1*, *EP300*, *CREBBP*), it is becoming evident that chromatin modifications and epigenetic reprogramming have great importance in renal tissue carcinogenesis.

The phosphoinositide 3-kinase (PI3K) and mechanistic target of rapamycin (mTOR) signaling pathway is activated by various lesions and affects cell growth, proliferation, migration, metabolism, and survival [156,157,229]. Due to the widely observed gain of chromosome 5q, harboring the *FGFR4* (fibroblast growth factor receptor 4) gene, encoding PI3K inducing receptor, this pathway is altered in up to 78% of ccRCC [157]. Among the principal players of this pathway, *MTOR* is the most commonly mutated gene observed

in 6-7% of cases [156,223], and patients carrying this mutation display a better response from rapalogs (mTOR-targeted) treatment [230], widely used for metastatic ccRCC. Catalytic subunit of PI3K encoding gene *PIK3CA* is mutated in 3-5% of ccRCC, while mutation of tumor suppressor gene *PTEN*, the most critical negative regulator of PI3K, observed in 2-4% of cases [156,157,229]. Patients with PTEN-mutant tumors were more prone to distant metastasis and recurrence of disease with worse survival [231,232].

Various genetic alterations in genes involved in cell cycle control were observed in 40% of ccRCC [157]. These alterations comprise gain of oncogene *MYC* (23%), deletion of tumor suppressor gene *CDKN2A* (cyclin-dependent kinase inhibitor 2A; 16%), and mutations in several other genes with the most prevalent of *TP53* (up to 3%) correlating with decreased survival in ccRCC [157,223].

1.2.3. Cancer evolution and tumor heterogeneity

The recent studies analyzing multiregional and sequential tumor samples by genome-wide mutation analyses provided much higher frequencies of driver mutations in ccRCC tumors, suggesting high heterogeneity of such tumors, which is overlooked in the single biopsy studies [6-9,233]. Furthermore, those studies underlined the loss of chromosome 3p and *VHL* as a trunk initiating event in ccRCC and that these tumors often display branched evolution. Branched evolution means that the different regions of the tumors display significant variations in their mutational signature, and even 73-75% of driver alterations were found to be subclonal [7]. Moreover, parallel evolution has been observed whereby genomically distinct but functionally equivalent alterations occur within the different tumor regions. In addition, several studies noted the convergence of genetic characteristics [234-236]. According to this, mutations in genes occur at different time points but lead to a similar overall genomic and phenotypic profile.

In the recent study, Turajilic *et al*. [8,9] described seven distinct evolutionary subtypes of ccRCC, characterized by the different degrees of intratumor heterogeneity (ITH) and genomic instability (GI). The lowest ITH and GI was established in the subtype consisted of the *VHL* as a lone mutational driver, displaying limited branching and a monoclonal structure. Intermediate ITH was determined in five other subtypes, characterized by moderate to high GI. The first subtype consists of tumors with multiple clonal drivers (≥2 clonal mutations in *BAP1*, *PBRM1*, *SETD2,* or *PTEN*). A second subtype comprises cases with *BAP1* as a lone mutational driver in addition to *VHL.* The third subtype consisted of *VHL*-wild type tumors with sarcomatoid

differentiation. The fourth and fifth subtypes were *PBRM1* → *PI3K* and *PBRM1* → SCNA (somatic copy number alterations), characterized by the early *PBRM1* mutation followed by activation of PI3K-mTOR pathway or subclonal SCNAs, respectively, enriched for lower grade tumors. And the final evolutionary subtype, namely *PBRM1* → *SETD2* driven, is characterized by extremely high ITH (about ten clones per tumor), frequent parallel evolution events, and advanced disease stage.

From the clinical perspective, such a variety of evolutionary subtypes may contribute to the distinct course of the disease and heterogenous clinical outcomes observed in ccRCC patients [57,58]. For example, Turajilic *et al*. [8,9] established that tumors with low ITH and high GI were more likely to progress rapidly and widely, suggesting the presence of occult metastases at diagnosis. In contrast, heterogeneous tumors with or without high GI were more likely to have an attenuated progression pattern, often with solitary metastasis. Particularly, multiple clonal drivers, *VHL*-wild-type and *BAP1* driven evolutionary subtypes, were attributed to rapidly progressing tumors, while *PBRM1* → *SETD2* and *PBRM1* → *PI3K* were characterized by attenuated progression. In addition, *VHL* mono-driver tumors were presented at an early stage (mean tumor size 45 mm), suggesting they may be an early evolutionary ancestor for the more complex subtypes.

The analysis of metastatic ccRCC showed that metastatic sites are more homogenous and harbor fewer driver somatic alterations than the primary tumor. Only 5.4% of driver events were found to be *de novo* in metastases [9]. Hence, most genetic alterations accumulate in the primary tumor, serving as a substrate for selecting metastasis-competent subclones.

To sum up, in clinical practice, such heterogeneity and a wide variety of evolutionary subtypes complicate precision medicine because tumor biopsies may not represent the overall spectrum of genetic alterations required for selecting treatment regimens. Moreover, such tumor heterogeneity may explain the difficulties in the validation of new oncology biomarkers. Thus, other sources to fulfill these objectives are needed.

1.3. Aberrant DNA methylation and renal clear cell carcinoma

Epigenetic modifications are reversible and heritable changes in gene expression without alterations in the primary DNA sequence. Epigenetic phenomena encompass histone modifications, DNA methylation, and non-coding RNA. DNA methylation in mammalian cells is characterized by the addition of a methyl group (-CH3) at the carbon-5 position of cytosine residues in the context of CpG dinucleotides through the action of DNA

methyltransferase (DNMTs) enzymes, forming 5-methylcytosine (5mC). It is the most widely studied epigenetic mechanism, responsible for the various biological processes, including normal development of mammals, differentiation, and regulation of gene expression [237]. There are approximately 28 million CpG sites in the genome, but these are not evenly distributed. About a half of CpG dinucleotides tend to concentrate into short CpG-rich regions, called CpG islands, located near gene transcription start site and span the promoters or other regulatory sequences (e.g., enhancers). Such CpG island-associated genes are either actively transcribed or poised for transcription [238]. While another part of CpGs are scattered individually within repetitive genome sequences [238]. Promoter CpG islands in normal cells generally remain unmethylated/hypomethylated and are associated with active gene expression during differentiation. On the contrary, CpGs within repetitive sequences are hypermethylated and associated with the repression of such regions and maintenance of genome stability [237].

The presence of methyl groups in specific DNA regions is carried out by DNMTs (DNMT1, DNMT3A, and DNMT3B), which are frequently overexpressed in various malignancies [239]. The expression of DNMTs is also promoted by HIF1α [240], which is relevant for ccRCC. Proteins containing methyl-CpG binding domains (MeCP2, MBD2, and MBD3) or C2H2 zinc fingers (e.g., ZBTB4, ZBTB33, ZBTB38) recognize methylated DNA and determine its transcriptional silencing [238]. For example, MBDs recruit histone deacetylases (related to transcriptional repression) to the methylated promoter, which induces chromatin condensation, making the DNA inaccessible for transcription leading to gene silencing [239].

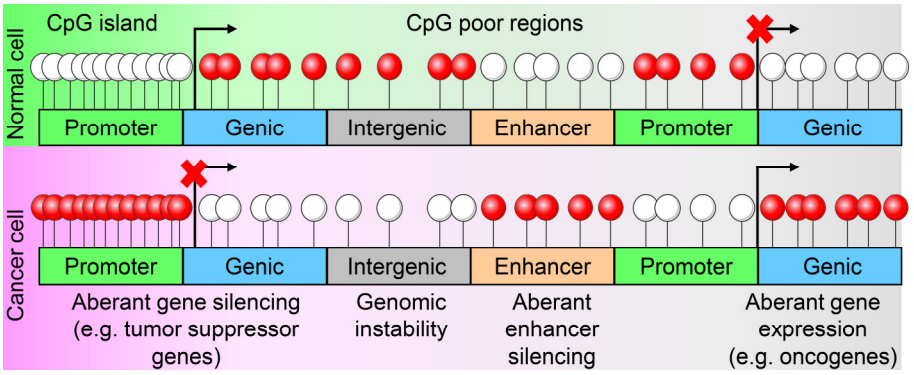

Fig. 1.7. The schematic pattern of DNA methylation in the normal and cancer cells. (Adapted from [237]). The white circles represent unmethylated CpG sites, while red circles – methylated CpG.

Normal epigenetic processes, including genome-wide changes in DNA methylation patterns, are disrupted during the initiation and progression of cancer [241,242]. Hypermethylation of the CpG islands is a common event in various cancer types, including kidney cancer, and is often associated with the silencing of tumor suppressor genes and their regulated signaling pathways (**Fig. 1.7**) [237,243]. Besides, enrichment of aberrant enhancers methylation is related to transcriptional alterations as well and, in the case of RCC, has important clinical significance [244]. On the contrary, DNA methylation in repetitive regions of various cancers is decreased and leads to genomic instability and activation of oncogenes [245].

The importance of epigenetic aberrations for ccRCC development is aptly illustrated by the common genomic alterations in genes encoding histones and chromatin modifiers, influencing DNA methylation changes. Among the most frequent RCC subtypes, ccRCC is characterized by the most prevalent DNA hypermethylation events with more than 200 hypermethylated CpG islands [156,223]. Aberrations in DNA methylation occur early during cancer development and, in the case of ccRCC, are observable even in the precancerous stage [10,246] with increasing promoter hypermethylation frequencies in higher stage and grade tumors [156]. Hence, DNA methylation could be precious clinical cancer biomarkers for early disease diagnosis and prognosis, considering the relatively infrequent number of somatic mutations and asymptomatic course of the disease (**Fig. 1.8**).

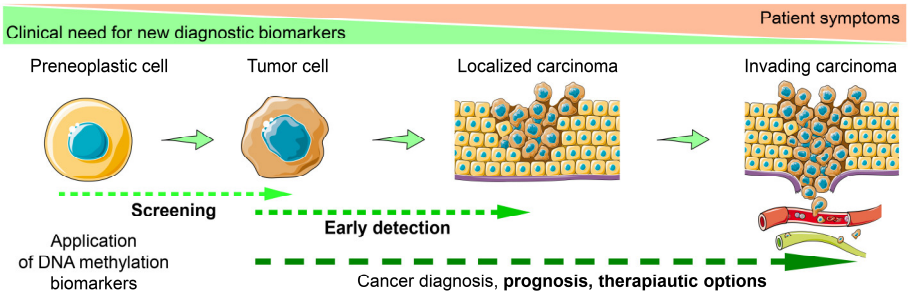

Fig. 1.8. The need and applicability of DNA methylation biomarkers in cancer detection, diagnosis, and prognosis. (Adapted from [247]).

DNA methylation has several additional superiorities over other commonly used biomarkers. For example, compared to mRNA or protein-based biomarkers, DNA methylation is much more stable. It can withstand harsh conditions for an extended period of time. In addition, DNA can be amplified and thus increase sensitivity, allowing the detection of such biomarkers on limited amounts and quality samples. Moreover, as a single

biopsy of ccRCC does not reflect the whole spectrum of (epi)genetic alterations [9], the applicability of DNA methylation-based biomarkers to a wide variety of clinical samples, particularly body fluids, bypasses the tumor heterogeneity-caused difficulties to validate new oncology biomarkers. Finally, DNA methylation is easily detectable in body fluids by conventional and inexpensive qualitative or quantitative PCR methods. All these features make DNA methylation particularly attractive for searching ccRCC biomarkers with the ability to use in clinical practice.

1.3.1. Frequently methylated genes and dysregulated pathways

Until today, most DNA methylation studies of ccRCC have focused on the selection of candidate biomarkers. These studies described plenty of hypermethylated genes affecting various cancer hallmarks, including cell cycle regulation (*CDKN2A/P16*, *CDKN2A/P16, RASSF1*), apoptosis (*DAPK1*, *APAF1*), invasion and metabolism (*GSTP1*, *CDO1*). In addition to cancer hallmarks, several signaling pathways important for ccRCC development are affected by DNA methylation, such as VHL-HIF and angiogenesis, cell adhesion, and EMT as well as WNT/β-catenin signaling pathway. These pathways form a complex network contributing to RCC cancerogenesis [248].

Dysregulation of the VHL-HIF signaling pathway in ccRCC is observed not only due to genetic alterations (described above), but promoter methylation-mediated inactivation of *VHL* occurs in up to 30% of cases as well (**Table 1.3**). In addition, other tumor angiogenesis regulating gene *GREM1*, encoding gremlin 1, which directly binds to the VEGF receptor, is frequently methylated in ccRCC. The inactivation of *GREM1* is interpreted by immature and unstable tumor vasculature formation, which facilitates an escape of tumor cells into the circulation leading to the development of cancer metastasis [249]. By contrast, *TIMP3* encoding tissue inhibitor of metalloproteinase 3 blocks the binding of VEGF to VEGFR2 and inhibits angiogenesis [250], and is frequently methylated in RCC. Besides, it also inhibits matrix metalloproteinases (MMPs), a crucial mediator of cancer EMT influencing invasiveness and metastasis by proteolysis of extracellular matrix [250,251]; therefore, inactivation of *TIMP3* enable metastatic spread as well.

Epithelial-mesenchymal transition related to both cancer initiation and progression to metastatic disease is also widely deregulated by DNA methylation events. *CDH1* encoding E-cadherin, required to preserve renal epithelial morphology [291], is frequently inactivated by methylation in ccRCC (**Table 1.3**). Protocadherins family member *PCDH8*, encoding

adhesion protein, necessary for the maintenance of epithelial phenotype as well [292], is also frequently silenced by methylation in ccRCC (58-68%) and correlated with poor patients survival [293]. EMT signaling might be further enhanced by promoter methylation of *FBN2* (fibrillin 2), considered the most common epigenetic mark in RCC [293]. Fibrillin-2 is an extracellular matrix protein, interrupting EMT induction by sequestration of transforming growth factor-β (TGF-β), a well-known inducer of EMT; thus, methylation of *FBN2* increased RCC tumorigenicity [270]. Another TGF-β superfamily protein, BMPs (bone morphogenic proteins), are characterized by the suppression of EMT [294], and their expression in RCC is also reduced by promoter methylation. Other genes involved in cell adhesion, invasion, and EMT are also frequently methylated in RCC (**Table 1.3**).

Table 1.3. Promoter methylation frequencies of commonly studied genes by targeted approach in primary RCC (mostly ccRCC) tumors.

Signaling pathway	Genes	Methylation frequency*	Type of biomarker	References
VHL–HIF, angiogenesis	*VHL*	4–31%	D	[14,252-263]
	GREM1	20–55%	Pg	[256,164-266]
	TIMP3	19–71%	D	[14,15,253,267, 269]
EMT, cell adhesion, motility and invasion	*CST6*	0–46%	Pg	[264,265]
	FBN2	21–34%	-	[270,271]
	CDH1	11–83%	D	[15,253,267]
	PCDH8	58–68%	Pg	[270,272]
	LAD1	27–35%	Pg	[256,265]
	NEFH	28–63%	Pg	[256,265,273]
	BMP2	48–83%	Pg	[265,274]
	NEURL	41–47%	Pg	[256,265]
WNT signaling	*SFRP1*	19–68%	D and Pg	[256,264,275-277]
	DKK1/3	50–52%	D and Pg	[275,278]
Cell cycle, growth, proliferation and apoptosis	*P14*	0–69%	D	[14,15,253,254,267, 279]
	P16	0–72%	D	[14,15,253-255, 267,268,279-281]
	RASSF1A	23–97%	D and Pg	[14,15,253,254,267, 268, 282-285]
	RARB	2–53%	D	[15,253,267,268]
	PTGS2	10–96%	D	[267,279]
	APC	5–29%	D	[14,15,253,267,268]
	DAPK1	8–64%	Pg	[279,286-289]
	APAF1	41–100%	Pg	[286-289]
Metabolism	*CDO1*	38–40%	Pg	[256,290]

*Only studies that analyzed ≥20 RCC tissue samples and genes with a methylation frequency of ≥15% are included. D – diagnostic, Pg – prognostic.

The WNT/β-catenin signaling pathway is frequently disturbed in ccRCC by promoter methylation of various pathway inhibitors that increase the tumorigenicity of renal cells as well [295]. Two classes of inhibitors protein regulate the WNT/β-catenin pathway, including secreted frizzled-related proteins (SFRPs), which bind directly to WNT and suppress downstream signaling, and the Dickkopf-related proteins (DKK) as well as insulin-like growth factor binding proteins (IGFBP), which bind to other receptor complex component (Frizzled receptor and LRPs) [296]. Frequent promoter methylation of these proteins encoding genes is observed in RCC, and analysis of TCGA data identified *SFRP1* methylation as a marker of poor patient survival [293].

Through decades of reports have suggested the described methylated genes in RCC as the candidates for diagnostic and prognostic biomarkers, no marker has reached the clinic yet. Meanwhile, DNA methylation-based tests for the diagnosis and/or prognosis of other urological cancers such as prostate (ConfirmMDx) and bladder (AssureMDx) cancer [13] are commercially available long before and even have been included in EAU (European Association of Urology) Guidelines. Considering the highest mortality rate of renal cancer among all urinary system neoplasms, this stimulates the search for novel biomarkers with better performance.

1.3.2. Methylome of ccRCC and identification of novel biomarkers

Most of the above-described studies based their biomarkers selection procedure on literature reporting on methylated biomarkers in several other cancer types, whereas only a few studies based their biomarkers selection on genome-wide DNA methylation or RNR expression data, thereby focusing on the identification of cancer type-specific candidate biomarkers. The advent of high throughput technologies encompassing the whole genome has enabled genome-wide analysis of DNA modifications and led to new insights into epigenomic profiles of ccRCC.

The TCGA project analysis of DNA methylation profile in ccRCC revealed three distinct clusters that were characterized by different DNA methylation levels, including clusters with high, intermediate, and low methylation levels, determined using a total of 1288 differentially methylated genes [157]. Another independent study also observed a similar methylation pattern, oriented to promoter methylome of small renal masses (≤ 4 cm tumors) [297]. In contrast, other studies based on promoter CpGs methylation revealed only two clusters with high and low methylation levels [298,59]. The cluster with high methylation was also characterized by a higher number of

somatic mutations, especially *SETD2* and *BAP1,* and other genetic alterations, like loss of 3p, 9p, 14q, etc. [157, 223]. Increased hypermethylation was also associated with various adverse clinical-pathological parameters and increased probability of metastasis, and decreased patient survival [59,157,223,298].

Table 1.4. Several novel putative DNA methylation biomarkers of renal cell carcinoma identified by genome-wide methylation analysis and validated in at least one cohort.

Selection + validation methods	Gene symbol	Gene name	Type of biomarker	Ref.
*HM450 + PSQ	*ZNF278*	Zinc finger protein 278	Pg	[299]
	FAM155A	Family with sequence similarity 155, member A	Pg	
	DPP6	Dipeptidyl peptidase like 6	Pg	
*HM450 + PSQ	*ZNF492*	Zinc finger protein 492	Pg	[300]
	GPR149	G protein-coupled receptor 149	Pg	
*Microarrays + BSQ	*HOXA5*	Homeobox A5	NA	[301]
	MSH2	MutS homolog 2	NA	
HM27 + COBRA	*SLC34A2*	Solute carrier family 34 member 2	NA	[271]
	TM6SF1	Transmembrane 6 superfamily member 1	NA	
	COL1A2	Collagen type I alpha 2 chain	NA	
	OVOL1	Ovo like transcriptional repressor 1	NA	
	TMPRSS2	Transmembrane serine protease 2	NA	
	DLEC1	DLEC1 cilia and flagella associated protein	NA	
	SST	Somatostatin	NA	
	BMP4	Bone morphogenetic protein 4	NA	
HM27 + BSQ/PSQ/ QMSP	*GRIK1*	Glutamate ionotropic receptor kainate type subunit 1	NA	[297]
	CHODL	Chondrolectin	NA	
	BCAN	Brevican	NA	
	ZNF177	Zinc finger protein 177	NA	
	ATP2A3	ATPase sarcoplasmic reticulum Ca2+ transporting 3	NA	
	OXR1	Oxidation resistance 1	NA	

*Studies included ccRCC subtype only. HM450/HM27 – Illumina Infinium HumanMethylation 450/27K BeadChip; COBRA – Combined Bisulfite Restriction Analysis; QMSP – quantitative methylation-specific PCR; PSQ – pyrosequencing; BSQ – bisulfite sequencing; Pg – prognostic; NA – not available.

According to another TCGA data analysis, different DNA methylation subgroups were found in the tumors with the same clinical stage and grade and *vice versa*; tumors with distinct stages and grades may share the same DNA methylation characteristics [11]. The study revealed that DNA methylation status represents a more elaborate classification analysis for RCC than clinical-pathological parameters. DNA methylation profiles can help understand the etiology of RCC. Most importantly, they demonstrated clinically applicable biomarkers for use in the early stages of kidney cancer detection and/or prognosis.

Genome-wide DNA methylation studies have produced a considerable amount of novel candidate ccRCC biomarkers (**Table 1.4**) and significantly increased the knowledge of epigenetic changes in renal cell carcinoma. However, most of the recently published studies used relatively small and heterogeneous (comprising various cancer subtypes) RCC sample cohorts for the validation of putative biomarkers or lack this analysis step at all, and only a few reports stated the selected genes as prognostic markers with a lack of diagnostic ones. Therefore further attempts are needed in order to choose novel diagnostic and/or prognostic DNA methylation biomarkers for ccRCC.

1.3.3. DNA methylation biomarkers in urine

To date, "liquid biopsy" is emerging as a revolutionary tool in cancer care, allowing analysis of genetic material, such as proteins, tumor cells, or cell-free DNA shed from primary or metastatic tumors into bodily fluids for non-invasive cancer detection or prognosis. Renal cell carcinoma-derived methylated DNA is easily detectable in body fluids, such as urine [14-19], serum [15,275,302,303] or plasma [304,305]. This potentially allows for the development of non-invasive molecular tests, which alone or in combination with imagining, could transform clinical management by enabling early detection of renal cancer and reducing unnecessary kidney biopsies and nephrectomies [20].

For urological cancers, including renal cancer, urine is, in many situations, the preferred "liquid biopsy" source containing both exfoliated tumor cells and cell-free tumor DNA and can be obtained easily, non-invasively, and repeatedly [306]. Furthermore, as ccRCC is considered to be a heterogeneous malignancy with high intra-tumor and inter-tumor heterogeneity that complicates diagnosis and prediction of the course of the disease, DNA methylation in urine bypasses this situation, providing a better reflection of tumor heterogeneity compared to the tissue sample. In addition, due to the easily available repeatability of the sample acquisition, urine-based

biomarkers can be checked periodically in patients at risk, allowing the detection of small tumors at an early stage or following the real-time state of the cancer progression. Despite these advantages, no clinically validated non-invasive DNA methylation biomarkers exist for RCC detection.

Table 1.5. Urinary DNA methylation biomarkers for the detection of RCC.

The size of investigated cohorts		Method	Biomarker	DSe, %	DSp, %	Ref.
Cancer	Control					
50 (35 ccRCC, 6 pRCC, 2 chRCC, 7 other (sub)types)	12 (healthy individuals)	MSP	*VHL*	12	100	[14]
			P16	8	100	
			P14	18	100	
			APC	16	100	
			RASSF1A	50	100	
			TIMP3	52	100	
			Panel of all biomarkers	90	100	
26 RCC (23 ccRCC, 1 pRCC, 1 chRCC, 1 other type)	91 (various diseases)	QMSP	*APC*	38	96	[15]
			P14	31	100	
			CDH1	38	95	
			GSTP1	15	100	
			MGMT	8	100	
			P16	35	100	
			RARB2	31	91	
			RASSF1A	65	89	
			TIMP3	46	91	
			Panel of all biomarkers	88	-	
19 RCC (not specified)	20 (not specified)	QMSP	*GDF15*	5	100	[16]
			HSPA2	11	100	
			TMEFF2	11	100	
			VIM	5	100	
50 RCC (not specified)	48 (healthy individuals)	QMSP	*TCF21*	28	100	[17]
			PCDH17	10	100	
			Panel of both biomarkers	32	100	
15 RCC (not specified)	15 (healthy individuals)	PSQ	*TCF2L*	79	100	[18]
53/171 ccRCC	57/86 (healthy individuals)	QMSP	MicroRNA 30a-5p*	83/63	53/67	[19]

RCC – renal cell carcinoma; ccRCC – clear cell RCC; pRCC – papillary RCC; chRCC – chromophobe RCC; MSP – methylation-specific PCR; QMSP – quantitative MSP; PSQ – pyrosequencing. *Stated as a prognostic biomarker.

Six studies analyzed urinary DNA methylation biomarkers for renal cell carcinoma detection encompassing 17 different biomarkers (**Table 1.5**). The sensitivities (proportion of patients with RCC positive for biomarker) of single biomarkers vary between 5% and 83%; however, specificities (probability of negative test results in individuals without cancer) were generally high, reaching >90% in most cases. Two first studies by Battagli *et al.* [14] and Hoque *et al.* [15] analyzed methylated DNA of well-known tumor suppressor genes and the methylations frequencies of *APC*, *P14*, *P16,* and *RASSF1A* were considerably higher in the latter study, while specificities were less varied. As discussed by Larsen *et al*. [306], the varying sensitivity is most probably affected by the variability in the pathology as larger tumors will shed more material than smaller ones and studies having a higher proportion of advanced cancers, achieving higher sensitivity. *TCF21* is another biomarker tested in more than one study; both of them achieved 100% of specificity, but the sensitivity varied from 28% to 79 %.

In order to overcome the low sensitivities of a single biomarker test, methylation of various gene panels has been evaluated in three studies. The best performing combination consisting of *VHL*, *P16*, *P14*, *APC,* and *TIMP3* achieved a sensitivity of 90 % and specificity of 100%. A similar sensitivity (88%) was reported by combining nine biomarkers, particularly *APC*, *P14*, *CDH1*, *GSTP1*, *MGMT*, *P16*, *RARB*, *RASSF1A*, *TIMP3*, with no indication of specificity. In contrast, a panel of *TCF21* and *PCDH17* reached a sensitivity of 32% only.

To date, only one study has identified prognostic ccRCC biomarkers in urine. Outeiro-Pinho *et al*. [19] found that methylation of the *mir-30a* gene in the urine sediments remarkably discriminated patients with metastasis from those without metastatic disease with 80% of sensitivity and 71% of specificity. Besides, this is the only study that included a considerable amount (>200 of samples) of homogenous (ccRCC only) cases, while other studies conducted their analysis in much smaller (≤50 of samples) and heterogeneous cohorts. Thus, despite high diagnostic parameters observed for gene panels, none of them are commercially available to date, and further thorough studies are needed in this field.

2. STUDY COHORTS AND METHODS

2.1. Patients and samples

Approval from the Lithuanian Bioethics Committee (Nr. 158200-18/12-1077-585) was obtained, and all patients gave informed consent for participation.

Retrospectively recruited patient cohorts were available for this study. Human kidney tissue samples from 123 patients primarily diagnosed with ccRCC who underwent partial or radical nephrectomy without any neoadjuvant therapy at the Urology Centre of Vilnius University Hospital "Santaros Klinikos" (Lithuania) were collected between 2013 and 2016. Noncancerous renal tissue (NRT) samples were available from 51 ccRCC patients as a control group and were collected as described previously [307]. From that sample collection, 11 pairs of ccRCC and morphologically normal tissue were used for DNA methylation microarray analysis, 4 pairs of ccRCC and NRT for mRNA expression microarray analysis, while 123 ccRCC and 45 NRT for the validation. All tissues were sampled and evaluated by an expert pathologist at the National Center of Pathology (NCP). Positive surgical margins were obtained in 11 patients, while the remaining cases were negative for surgical margin status. Tumors were categorized based on pathological stage and histological subtype, and nuclear differentiation was graded according to the Fuhrman [67] and World Health Organization/International Society of Urological Pathology [75] grading systems. The overall survival data were available for 87% of patients (107/123) with a median follow-up time of 59 months (range, 1–79 months). Follow-up data for all the cases involved in the study were updated in February 2020.

Urine sediments from voided urine samples were available for all ccRCC patients (N=123) and from an additional 92 age- and sex-matched asymptomatic volunteers named as asymptomatic control (ASC).

All collected demographic and clinical-pathological data of the study subgroups are provided in **Table S1**.

2.2. Sample preparation for nucleic acid extraction

Renal tissue samples were homogenized using liquid nitrogen and cryoPREP™ CP02 Impactor with tissue TUBE TT1 (Covaris, Woburn, MA, USA).

Urine samples were centrifuged at 1000 rpm for 15 min at 4 °C (Hettich Universal 320R Centrifuge, DJB Labcare, Buckinghamshire, United Kingdom) at NCP; then sediments were washed twice with 1× PBS and resuspended in the same buffer for storage at -80 °C until use. Just before the lysis step, about 1.5-2.0 mL of thawed urine sediment samples were washed with 1× PBS one more time and concentrated to ≤100 µL of total sample volume.

2.3. DNA extraction and bisulfite conversion

Homogenized tissue powder and/or urine sediments were treated for up to 18 h at 55 °C with 10-25 µl of proteinase K (Thermo Scientific™, Thermo Fisher Scientific, Wilmington, DE, USA) and 500 µl of lysis buffer, consisting of 50 mM Tris-HCl pH 8.5, 1 mM EDTA, 0.5% Tween-20 (all from Carl Roth, Karlsruhe, Germany) for tissue samples, and 10 mM Tris-HCl pH 8.0, 1% SDS, 75 mM NaCl (all from Carl Roth) for urine samples. DNA was extracted following the standard phenol-chloroform purification and ethanol precipitation protocol.

The concentration and purity of the isolated DNA were evaluated by NanoDrop™ 2000 spectrophotometer (Thermo Scientific™, Thermo Fisher Scientific, Wilmington, DE, USA). DNA integrity of the samples selected for genome-wide DNA methylation profiling was checked electrophoretically (**Fig. 2.1 A**).

For targeted DNA methylation analysis, up to 400 ng of purified DNA were modified with bisulfite, using EZ DNA Methylation™ Kit (Zymo Research, Irvine, CA, USA) according to the manufacturer's protocol, except that the initial incubation of samples was performed at 42 °C for 15 min as better results compared to 37 °C were observed.

2.4. RNA extraction

Total RNA from homogenized tissue powder was isolated with mirVana Kit (Ambion, Thermo Fisher Scientific, Foster City, CA, USA) according to the manufacturer's recommendations. Briefly, tissue samples were treated with 500 µL Lysis/ Binding Buffer for 10 min on ice and 50 µL of miRNA Homogenate (for possible miRNA assays) for an additional 10 min. Total RNA was extracted with 500 µL of acid-phenol: chloroform and purified using the supplied Filter Cartridges. For the elution of total RNA, 100 µL of preheated (95 °C) Elution Solution was used.

The concentration and purity of the isolated total RNA were measured spectrophotometrically with NanoDrop 2000 (Thermo Scientific™). Additionally, the RNA integrity of the samples selected for global mRNA expression analysis was checked electrophoretically.

2.5. Genome-wide DNA methylation profiling

2.5.1. DNA methylation microarrays

The genome-wide DNA methylation profiling of 11 paired ccRCC and NRT samples with thorough clinical-pathological data was performed in order to identify potential ccRCC biomarkers. The samples were processed using the two-color Human DNA Methylation 1×244K Microarrays (Gene Expression Omnibus, GEO, accession identifier GSE166734; https://www.ncbi.nlm.nih.gov/geo/) according to the manufacturer's protocol G4170-90012 v2.3 (Agilent Technologies, Santa Clara, CA, USA). Briefly, 5 µg of purified DNA in 1×PBS was sonicated into fragments of 150-1000 bp in size using Covaris M220 focused-ultrasonicator (Woburn, Massachusetts, USA) (**Fig. 2.1 A**).

For the methylated DNA immunoprecipitation (IP-DNA), 200 µL (~4 µg) of the sonicated sample was mixed with 50 µL of the prepared magnetic beads (DynaBeads Pan Mouse IgG, Invitrogen™, Thermo Fisher Scientific, Carlsbad, CA, USA) labeled with 5-methylcytosine (5-mC) monoclonal antibody 33D3 (Diagenode) and 250 µL of 2×IP buffer, and gently mixed for 18 hours at speed 40 in Stuart tube rotator SB3 (Cole-Parmer, Vernon Hills, IL, USA) at 4 °C. IP-DNA and untreated reference DNA (Ref-DNA) were purified with phenol-chloroform (Carl Roth) using MaXtract High-Density gel-filled tubes (Qiagen, Valencia, CA, USA).

After purification IP-DNA and Ref-DNA were labeled by Cy5 and Cy3 (**Fig. 2.1 B**) using SureTag DNA Labeling kit followed by manufacturer's protocol (Agilent Technologies). The yields of samples and the specific activity of the dyes were evaluated spectrophotometrically. IP-DNA and Ref-DNA of the same sample were mixed and hybridized onto Human DNA Methylation 1×244K microarrays (**Fig. 2.1 C**), design ID023795 (Agilent Technologies), for 40 hours at 65 °C in a rotating hybridization oven (Agilent Technologies). After hybridization, microarrays were washed in a buffer system and scanned with Agilent G4900DA SureScan microarray scanner (Agilent Technologies) (**Fig. 2.1 D-F**).

Feature Extraction software v10.7.3.1 (Agilent Technologies) was used for data extraction from microarray TIFF images. The obtained data were further subjected to quality control, pre-processing, and differential analysis.

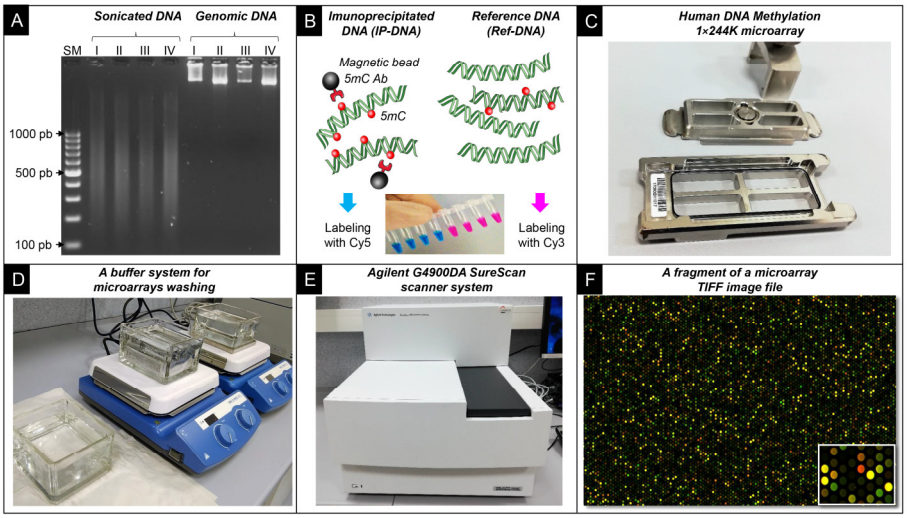

Fig. 2.1. The particular steps of DNA methylation analysis by means of microarrays. A – genomic DNA and sonicated DNA analysis in 3% agarose gel; B – immunoprecipitated methylated DNA and reference DNA samples after labeling; C –microarray slide placed on the hybridization chamber; D – microarray washing in the buffer system after hybridization; E – microarray scanner system Agilent G4900DA SureScan (Agilent Technologies); F – a magnified fragment of a microarray TIFF image file. Abbreviations: SM – DNA size marker GeneRuler 50 bp DNA Ladder (#SM0373, Thermo Scientific); bp – base pair; I-IV – renal tissue DNA samples; 5mC – 5-methylcytosine; Ab – antibody; Cy5/3 – cyanine 5/3 dye.

2.5.2. Microarray data processing and analysis

All calculations were performed with GeneSpring GX v14.9 software (Agilent Technologies), and all microarray datasets were normalized using the same procedure. Saturated, non-uniform, and outlier probe signals were treated as compromised, and probes undetected in at least one sample were removed from the analysis. The signal was filtered on expression (20.0–100.0th) percentile in the raw data, and all samples have values within the range. Normalized log ration (Cy5/Cy3) representing IP-DNA/Ref-DNA was used for further calculations. Probe annotations were uploaded from the SureDesign platform (https://earray.chem.agilent.com/suredesign). For group comparison, fold change (FC) values were estimated, and a paired (if applicable) or unpaired t-test was applied. The resulting P values were

corrected for multiple testing using false discovery rate (FDR). As the stringent filtering, i.e., absolute FC ≥ 1.5 and corrected P-value <0.050, did not yield any significant probes, no multiple testing correction was used. Methylation levels of the particular probes were considered as different if the absolute FC value was ≥1.5 and the non-adjusted P-value was <0.050 for different group comparisons.

2.6. Global gene expression profiling

Global gene expression profiling of 8 renal tissues samples from 4 ccRCC cases and paired NRT samples was performed onto SurePrint G3 Human Gene Expression (v2) 8×60 K microarrays (design ID 072363) according to the manufacturer's protocol G4140-90040 Version 6.9.1 (Agilent Technologies, Santa Clara, CA, USA). The data obtained are publicly available on GEO database (GEO accession identifier GSE168845). Sample processing (100 ng of input RNA) was performed according to One-Color Microarray-Based Gene Expression Analysis Low Input Quick Amp Labeling, version 6.5, a protocol using spike RNA (RNA Spike-In kit) and Low Input Quick Amp Labeling Kit, One-Color (Agilent Technologies). Prepared samples were hybridized at 65 °C for 17 hours. Then, slides were washed using the Gene Expression Wash Buffer Kit and scanned with Agilent G4900DA SureScan microarray scanner (Agilent Technologies).

Raw signal intensities from the obtained TIFF images were extracted and evaluated with Feature Extraction software v10.7.3 and further analyzed using GeneSpring GX v12.6.0 (Agilent Technologies). Probes with saturated, non-uniform, and outlier signal values were removed before further preprocessing. Probes having raw signal values of ≤ 20 were filtered out. Probe annotations were extracted from eArray platform according to the corresponding microarray design identifier. Fold change (FC) values were estimated, and a paired t-test was used for comparing the two groups. Differences in gene expression levels were considered significant if absolute FC was ≥2.0 and P<0.050.

2.7. Gene set enrichment analysis

Gene ontology (GO) and molecular pathways analysis was performed using publicly available GSEA (gene set enrichment analysis) tool and MSigDB v5.2 (Molecular Signatures Database; http://software.broadinstitute.org/gsea). The results were considered significant when the FDR q value was <0.050.

2.8. Targeted methylation analysis by methylation-specific PCR

Bisulfite-modified DNA served as a template for methylation-specific PCR (MSP). The MSP primers for unmethylated and methylated DNA were designed to overlap with the location of the microarray probes (if available) or at least next to that probe using Methyl Primer Express® Software v1.0 (Applied Biosystems™, Thermo Fisher Scientific, Carlsbad, CA, USA) and ordered from Metabion (Martinsried, Germany) (**Table S2**). The reaction mix of MSP (25 µl in total) consisted of 1× PCR Gold Buffer, 2.5 mM MgCl2, 0.4 mM of each dNTP, 1.25 U AmpliTaq Gold® 360 DNA Polymerase (Applied Biosystems™, Thermo Scientific™), 1 µL of 360 GC Enhancer, 1 µM of each primer, and ~10 ng of the bisulfite-treated DNA. Thermocycling conditions were optimized before the study and consisted of 10 min at 95 °C, 35-38 cycles of 45 s at 95 °C, primer annealing for 45 s at 58-65 °C (**Table S2**).

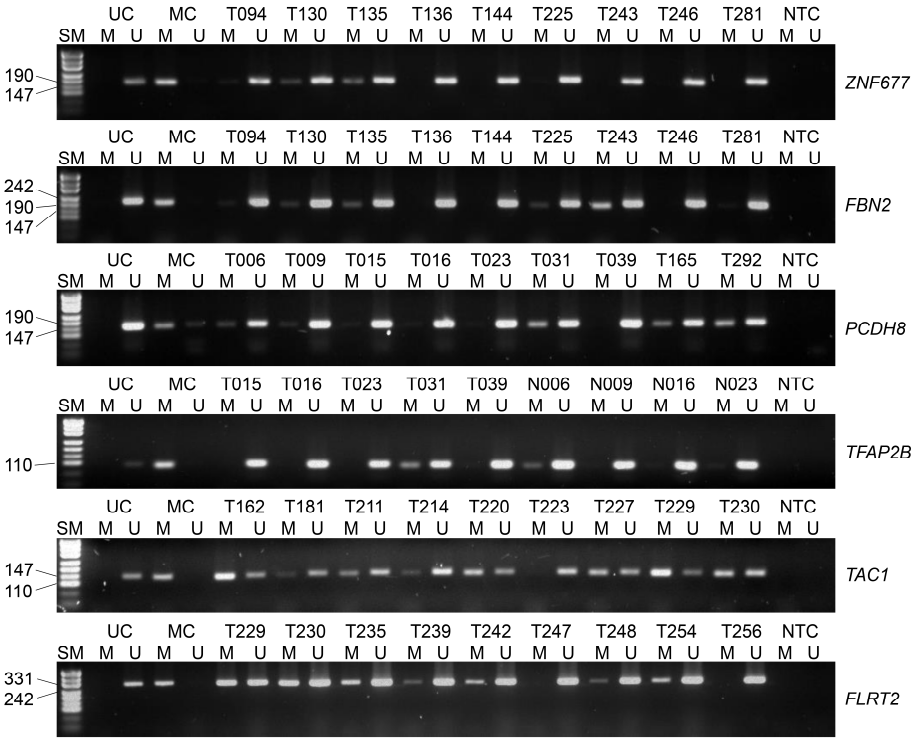

Fig. 2.2. An example of methylation-specific PCR results for several genes. The specific gene is indicated on the right. SM – DNA size marker with fragment lengths (in bp) on the left, UC – unmethylated control, MC – methylated control samples, T000/N000 – samples of renal tumors/non-cancerous tissues, NTC – no template control, M/U – amplification products with primers specific for methylated/unmethylated DNA.

For each primer pair, methylated control (*in vitro* fully methylated human leukocyte DNA, MC), unmethylated control (human leukocyte DNA, UC) and no-template control (NTC) were included in all MSP assays. Amplification products were analyzed in 3% agarose gels with 1X TAE buffer and visualized under UV light after ethidium bromide staining (Carl Roth GmbH, Co., KG). An example of MSP analysis results is provided in **Fig. 2.2**. The individual biomarker was considered as methylated if the amplification product in the sample with primers, specific for methylated DNA, was detected. A biomarker was considered as unmethylated if the amplification product in the sample with primers, specific only for unmethylated DNA, was detected, and there was no amplification product with the primers specific for the methylated DNA. Likewise, the panel of biomarkers was considered as methylated if at least one gene in the particular panel was methylated, and the panel was considered as unmethylated if all genes in the particular panel were unmethylated.

2.9. Quantitative methylation-specific PCR

Quantitative MSP (qMSP) primers specific for methylated DNA for genes *ZNF677*, *FBN2*, *PCDH8*, *TFAP2B*, *TAC1,* and *FLRT2* were designed using Methyl Primer Express® Software v1.0 (Applied Biosystems™, Thermo Fisher Scientific, Carlsbad, CA, USA) and ordered from Metabion (Martinsried, Germany) (**Table S3**). All primers and/or probes overlap at least a fragment of the MSP primers' sequence (**Table S4**). The primers for *ACTB*, which do not overlap with CpG dinucleotides, were selected from the previous study [308] and used in each run to normalize the DNA input.

Each qMSP reaction was performed in triplicates for each set of primers in separate wells. The reaction mix (20 µl in total) consisted of 1×TaqMan® Universal Master Mix II, no UNG (Applied Biosystems™), 300 nM of each primer, 50 nM of the probe, and ~10 ng of 20 bisulfite-converted DNA. All assays were carried out under the following conditions: 95 °C for 10 min followed by 50 cycles of 95 °C for 15 s and 60 °C for 1 min, using the ViiA7 qPCR System (Applied Biosystems™).

The results were generated using QuantStudio Real-Time PCR Software (Thermo Scientific) (**Fig. 2.3**). Only runs wherein MCs provided a positive signal, and the NTC gave no amplification product were considered valid. The background-based threshold algorithm was applied for the estimation of the cycle of quantification (Cq) value. The methylation level of a particular gene was estimated based on the ΔΔCq algorithm and expressed as a percentage of the MC according to **Formula 1**.

$$Methylation\ level, \% = \frac{100\%}{2^{(\boldsymbol{Cq}\ of\ X\ in\ sample\ -\ \boldsymbol{Cq}\ of\ ACTB\ in\ sample)-(\boldsymbol{Cq}\ of\ X\ in\ MC\ -\ \boldsymbol{Cq}\ of\ ACTB\ in\ MC)}}$$

Formula 1. The formula is used for calculating the methylation level of the particular gene (X). The methylation level is expressed in percentage. Cq – cycle of quantification value, MC – methylated (positive) DNA standard (control sample).

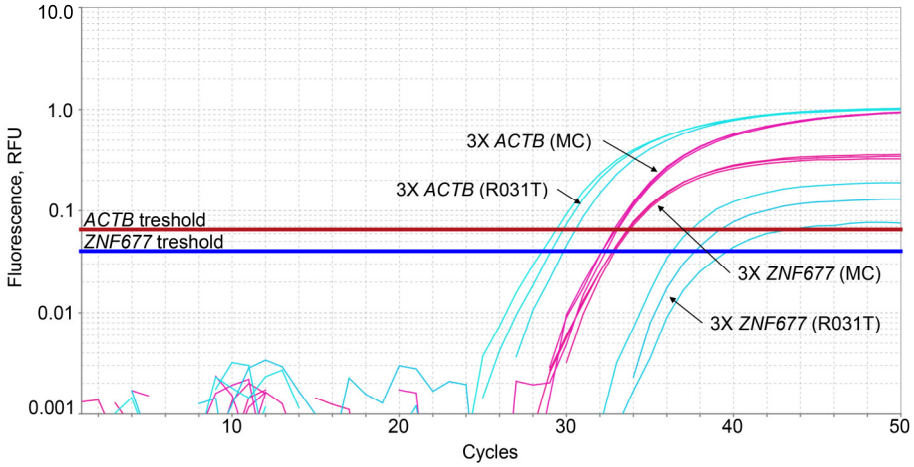

Fig. 2.3. An example of quantitative methylation-specific PCR amplification curves. Methylation of the gene *ZNF677* was analyzed using *ACTB* as an endogenous control in the urine sample (R031T). The baseline-subtracted fluorescence signal is provided in logarithmic scale in relative fluorescence units (RFU). MC – methylated control.

2.10. Gene expression analysis by RT-qPCR

For gene expression analysis by RT-qPCR, up to 100 ng of the RNA were reverse transcribed (RT) using Maxima First Strand cDNA Synthesis Kit with ds DNase according to the recommended protocol (Thermo Fisher Scientific).

Expression of the genes *ZNF677*, *FBN2*, *PCDH8*, *TFAP2B*, *TAC1*, *FLRT2* and endogenous control *HPRT1* was evaluated using TaqMan® Gene Expression Assays (Hs00737026_m1, Hs00266592_m1, Hs00159910_m1, Hs01560931_m1, Hs00243225_m1, Hs00544171_s1 and Hs02800695_m1, respectively; Applied Biosystems™) in duplicates per gene. The reaction mix (20 µL in total) consisted of 1× TaqMan® Universal Master Mix II, no UNG (Applied 20 Biosystems™), 0.6 µL of TaqMan® assay, and 2 µL of RT reaction product. Amplification was performed using ViiA7 qPCR System (Applied Biosystems™) under the following thermal cycling conditions: 40

cycles of 95 °C for 15 s and 60 °C for 1 min. NTCs (No-template control) were included in each qPCR run. Relative gene expression values (normalized to *HPRT1*) in a logarithmic scale were used for the analysis of the results, performed with GenEx v6.0.1 software (MultiD Analyses AB, Göteburg, Sweden). For survival analysis, gene expression levels were categorized as "high" or "low" if the log-transformed values were above or below the mean value of all samples for a particular gene, respectively.

2.11. Statistical analysis

Statistical analyses were performed using STATISTICA™ v8.0 (StatSoft, Tulsa, OK, USA), MedCalc® v14.0 software (MedCalc Software, Ostend, Belgium) and GraphPad Prism v8 software (GraphPad Software, La Jolla, CA, USA). All quantitative variables were tested for normality (Shapiro-Wilk, Kolmogorov-Smirnov, and Lilliefors tests), and because of abnormal distribution, the nonparametric Wilcoxon–Mann–Whitney test was applied to compare variables between two groups. Meanwhile, the 2-sided Fisher's exact test was applied for the comparison of categorical variables.

For multimarker panel analysis in the tissue samples by qualitative MSP, the particular panel of genes was considered as methylated if at least one gene was methylated. The panel was considered as unmethylated if all genes in that panel were unmethylated.

For the qMSP data analysis in the urine samples, the ability of biomarkers to distinguish ccRCC and ASC was evaluated by performing receiver operating characteristic (ROC) curve analysis and estimating the area under the curve (AUC) values. The diagnostic test's performance parameters – sensitivity and specificity, were obtained from the ROC curve analysis and based on the Youden index for the selection of optimal cut-off value. This cut-off value ensured perfect categorization of the samples as positive and negative for the methylation test. For various combinations of biomarkers, logistic regression analysis was applied.

For time-event analysis, Kaplan–Meier curves with the log-rank test were used to calculate survival estimates. The univariate and multivariate Cox proportional hazards modeling was performed to estimate the hazard ratio (HR) of death with 95% confidence intervals (CI). Differences and associations were considered statistically significant at $P < 0.050$.

3. RESULTS

The present study of DNA methylation biomarkers for renal clear cell carcinoma consisted of three stages (**Fig. 3.1**). During the first screening stage, genome-wide DNA methylation and global mRNA expression analysis were done. According to obtained data and available literature on genes presumably contributing to cancer development and progression, ten protein-coding genes as potential biomarkers for ccRCC were selected for the next step of the study. The second validation stage consists of targeted DNA methylation analysis of these genes in the cancerous and non-cancerous renal tissue (NRT) samples and the comparison of methylation frequencies with clinical-pathological parameters of the patients [309,310]. At this step, six genes were selected for further mRNA expression analysis in the renal tissue samples. The third stage encompassed DNA methylation intensity analysis of these six genes in the urine sediments of patients with ccRCC and asymptomatic controls (ASC) and the evaluation of the potential of such genes for the non-invasive diagnosis and prognosis of ccRCC [309].

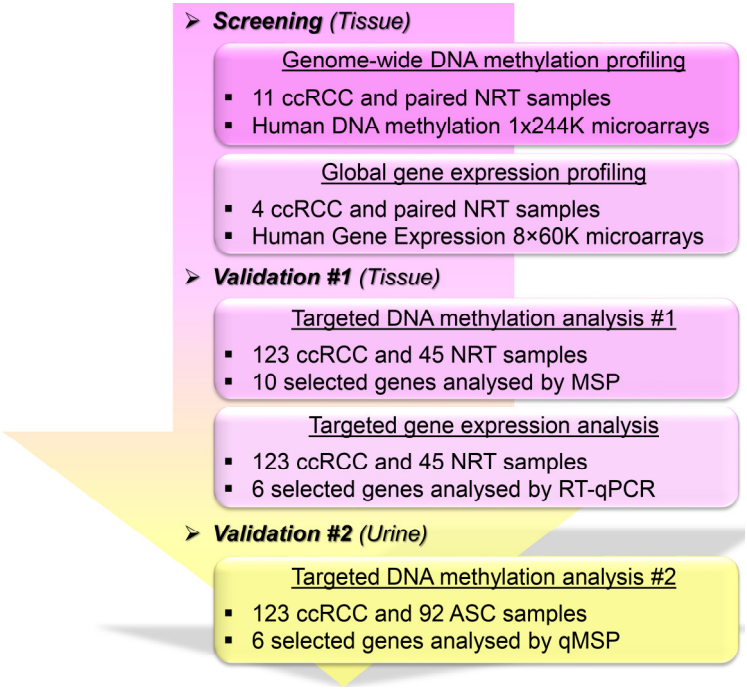

Fig. 3.1. The workflow for the search of novel DNA methylation biomarkers for kidney cancer. Abbreviations: ccRCC – clear cell renal cell carcinoma; NRT – non-tumor renal tissue; ASC – asymptomatic controls; MSP – methylation-specific PCR; qMSP – quantitative MSP; RT-qPCR – reverse transcription-quantitative PCR.

3.1. Genome-wide DNA methylation and gene expression profiling

In order to identify potential DNA methylation biomarkers of ccRCC and to determine the amount of DNA methylation changes in cancerous renal tissues compared to NRT, initially, the genome-wide DNA methylation profile was analyzed in 11 pairs of ccRCC and NRT samples.

Among ccRCC, four samples were of an early pT1a stage, while the remaining were of advanced pT3-4 stages. The comparison of cancerous and non-cancerous renal tissue samples revealed significant methylation differences (fold-change (FC) ≥ 1.5; P ≤ 0.050) in 766 probes, reflecting 367 genes in total. About a half of differently methylated genes, particularly 175 (48%), were hypermethylated (**Table S5**), and 192 (52%) were hypomethylated. Hierarchical clustering analysis revealed two main clusters of ccRCC, one with high methylation levels and another with low, which is more similar to NRT ones (**Fig. 3.2**).

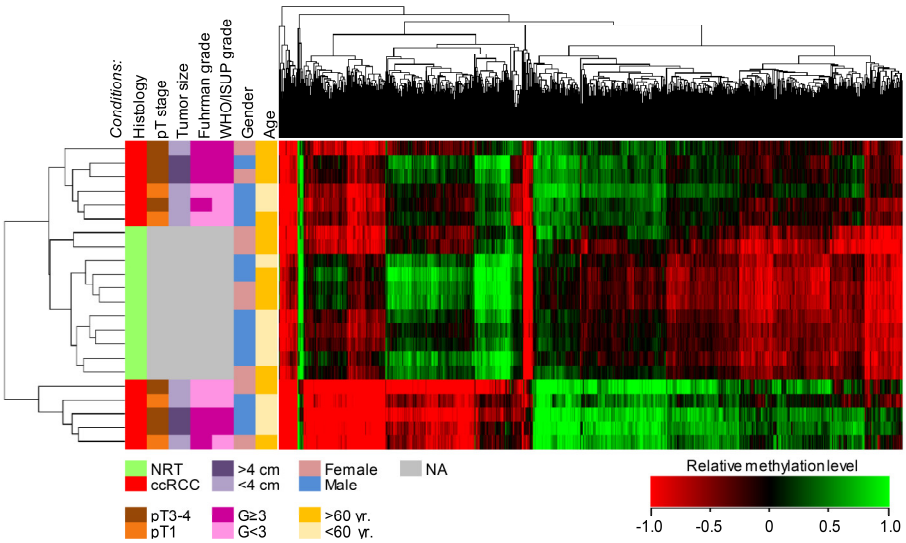

Fig. 3.2. Genome-wide DNA methylation analysis in cancerous and non-cancerous renal tissues. Heat map for hierarchical clustering analysis of 11 pairs of clear cell renal cell carcinoma (ccRCC) and non-cancerous renal tissue (NRT) samples from 11 patients. Only probes indicating statistically significant methylation differences (FC ≥ 1.5; P ≤ 0.050) between cancerous and non-cancerous tissues are included in the heatmap. The color scale indicates relative methylation level normalized by reference sample (genomic DNA), where -1 indicates hypomethylated while 1 hypermethylated status of the probe. Abbreviations: pT – pathological stage; WHO/ISUP – World health organization/International Society of Urological Pathology; G – grade; yr – years. NA – not applicable.

Comparison of the cases of different tumor stages with NRT revealed the most abundant DNA methylation differences in pT1 tumors. DNA methylation changes in pT1 tumors occurred in 1940 genes (FC ≥ 1.5; P ≤ 0.050) in total, of which 406 (21%) were hypermethylated, and 1526 (79%) were hypomethylated, including eight genes with concurrent changes observed according to different microarray probes. In the pT3-4 tumor stage, DNA methylation differences were less common and observed in 323 genes (FC ≥ 1.5; P ≤ 0.050), of which 210 (65%) were hypermethylated and 112 (35%) hypomethylated, including one overlapped gene. It is worth noting that these diversities between stages can be explained by a small number of samples being compared. However, the comparison of pT3-4 to pT1 revealed methylation differences (FC ≥ 1.5; P ≤ 0.050) in only eight genes. A considerable part of deregulated genes in the separate tumor stages was observed in the ccRCC *vs.* NRT comparison group as well (**Table S5, Fig. S1**).

Relatively scarce methylation differences were found when comparisons according to other clinical-pathological parameters were made. On the contrary, abundant methylation differences were observed among males and females as well as different age groups; however, only one of the genes overlapped with methylation changes determined in the ccRCC *vs.* NRT comparison group (**Table S6**).

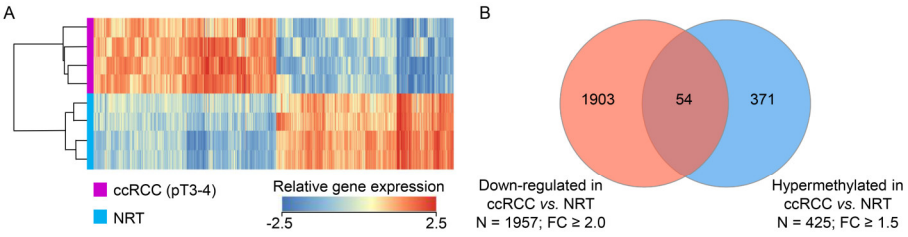

Fig 3.3. Global gene expression analysis in renal tissues and comparison with DNA methylation. A – The expression profile of genes that were differentially expressed (N = 3942, FC ≥ 2, P < 0.050) in the cancerous renal tissues (ccRCC) and non-cancerous (NRT) samples; B – Venn diagram of the down-regulated and hypermethylated genes of the same samples set.

Global gene expression analysis in 4 pairs of ccRCC (pT3-4 stage) and NRT samples, which have been used in methylation analysis, was also conducted. Microarray-based transcriptome analysis identified 3942 genes that were significantly deregulated (P < 0.050) with fold change (FC) value of ≥2 in 4 ccRCC samples while compared to NRT and half of these genes (N = 1957) were down-regulated (**Fig. 3.3 A**). While compared with DNA

methylation data of the same samples, 54 genes in total were simultaneously down-regulated and hypermethylated in the ccRCC tissues (**Fig. 3.3 B, Table S7**).

3.1.1. Functional term enrichment analysis of differentially methylated and expressed genes

In order to gain a better insight into the molecular mechanism that occurs during renal tissue carcinogenesis and ccRCC progression, gene set enrichment analysis (GSEA) of all aberrantly methylated and differentially expressed genes was performed.

Firstly, the Biological Process category of gene ontology (GO) terms was analyzed to elucidate the molecular mechanisms that occur during kidney carcinogenesis. Enrichment of the gene groups related to cell differentiation, cell fate commitment, epithelium development, cell population proliferation, cell migration, regulation of chromatin organization, gene expression, and transcription was identified, while differentially methylated genes were analyzed (**Fig. S2**). Among differentially expressed genes, the gene sets involved in various processes related to kidney development and regulation of the immune system process were commonly detected (**Table S8**).

To further clarify biological pathways involved in ccRCC development, Hallmark gene sets were identified. According to the collection of Hallmark pathways, gene sets involved in cell cycle regulation and DNA repair were among the most significantly enriched in ccRCC samples compared to NRT cases (**Fig. 3.4. A**). The increase of methylation levels was the most significant among the genes involved in epithelial-mesenchymal transition (EMT), however, observed in the pT1 stage tumors only. Among the differentially expressed genes, similar pathways were determined as well (**Fig. 3.4 B**). In addition, the upregulated genes were the most significantly and commonly involved in interferon-gamma response, inflammatory response, G2M checkpoint, and many others; meanwhile, downregulated genes were involved in oxidative phosphorylation, fatty acids metabolism, KRAS signaling, and others.

To sum up, GO biological process and Hallmark pathways analysis revealed that during ccRCC development and progression, deregulation in molecular processes commonly involved in cancer development was enriched.

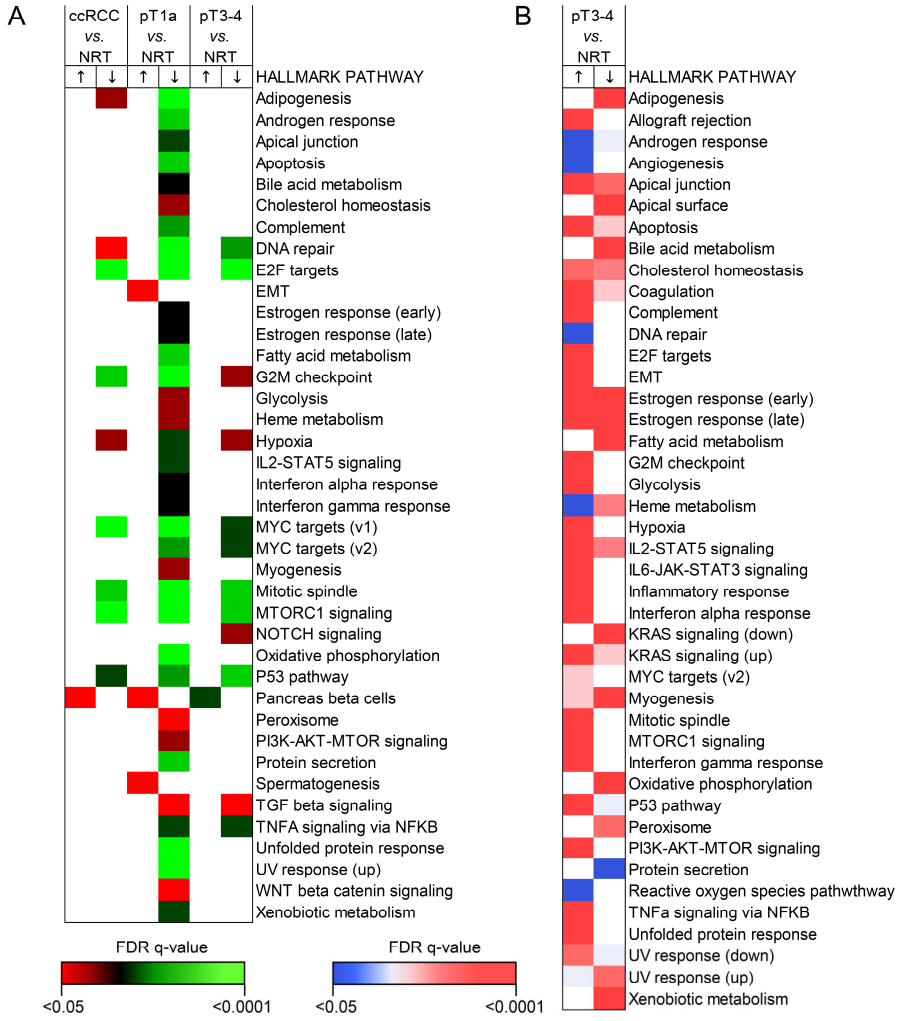

Fig. 3.4. Gene set enrichment analysis of differentially methylated and expressed genes identified in genome-wide methylation and global gene expression profiling, respectively. A – functional gene sets (hallmark pathways) for all identified differentially methylated genes; Only genes with significant methylation differences with fold change values ≥1.5 were included. B – functional gene sets (hallmark pathways) for all identified differentially expressed genes; Only genes with significant expression differences with fold change values ≥2.0 were included. The color intensities indicate the level of false discovery rate (FDR) adjusted P-values (q-values). Abbreviations: ccRCC – clear cell renal cell carcinoma; NRT – non-cancerous renal tissues; pT – pathological tumor stage; EMT – epithelial-mesenchymal transition. ↑ – hypermethylation or up-regulation; ↓ – hypomethylation or down-regulation.

3.1.2. The selection of genes for targeted methylation analysis

Based on methylation differences according to the renal tissue histology and/or tumor stage, as well as with regard to global gene expression analysis and the number of particular gene-associated probes showing significant methylation differences, nine genes *ZNF677*, *FBN2*, *PCDH8*, *TFAP2B*, *TAC1*, *FLRT2*, *ADAMTS19*, *BMP7*, and *SIM1* were selected for further targeted DNA methylation analysis (**Table 3.1, Fig. 3.5**). These genes were selected due to their putative contribution to the cancer hallmarks (according to GSEA analysis and literature data) and technical feasibility for targeted methylation-specific PCR analysis as well. In addition, the *SFRP1* was selected as a well-known methylated biomarker of ccRCC.

Table 3.1. Genes selected for methylation analysis.

Gene symbol	Gene name	Chromo-somal location (strand)	Cancer hallmark or signaling pathways	DNA methylation differences (probes, N (FC))			mRNA expre-ssion
				ccRCC *vs.* NRT	pT1 *vs.* NRT	pT3-4 *vs.* NRT	
ZNF677	zinc finger protein 677	19q13.42 (-)	Transcriptional regulation	1 (1.6)	1 (1.6)	2 (1.6)	down (10.0)
FBN2	fibrillin 2	5q23.3 (-)	Invasion, EMT	8 (1.8)	8 (2.0)	8 (1.8)	na
PCDH8	protocadherin 8	13q14.3 (-)	Cell adhesion, EMT	4 (1.7)	7 (2.0)	3 (1.6)	na
TFAP2B	transcription factor AP-2 beta	6p12.3 (+)	Transcriptional regulation, WNT signalling	1 (1.6)	1 (1.6)	1 (1.5)	down (349.5)
TAC1	tachykinin precursor 1	7q21.3 (+)	Cell motility, inflammation	1 (1.5)	0	5 (1.7)	down (7.7)
FLRT2	fibronectin leucine rich transmembrane protein 2	14q31.3 (+)	Cell adhesion, invasion	2 (1.7)	2 (1.7)	2 (1.7)	na
ADAMTS 19	ADAM metallopeptidase with thrombospondin type 1 motif 19	5q23.3 (+)	Cell adhesion, migration, proliferation, angiogenesis	4 (1.6)	3 (1.6)	3 (1.6)	down (2.1)
BMP7	Bone morphogenetic protein 7	20q13.31 (-)	Invasion, EMT	2 (1.5)	2 (1.5)	1 (1.6)	down (7.3)
SIM1	SIM bHLH transcription factor 1	6q16.3 (-)	Tumor metastasis	3 (1.7)	3 (1.7)	5 (1.7)	down (18.5)
SFRP1	Secreted frizzled related protein 1	8p11.21 (-)	WNT signalling	na	na	na	down (70.4)

FC – fold change; ccRCC – clear cell renal cell carcinoma; NRT – non-cancerous renal tissues; pT – pathological stage; EMT – epithelial-mesenchymal transition; WNT – Wingless and Int-1.

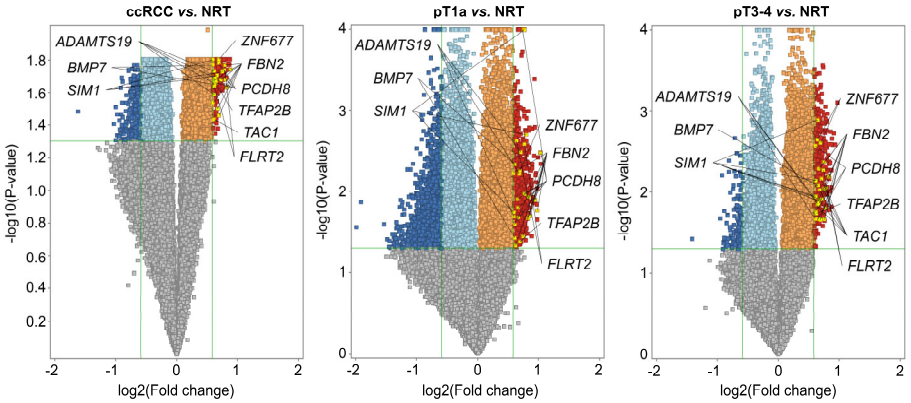

Fig. 3.5. Volcano plots of DNA methylation profiling in renal tissues. Methylation differences between A – ccRCC and NRT; B – pT1 stage tumors and NRT; C – pT3-4 stage tumors and NRT; Dark blue colored squares indicate hypomethylated and dark red – hypermethylated probes with fold change ≥ 1.5 and P < 0.050. Yellow labeled squares indicate microarray probes of the genes selected for further validation analysis. Abbreviations: ccRCC – clear cell renal cell carcinoma; NRT – non-cancerous renal tissues; pT – pathological tumor stage.

3.2. Targeted DNA methylation analysis of the selected genes in the renal tissue samples

DNA methylation status of *ZNF677*, *FBN2*, *PCDH8*, *TFAP2B*, *TAC1*, *FLRT2*, *ADAMTS19*, *BMP7*, *SIM1*, and *SFRP1* was analyzed qualitatively at regulatory regions of the genes in 123 ccRCC and 45 NRT samples.

Methylation of all selected genes was significantly more common in cancerous renal tissues as compared to NRT (P < 0.050; **Fig. 3.6**). Methylation of *ZNF677*, *FBN2*, *PCDH8*, *TFAP2B*, *TAC1*, *FLRT2*, *ADAMTS19*, and *SFRP1* was detected in at least one-third of ccRCC samples or even more frequently (from 33.3% to 60.2%), while less common methylation events were observed in *BMP7* and *SIM1* (20.3% and 18%). In addition, *ZNF677*, *FBN2*, *PCDH8*, *ADAMTS19*, *BMP7*, *SIM1*, and *SFRP1* were highly tumor-specific, whereas low methylation frequency of *TFAP2B*, *TAC1*, and *FLRT2*, ranging from 2 % to 11%, was observed in NRT samples as well.

3.2.1. The diagnostic potential of selected genes

Diagnostic test selectivity parameters were calculated in order to evaluate the ability of the biomarkers to distinguish ccRCC and NRT samples. The separate biomarkers had high specificity (≥88.9%); however, sensitivity was low to moderate, with the highest value for *TAC1* equal to 60% (**Table 3.2**).

The biomarkers were also analyzed for their diagnostic performance in various combinations. Panels of two-five biomarkers showed even better characteristics, which in most cases exceeded the respective values of the individual assays. Multimarker panel consisting of *ZNF677*, *FBN2*, *PCDH8*, *TAC1* & *SFRP1* either with or without *TFAP2B* was characterized with the best diagnostic potential and reached 83.7–85.4% of sensitivity and 95.8–97.8% of specificity.

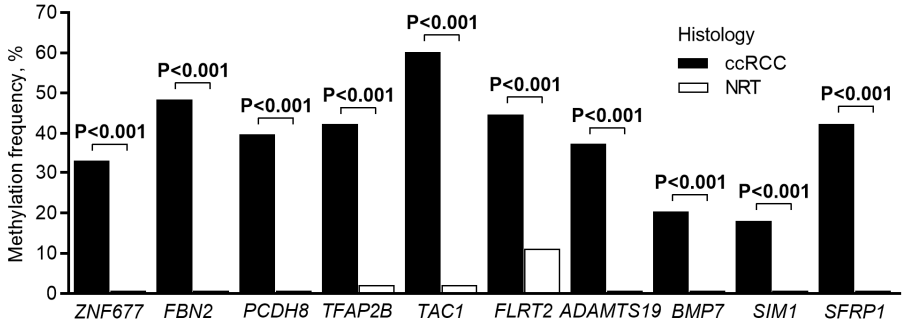

Fig. 3.6. Methylation frequencies of the selected genes in renal tissues. The results were obtained by qualitative methylation-specific PCR (MSP). Abbreviations: ccRCC – clear cell renal cell carcinoma, NRT – noncancerous renal tissues. Significant P-values are in bold.

Table 3.2 The diagnostic test performance characteristics of the analyzed methylation biomarkers in renal tissues.

Biomarkers	DSe, %	DSp, %	AUC
ZNF677	33.3	100.0	0.67
FBN2	48.4	100.0	0.74
PCDH8	39.8	100.0	0.70
TFAP2B	42.3	97.8	0.70
TAC1	60.2	97.8	0.79
FLRT2	44.7	88.9	0.67
ADAMTS19	37.4	100.0	0.69
BMP7	20.3	100.0	0.60
SIM1	17.9	100.0	0.59
SFRP1	42.3	100.0	0.71
FBN2 & TAC1	70.7	97.8	0.84
FBN2, TAC1 & SFRP1	77.2	97.8	0.88
ZNF677, FBN2, TAC1 & SFRP1	82.1	97.8	0.90
ZNF677, FBN2, PCDH8, TAC1 & SFRP1	83.7	97.8	0.91
ZNF677, FBN2, PCDH8, TAC1, TFAP2B & SFRP1	85.4	95.6	0.91

DSe – diagnostic sensitivity; DSp – diagnostic specificity; AUC – area under the curve.

3.2.2. Association of selected genes with demographic and clinical-pathological parameters

Aberrant methylation of the genes was further analyzed according to the demographic patients' characteristics, including sex and age.

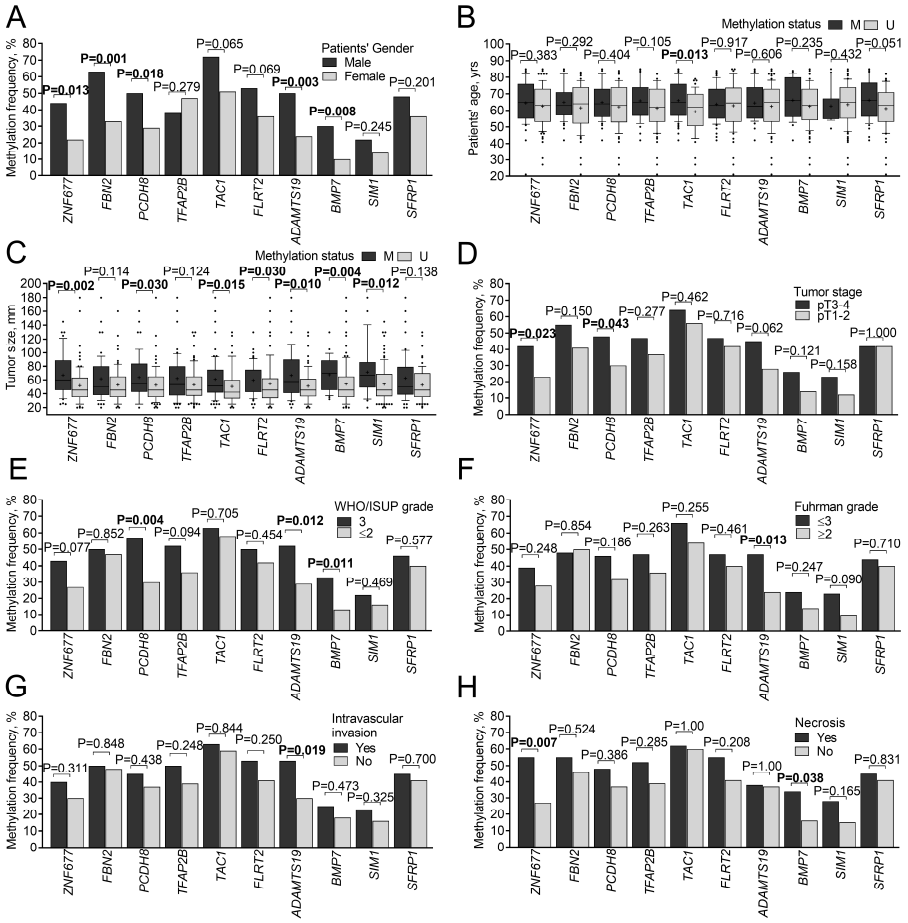

Fig. 3.7. Methylation frequencies of selected genes in renal tumor tissues according to demographic and clinical-pathological variables. A – Methylation frequencies according to patients' sex; B – methylation status association with patients' age and C – tumor size. Methylation frequencies according to tumor: D – stage; E – WHO/ISUP grade; F – Fuhrman grade; G – intravascular invasion; H – necrosis. The box depicts the 25th and 75th percentiles; the line inside the box reflects the median; the plus sign depicts the mean; the whiskers marked the 10-90% range, and data values out of that range are shown as dots. Abbreviations: M – methylated, U – unmethylated gene status; WHO/ISUP – World health organization/International Society of Urological Pathology, G – grade. Significant P-values are in bold.

Higher methylation frequency of all investigated genes, except *TFAP2B*, was observed in males, compared to females, and for *ZNF677*, *FBN2*, *PCDH8*, *ADAMTS19*, and *BMP7*, this tendency was statistically significant ($P < 0.050$; **Fig. 3.7 A**). Besides, the methylated status of *TAC1* was related to the older patients (66 vs. 59 yr., $P = 0.013$; **Fig. 3.7 B**).

Aberrant methylation of the genes was further analyzed according to clinical-pathological patients' characteristics. Methylated status of *ZNF677*, *PCDH8*, *TAC1*, *FLRT2*, *ADAMTS19*, *BMP7*, and *SIM1* was significantly associated with larger tumors ($P < 0.050$; **Fig. 3.7 C**). Furthermore, methylation frequencies of all of the genes, except *SFRP1*, showed an increasing tendency according to the tumor stage; however, the observed association was statistically significant only for *ZNF677* and *PCDH8* ($P = 0.023$ and $P = 0.043$ respectively; **Fig. 3.7 D**). Methylation frequency of all genes was also elevated in tumors with higher WHO/ISUP grade and for *PCDH8*, *ADAMTS19* and *BMP7* this tendency was significant ($P = 0.004$, $P = 0.012$ and $P = 0.011$ respectively; **Fig. 3.7 E**). Moreover, almost all genes, except *FBN2*, were more commonly methylated in tumors with higher Fuhrman grade, but only for *ADAMTS19*, this association was statistically significant ($P = 0.013$; **Fig. 3.7 F**) as in the case of intravascular tumor invasion ($P = 0.019$; **Fig. 3.7 G**) as well. Lastly, frequent methylation of *ZNF677* and *BMP7* was related to the presence of tumor necrosis ($P = 0.007$ and $P = 0.038$, respectively; **Fig. 3.7 H**).

3.2.3. Prognostic value of selected gene methylation in ccRCC tissues

For the investigation of the prognostic value of selected putative ccRCC biomarkers, the patient's overall survival (OS) as an endpoint was used.

Aberrant methylation of all genes except *TFAP2B* and *SIM1* was more frequent in the case of death than survived patients, and for *FBN2*, this difference was significant ($P < 0.050$; **Fig. S3**). Further Kaplan-Meier curves survival analysis was done, and significantly shorter OS for ccRCC patients with a methylated status of *ZNF677* and *FBN2* ($P = 0.023$ and $P = 0.019$, respectively; **Fig. 3.8 A, B**) was revealed. Although no associations with OS were observed for another single gene ($P > 0.050$; **Fig. 3.8 C-J**), various combinations of the biomarkers were significantly associated with the poorer overall survival of ccRCC patients (**Fig. 3.8 K-T**).

Univariate Cox proportional hazard analysis confirmed the association of the methylated status of single genes *ZNF677* and *FBN2* ($P < 0.050$; HR: 2.61, 95% CI: 1.10-6.17 and HR: 2.96, 95% CI: 1.14-7.66 respectively) and various panels of two-four genes ($P < 0.050$; HR from 2.39 to 4.29) with overall

survival (**Table S9**), that even outperform the prognostic value of some demographic and clinical pathological variables. Among the latter, patients' age (HR: 1.09, 95% CI: 1.04-1.14), gender (male *vs.* female, HR: 2.73, 95% CI: 1.06-7.08), tumor size (HR: 1.01, 95% CI: 1.00-1.02), tumor stage (pT3-4 *vs.* pT1-2, HR: 5.12, 95% CI: 1.72-15.24), WHO/ISUP grade (G3 *vs.* G1-2, HR: 3.04, 95% CI: 1.28-7.24), fat invasion (yes *vs.* no, HR: 4.83, 95% CI: 1.87-12.48), and necrosis (yes *vs.* no, HR: 4.97, 95% CI: 2.10-11.76) showed an independent prognostic value of overall survival (P < 0.050; **Table S9**).

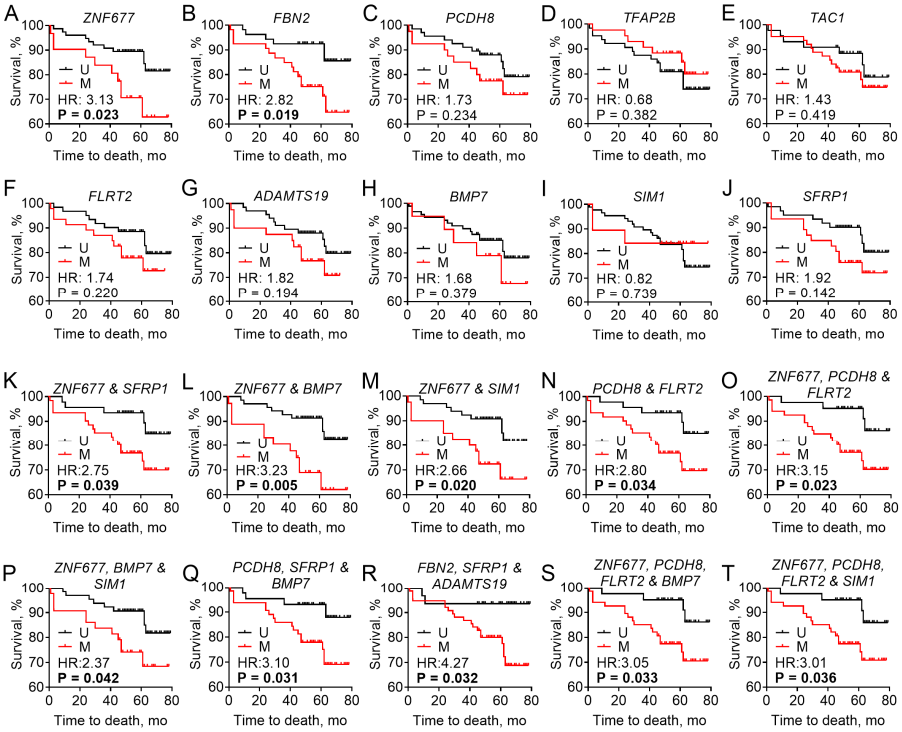

Fig. 3.8. The relationship between methylation status of selected genes and overall survival. Kaplan-Meier survival curves according to the gene methylation status of A-J – single gene and K-T – various combinations of two-four genes. For the gene combinations, only panels showing the significant association with the patient's overall survival in the univariate Cox analysis are depicted. Abbreviations: M/U – methylated/unmethylated gene status; HR – hazard ratio (when gene or panel is methylated). Significant P-values are in bold.

In the backward multivariate analysis, *FBN2* showed a better prognostic value than *ZNF677* (**Table S9**). Meanwhile among panels of two, three or four genes, the best prognostic potential was established for *ZNF677 & BMP7* (M *vs.* U, HR: 3.27, 95% CI: 1.38-7.78), *ZNF677*, *PCDH8 & FLRT2* (M *vs.* U,

HR: 3.18, 95% CI: 1.07-9.45) and *ZNF677*, *PCDH8*, *FLRT2 & BMP7* (M *vs*. U, HR: 3.08, 95% CI: 1.04-9.15) respectively. However, while adjusting for demographic and clinical-pathological variables, no single gene nor the combination of genes retained an independent prognostic value (**Table S9**).

3.2.4. mRNA expression analysis of selected genes and association with promoter methylation and clinical-pathological parameters

Based on promoter methylation frequencies and with regard to correlations with clinical-pathological variables as well as prognostic value, genes *ZNF677*, *FBN2*, *PCDH8*, *TFAP2B*, and *TAC1* and *FLRT2* were selected for mRNA expression analysis.

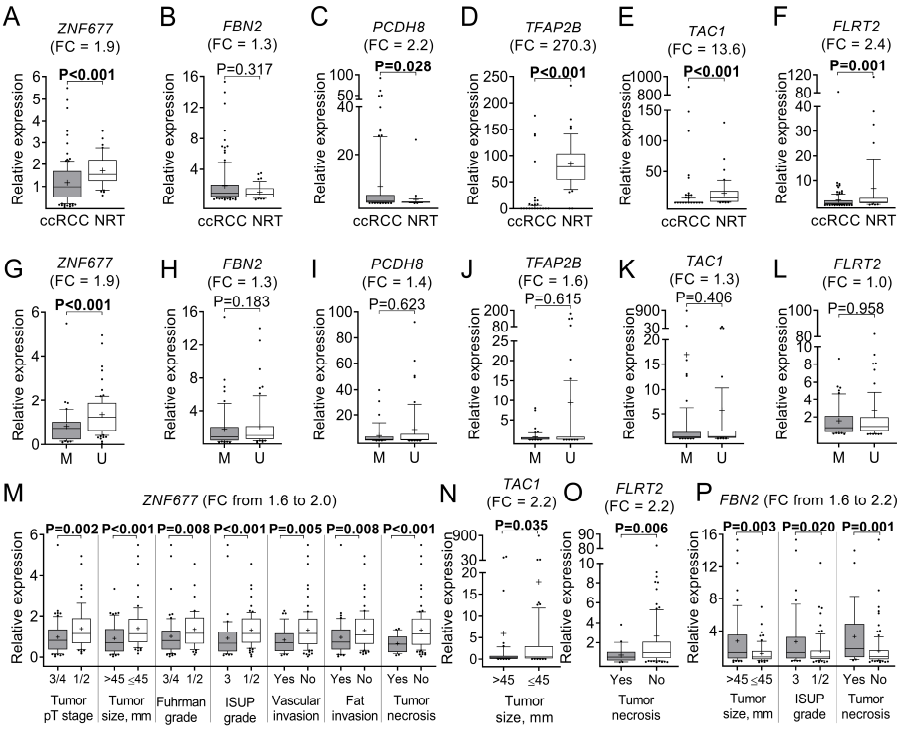

Fig. 3.9. Transcriptional expression analysis of the selected genes. A–F – relative expression levels of genes according to renal histology; G–L – a relative expression of genes according to methylation status; M–P – a relative expression of genes according to clinical-pathological parameters of ccRCC patients. The box depicts the 25th and 75th percentiles; the line inside the box reflects the median; the plus sign depicts the mean; the whiskers marked the 10-90% range, and data values out of that range are shown as dots. Abbreviations: FC – fold change; ccRCC – clear cell renal cell carcinoma; NRT – noncancerous renal tissues; ISUP –International Society of Urological Pathology; pT – pathological tumor stage. Significant P-values are in bold.

Transcriptional expression of *ZNF677*, *FBN2*, and *FLRT2* was detected in all ccRCC and NRT samples, while mRNA of *TFAP2B*, *TAC1*, and *PCDH8* was observed in a part of ccRCC and NRT samples (118, 112, 91 and 45, 45, 26, respectively). Expression levels of *ZNF677*, *TFAP2B*, *TAC1*, and *FLRT2* were significantly lower in ccRCC tissues as compared to NRT samples (all $P < 0.050$), while higher expression of *PCDH8* was found in ccRCC ($P < 0.050$), and no significant differences was observed for *FBN2* (**Fig. 3.9 A-F**). Lower expression levels of *ZNF677* in ccRCC tissues were significantly associated with methylated promoter status ($P < 0.001$), meanwhile no such correlation was observed for the other selected genes (**Fig. 3.9 G-L**).

In comparison with clinical-pathological parameters, down-regulated *ZNF677* was significantly correlated with the higher tumor stage, Fuhrman and WHO/ISUP grade, larger (> 45 mm) tumor size, presence of tumor vascular and fat invasions as well as necrosis (all $P < 0.050$; **Fig. 3.9 M**). The lower expression level of *TAC1* and *FLRT2* was also related to larger (> 45 mm) tumor size and the presence of tumor necrosis, respectively ($P = 0.035$ and $P = 0.006$; **Fig. 3.9 N, O**). On the contrary, a higher mRNA level of *FBN2* was significantly associated with larger tumors, higher WHO/ISUP grade, and tumor necrosis ($P = 0.003$, $P = 0.020$, and $P = 0.001$ respectively; **Fig. 3.9 P**). In addition, Kaplan-Meier survival analysis and log-rank test results suggested that patients with low expression of *ZNF677* had significantly shorter overall survival than patients with high expression of *ZNF677* ($P = 0.021$; **Fig. S4**).

3.3. Targeted DNA methylation analysis of the selected genes in urine sediments

In urine samples, quantitative DNA methylation analysis of *ZNF677*, *FBN2*, *PCDH8*, *TFAP2B*, *TAC1*, and *FLRT2* was performed by the qMSP method. For the qualitative interpretation of the results, the threshold, calculated according to ROC curve analysis and based on the Youden index for the selection of optimal cut-off value, was applied.

The average methylation levels and hypermethylation frequencies of all genes were significantly higher in the urine of ccRCC cases as compared to the ASC group ($P < 0.050$; **Fig. 3.10 A, B**). However, DNA methylation of the genes in the urine sediments was not significantly associated with the methylation status in the tissue samples (data not shown). As expected, DNA methylation intensity was significantly lower in randomly selected 20 ccRCC patients' urine samples than in paired ccRCC tissues (all $P < 0.050$; **Fig. S5**).

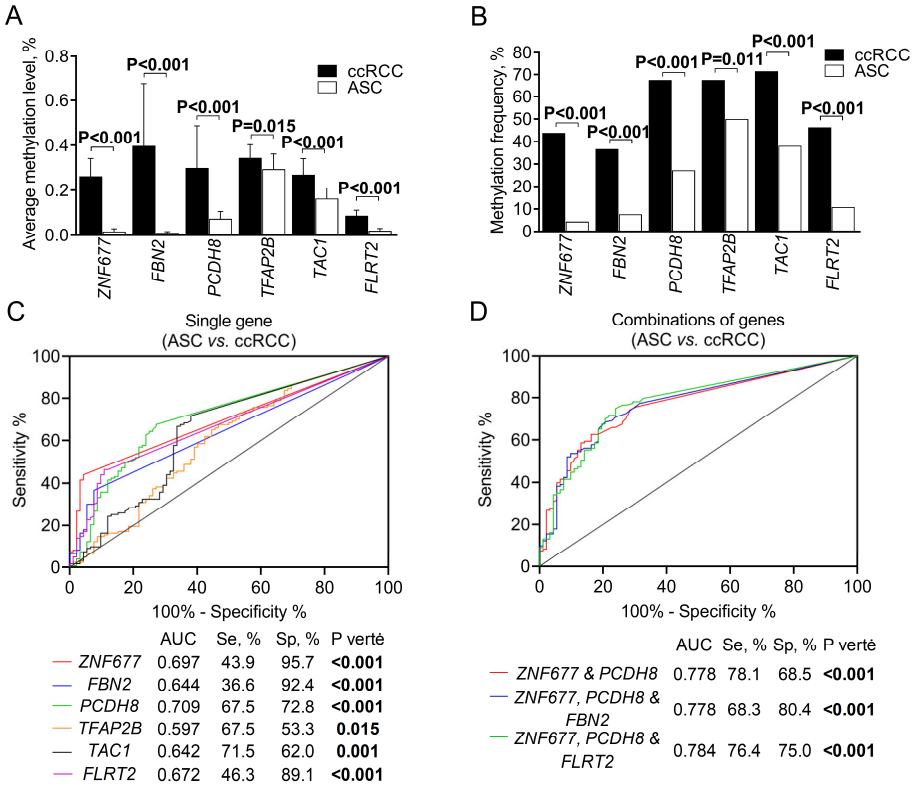

Fig. 3.10. DNA methylation analysis in urine sediments. A – Methylation levels and B – methylation frequencies of selected genes in urine sediments of patients diagnosed with clear cell renal cell carcinoma (ccRCC) and asymptomatic control (ASC) cases. ROC curve analysis for C – single gene and D – a combination of two-three genes in discriminating patients with ccRCC and ASC. Abbreviations: ROC – receiver Operating Characteristic; AUC – area under the curve; Se – sensitivity; Sp – specificity. Significant P-values are in bold.

3.3.1. The potential of selected genes for non-invasive diagnosis of ccRCC

The power of selected urine biomarkers methylation intensities to discriminate ccRCC cases from asymptomatic controls was analyzed by the ROC curve method.

The area under the curve (AUC) value for all genes was 0.60 or higher with the highest value for *PCDH8*, which was 0.71 with 67.5% of sensitivity and 72.8% of specificity (all $P < 0.050$; **Fig. 3.10 C**). As expected, panels of two-six genes had a better ability to discriminate between ccRCC and ASC (all $P < 0.001$; **Table S10**). The highest diagnostic power (AUC=0.78) were observed for the panels, consisting of two – *ZNF677* & *PCDH8* (sensitivity – 78%; specificity – 69%) and three – *ZNF677*, *PCDH8* & *FBN2* (sensitivity –

68%; specificity – 80%) or *ZNF677*, *PCDH8* & *FLRT2* (sensitivity – 78%; specificity – 75%) genes (all P < 0.001; **Fig. 3.10 D**).

3.3.2. Association of selected genes methylation in the urine samples with clinical-pathological parameters

Aberrant methylation of selected genes in the urine samples was further analyzed according to demographic and clinical-pathological characteristics.

In contrast to the results obtained in tissue samples, no associations between methylation of selected genes and patients' gender were observed (data not shown). However, methylation intensities of all genes, but *FLRT2*, in urine sediments were significantly correlated with patients' age (all P < 0.050; **Fig. 3.11 A**), however, no such correlation was observed in the asymptomatic control group (data not shown).

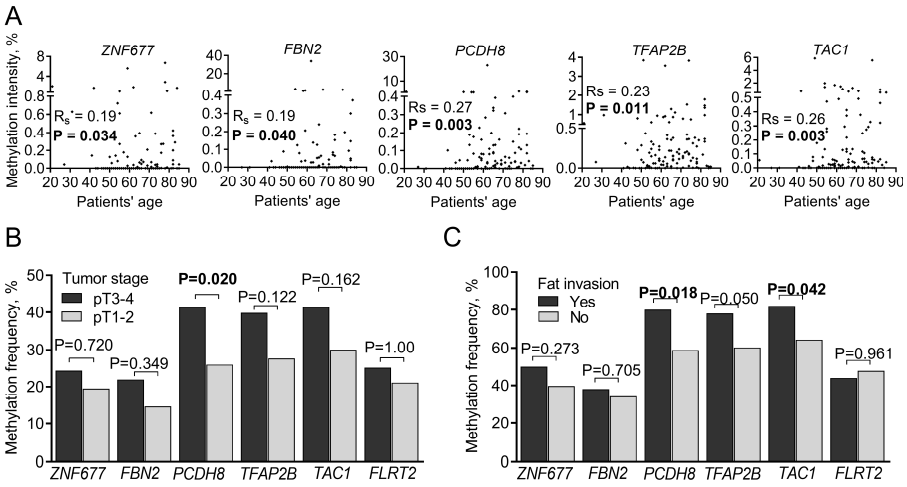

Fig. 3.11. The association of selected genes methylation in urine sediments with clinical-pathological parameters. A – the association of methylation intensity with patient's age; B – the association of methylation frequencies with pathological tumor stage. C – the association of methylation levels with tumor fat invasion. Significant P-values are in bold.

Among clinical-pathological characteristics, higher methylation frequencies of all genes were detected in pT3-4 stage tumors as compared to the pT1-2 stage; however, only for *PCDH8,* this difference was significant (P = 0.002; **Fig. 3.11 B**). Meanwhile, higher methylation frequencies of *PCDH8* and *TAC1* were observed in the urine samples from patients diagnosed with locally advanced ccRCC, particularly characterized by the fat invasion (P = 0.018 and P = 0.042 respectively; **Fig. 3.11 C**). However, no significant

associations were detected between other clinical-pathological parameters and genes methylation intensity or frequency in urine sediments (**Table S11**).

3.3.3. The potential of selected genes for non-invasive prognosis of ccRCC

To investigate the prognostic value of the newly identified genes showing tumor-specific methylation in the urine sediments, the overall survival analysis was performed.

Aberrant methylation of all genes in the urine samples was more frequent in the case of death, while compared to survived patients, but only for *PCDH8,* this tendency was significant (P = 0.005; **Fig. S6**). Kaplan-Meier survival curves also revealed significant associations between the methylated status of *PCDH8* and shorter patients' overall survival (P = 0.024; **Fig. 3.12 A**). Meanwhile, no other single gene showed significant results (data not shown). However, the prognostic value of *PCDH8* considerably increased in combination with *ZNF677* (both P = 0.022; **Fig. 3.12 B**), while no other combinations showed better results (**Fig. S7**).

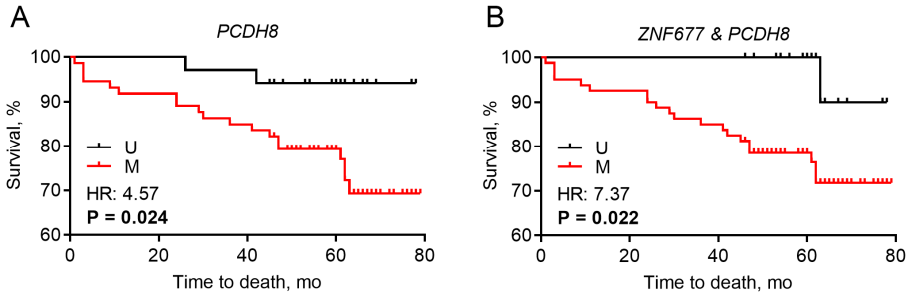

Fig. 3.12. The relationship between methylation status of investigated genes in urine sediments samples and patient's overall survival. Kaplan-Meier survival curves according to the methylation status of A – *PCDH8* alone or B – panel of *ZNF677 & PCDH8*. Abbreviations: M/U – methylated/unmethylated gene (panel) status; HR – hazard ratio (when gene or panel of genes are methylated). Significant P values are in bold.

Univariate Cox proportional hazard analysis confirmed the association of the methylated status of *PCDH8* and the combination of *ZNF677 & PCDH8* with shorter overall survival (**Table 3.3**). Moreover, multivariate analysis revealed the methylation status of *PCDH8* alone or panel of *ZNF677 & PCDH8* is an independent predictor for ccRCC patients OS with HR: 5.7, 95% CI: 1.16-28.12 and HR: 12.5, 95% CI: 1.47-105.58, respectively, while adjustment according to the most important prognostic factors of ccRCC, including patients' age, gender, tumors stage, size, grade, and necrosis, was

done (**Table 3.3**). Besides, the prognostic value of other combinations of biomarkers was also rather promising (**Fig S7, Table S12**). Altogether, this indicates the potential to develop a molecular test for predicting ccRCC progression based solely on DNA methylation biomarkers.

Table 3.3. Univariate and multivariate Cox proportional hazard analysis of overall survival according to molecular and/or clinicopathologic variables while analyzing the urine samples.

UNIVARIATE ANALYSIS			
Covariates	HR [95% CI]	P-value	Model P-value
PCDH8 (M vs U)	4.58 [1.07 - 19.54]	**0.041**	**0.013**
ZNF677 & PCDH8 (M vs. U)	7.38 [1.00 - 54.46]	0.051	**0.008**
Age, years (cont.)	1.09 [1.04 - 1.14]	**<0.001**	**<0.001**
Gender (male vs. female)	2.73 [1.06 - 7.08]	**0.038**	**0.029**
Stage (pT3-4 vs. pT1-2)	5.12 [1.73 - 15.16]	**0.003**	**<0.001**
Tumor size (cont.)	1.01 [1.00 - 1.02]	**0.036**	0.063
WHO/ISUP grade (G=3 vs. G≤2)	3.04 [1.28 - 7.21]	**0.012**	**0.012**
Necrosis (yes vs. no)	4.97 [2.11 - 11.71]	**<0.001**	**<0.001**
MULTIVARIATE ANALYSIS			
MODEL 1			
PCDH8 (M vs U)	5.70 [1.16 - 28.12]	**0.033**	
Age, years (cont.)	1.10 [1.04 - 1.16]	**0.001**	
Gender (male vs. female)	2.72 [0.99 - 7.45]	0.053	
Stage (pT3-4 vs. pT1-2)	1.76 [0.51 - 6.08]	0.372	**<0.001**
Tumor size (cont.)	1.02 [1.00 - 1.03]	**0.044**	
WHO/ISUP grade (G=3 vs. G≤2)	0.69 [0.22 - 2.18]	0.527	
Necrosis (yes vs. no)	4.73 [1.45 - 15.46]	**0.010**	
MODEL 2			
ZNF677 & PCDH8 (M vs. U)	12.47 [1.47 - 105.58]	**0.021**	
Age, years (cont.)	1.10 [1.04 - 1.16]	**<0.001**	
Gender (male vs. female)	3.42 [1.26 - 9.30]	**0.016**	
Stage (pT3-4 vs. pT1-2)	1.93 [0.58 - 6.43]	0.285	**<0.001**
Tumor size (cont.)	1.01 [1.00 - 1.03]	0.123	
WHO/ISUP grade (G=3 vs. G≤2)	0.92 [0.31 - 2.70]	0.874	
Necrosis (yes vs. no)	4.67 [1.64 - 13.26]	**0.004**	

M/U – methylated/unmethylated status; cont. – continuous variable; WHO/ISUP – World Health Organisation/Internation Society of Urological Pathology; pT – pathological tumor stage; G – grade; HR – hazard ratio; CI – confidence interval. Significant P-values are in bold.

To sum up, the newly identified genes, especially *ZNF677* and *PCDH8,* showed promising potential for the non-invasive diagnosis and prognosis of ccRCC patients, however further studies with the larger patient cohorts and comprehensive follow-up data are mandatory to prove this potential.

4. DISCUSSION

Renal cell carcinoma (RCC) originating from the epithelium of nephron tubules is the most common type of kidney cancer, accounting for 90% with clear cell RCC (ccRCC) as the leading subtype representing the most aggressive and lethal cancer of the urinary system [1-3]. While the majority of patients will present with localized disease, more than a quarter of those will develop the distant disease, while at least one-fifth of patients will present with metastatic disease at diagnosis [4] that presumably caused the significant health burden of RCC. This is attributed to the typical lack of symptoms of the primary RCC, and currently, the majority of patients are diagnosed incidentally due to extensive use of radiology imaging for investigation of various non-specific symptoms [1,5]. For patients with surgically resectable RCC, the standard of care is surgical excision. However, none of the imagining methods are able to distinguish benign renal lesions from neoplastic, and as a consequence, some of the patients suffer from overtreating [60-62,311]. Thus, there is a vital need for new molecular biomarkers which would provide valuable information about disease presence, aggressiveness, and prognosis, as well as assist in treatment decision making.

As changes in the DNA methylation occur at the very beginning of renal tissue cancerogenesis and are often related to clinical-pathological parameters [10,312], they might be helpful not only to early detection of kidney cancer but prognosis prediction as well. Moreover, DNA methylation can be easily detected in the body fluids such as urine by conventional and inexpensive qualitative or quantitative PCR methods. Thus, it may serve as non-invasive biomarkers that could provide clinicians with rapid, objective, and accurate tools for disease detection and follow-up. However, despite the efforts made [271,297,299-301], no DNA methylation biomarker has reached the clinic yet. Therefore further investigations are needed.

4.1. Identification of novel DNA methylation biomarkers for renal clear cell carcinoma

Up to now, genome-wide DNA methylation studies have produced a considerable amount of novel candidate ccRCC biomarkers and significantly increased the knowledge of epigenetic changes in renal cell carcinoma. However, most of the recently published studies used relatively small and heterogeneous RCC sample cohorts for the validation of putative biomarkers or lacked this analysis step at all. Therefore further attempts are needed in

order to select novel diagnostic and/or prognostic DNA methylation biomarkers for ccRCC.

In the current study, human DNA methylation microarrays were used for screening of diagnostic and prognostic DNA methylation biomarkers in a small set of ccRCC and paired NRT samples. In agreement with other studies [59,298], two clusters of ccRCC samples with high and low methylation levels have been identified. Compared to previous studies [297,299,300], more common methylation events in ccRCC samples as compared to NRT were detected in the current study. Deregulated genes were significantly enriched in various pathways commonly contributing to cancer development. Several previously reported genes, such as *PCDH8* [272], *GPR149* [300], *FBN2* [270], *CHODL* [297], *FAM155A*, *DPP6* [299], *GREM1* [266] was also found as hypermethylated in the present study. However, the majority of identified differentially methylated genes have never been analyzed in the case of renal cancer. Interestingly, none of the most widely studied hypermethylated genes in kidney cancer, like *VHL*, *TIMP3, SFRP1, P14, P16, RASSF1A, RARB, APC, DAPK1, SFRP1* was detected in any of the comparison groups.

While the design of the microarray used in the present study covered various CpGs, regardless of their association to the gene regulatory elements, for the further gene-targeted DNA methylation validation, we focused on promoter or enhancer associated significantly methylated probes and their related genes. As DNA methylation at these sites usually influences the regulation of gene expression and most likely has a clinical value [13]. As a comparison between DNA methylation profile and transcriptome was made, only 54 genes showed simultaneously occurred hypermethylation and downregulation. However, it is worth mentioning that only four samples were examined for the transcriptome in the current study and presumably did not fully reflect DNA methylation impact on gene expression. Thus further gene selection as potential ccRCC biomarkers was based not only on that mRNA expression data, but their possible role in cancer development was evaluated as well.

Among the large number of differentially methylated genes identified in the present study, ten protein-coding genes, particularly *ZNF677, FBN2, PCDH8, TFAP2B, TAC1, FLRT2, ADAMTS19, BMP7, SIM1,* and *SFRP1,* were selected for further validation in 123 ccRCC, and 45 non-cancerous renal tissue samples. Hypermethylation of *FBN2*, *PCDH8* and *SFRP1* in the case of renal cancer are known from the previous studies [270,272,293,313], while the remaining genes were investigated for the first time. Hypermethylation of all ten genes was highly (from 89% to 100%) ccRCC-specific, but sensitivity was low to moderate. However, a multimarker panel consisting of *ZNF677*,

FBN2, *PCDH8*, *TAC1* & *SFRP1* either with or without *TFAP2B* was characterized with even 83.7–85.4% of sensitivity and 95.8–97.8% of specificity.

Our study further assisted in the identification of new genes and pathways possibly involved in renal carcinogenesis.

One of the most promising genes, *ZNF677 (zinc finger protein 677),* encodes the transcription factor belonging to the zinc finger protein family, which has a wide variety of functions in human diseases, including cancers [314]. ZNF677 may function as a tumor suppressor regulating transcription of many genes, and its overexpression in cancer cells was related to the inhibition of cell proliferation, migration, invasion, tumorigenic potential, and induction of cell-cycle arrest and apoptosis; while down-regulation has an opposite effect [315,316]. More specifically, it is observed that ZNF677 induces G0–G1 phase arrest, inhibits Akt phosphorylation, and activates p53 signaling, partially through transcriptionally repressing its targets, e.g., *CDKN3* [316]. Down-regulation of *ZNF677* due to promoter methylation previously was found in the lung [315], thyroid [316], and oral cancer tissues [317], but no studies exist on renal cancer. This study has linked for the first time the hypermethylation of *ZNF677* in ccRCC with transcriptional downregulation and various adverse clinicopathological features of the tumors, including larger size, higher stage, necrosis, as well as shorter patient survival, confirming its considerable contribution to the tumor development and progression.

Another investigated gene, *FBN2,* encodes extracellular matrix glycoprotein fibrillin-2, a key component of human microfibrils, regulating TGF-β bioavailability by sequestering their at the extracellular matrix (ECM) [318]. In the case of renal cancer, loss of fibrillin-2 may contribute to a malignant phenotype by the dysregulation of the signaling pathways regulated by TGF-β, as well as give angiogenic and metastatic advantages to RCC [270]. Specifically, deficiency of fibrillin-2 causes aberrant latent TGF-β activation [59], which in turn may promote cell transformation, proliferation, and migration, possibly by induction of epithelial-mesenchymal transition (EMT) contributing to RCC development [174,270]. Although hypermethylation of *FBN2* lacks significant associations with any clinical-pathological parameters in the present study, its methylated status has been related to shorter patient survival, while no such link was found previously [293]. Thus, further studies are required in order to clarify the clinical significance of this gene in ccRCC.

PCDH8 (Protocadherin-8) encodes a transmembrane protein belonging to the protocadherins, the largest subgroup of the cadherin superfamily, participating in cell adhesion, proliferation, differentiation, and migration

processes [319]. The significance of *PCDH8* in tumorigenesis is controversial. Some studies reported *PCDH8* as a tumor suppressor, inhibiting cell proliferation, migration, and inducing apoptosis and thus are frequently inactivated by promoter methylation in various types of carcinomas [320-322]. However, other studies showed that *PCDH8* might have metastasis-enhancing properties, and its overexpression remarkably promoted cell invasion and migration, possibly through encouraging various ECM receptor interaction pathways [323,324]. Interestingly, in the present study, we find both hypermethylation and up-regulation of *PCDH8* in ccRCC tissues; however, its overexpression was not linked with promoter methylation status; thus, further studies are needed to explain this phenomenon. Nevertheless, hypermethylation of *PCDH8* was significantly related to the larger tumors, higher tumor stage, and differentiation grade, confirming the previous observations [272] and its relation to ccRCC development and progression.

Gene *TFAP2B (transcription factor AP-2 beta)* encodes a member of the AP-2 family of transcription factors, specifically AP-2β. AP-2 proteins stimulate cell proliferation and suppress the terminal differentiation of various cell types. Specifically, TFAP2B is indispensable for kidney development by participating in the differentiation and function of normal renal tubular epithelia [325,326] and takes a role in tumors differentiation as well [327,328], possibly by promoting the WNT/β-catenin pathway [329]. The modulation of TFAP2B in tumorigenesis may be both inhibitory or promoting, depending on the specific tissues and stages of cancer progression [330]. Nuclear *TFAP2B* expression was linked with the small localized and low malignant phenotype of RCC tumors, possibly due to its induction of p21 expression, which inhibits cell transition from G1 to S phase [331]. In addition, upregulated TFAP2B inhibits VEGFR2 expression; meanwhile, loss of TFAP2B enhances VEGFR2 expression [332], widely contributing to the angiogenesis and progression of ccRCC tumors [171,172]. In this study, considerably reduced expression of *TFAP2B* was found in ccRCC tissues, which nicely confirms the previous observation [333]. Relatively high methylation frequency of *TFAP2B* has been established as well, and regardless of the absence of the associations with clinical-pathological features, this gene still represents a promising novel biomarker for ccRCC.

TAC1 (tachykinin-1) encodes a secreted protein tachykinin, a member of the neuropeptide family, which may influence cell secretion, motility, inflammatory reactions as well as inhibits cell proliferation in the normal cell [334]. Therefore, *TAC1* is considered a tumor-suppressor gene. The inclusion of this gene in the validation set was based on the previously observed association with the immune response [335]. For example, proteins encoded

by *TAC1* regulate the maturation of T-cells and recruitment of macrophages in the inflammatory tissues, which is highly observed in immunogenic ccRCC tumors [336,337]. Although, the exact function of *TAC1* in tissue cancerogenesis is unclear. Previously hypermethylation of *TAC1* was observed in various types of carcinomas, including lung cancer [338], colon cancer [339], head and neck cancer [340], pancreatic cancer [341], esophageal cancer [342], breast cancer [343], and was associated with disease prognosis. In the present study, hypermethylation of *TAC1* in ccRCC tissues was the most frequent (60%) among all genes investigated and, together with decreased expression, was related to the larger tumors. Thus, due to frequent hypermethylation, *TAC1* represents a promising diagnostic biomarker of ccRCC.

FLRT2 (Fibronectin leucine-rich transmembrane protein 2) encodes a glycosylated transmembrane protein with extracellular leucine-rich repeats domain acting as both adhesion and signaling molecule [344]. FLRT2 acts as an adhesion protein interacting with ECM-localized fibronectin in either a repulsive or adhesive manner [345], suggesting its possible link with tumor metastasis. In the case of breast cancer, down-regulation of *FLRT2* due to promoter methylation increased cell proliferation and migration, while overexpression had the opposite effect [346], indicating *FLRT2* as a potential tumor suppressor. The present study showed down-regulation and frequent hypermethylation of *FLRT2* in ccRCC tissues for the first time. The down-regulation was related to tumor necrosis, while hypermethylation with larger tumor size, confirming its possible tumor-suppressive activity.

ADAMTS19 (ADAM metallopeptidase with thrombospondin type 1 motif 19) encodes a member of the ADAMTS secreted metalloproteinases family, which can cleave or interact with a wide range of extracellular matrix (ECM) components or regulatory factors, affecting cell adhesion, migration, proliferation, and angiogenesis [347]. Although the exact biological function of ADAMTS19 remains uncharacterized, due to its close relation to ADAMTS17, it is speculated that ADAMTS19 may participate in the biogenesis of ECM fibrillin microfibrils [348]. Thus downregulation of *ADAMTS19* may be associated with the loss of tissue integrity and allowing tumor progression. This is the first study reporting *ADAMTS19* promoter methylation in ccRCC that linked it with various adverse clinical-pathological parameters, including larger tumor size, intravascular invasion, and a higher tumor grade, confirming its relation with tumor development and progression.

BMP7 (bone morphogenetic protein 7) is a member of the TGF superfamily growth and differentiation factor possibly stored bound to fibrillin in ECM [349,350]. Kidney tissues are the major sources for BMP7 in adults

and may contribute to the maintaining of structure and function of renal tissues and have an anti-inflammatory effect; meanwhile, its loss leads to the development of kidney injuries and neoplasia [351,352]. It is observed that BMP7 inhibits differentiation and epithelial-to-mesenchymal transition (EMT) of the kidney proximal tubular epithelial cells by reducing the production of EMT inductor TGF-β [349,351,353]. Thus downregulation of this gene may stimulate cancer development and progression by promoting EMT, which contributes to ccRCC development [174]. Indeed, the decreased expression of *BMP7* was found in RCC [353,354]; however, the promoter methylation has not been investigated so far. The present study related the methylated status of *BMP7* with larger tumors, higher WHO/ISUP grade, and tumor necrosis, supplementing its relation to the tumor progression.

SIM1 (single-minded family bHLH transcription factor 1) encodes a transcription factor involved in the developmental processes [355], but its role in cancerogenesis remains unclear. There is a link between SIM1 and human obesity [356], and the methylation of obesity-related genes previously was linked with poorer RCC prognosis [357]. To date, the DNA methylation of *SIM1* has been described in several cancers, including breast [358], lung [359], and cervical [360], and was related to tumor metastasis; however, no data exist on RCC. In the present study, *SIM1* was rarely methylated in ccRCC tissues but was associated with larger tumors; however, its role in ccRCC development and progression remains to be elucidated in the future.

SFRP1 (Secreted frizzled-related protein 1) is the frizzled protein family member acting as the inhibitor of the WNT signaling pathway [361]. It is well known that the active WNT pathway promotes cell proliferation, survival, and invasion, thereby contributing to RCC pathogenesis [197,361]. Thus, *SFRP1* serves as a tumor suppressor gene, which down-regulation increases ccRCC cells' growth by releasing WNT signaling [264,361]. Although SFRP1 showed no evidence of differential methylation in microarray-based screening, the inclusion of this gene in the validation set was based on the previous widely conducted studies on its methylation in renal cancer [361]. The methylation frequencies of *SFRP1* varied among these studies [264,293,313] and were higher in our study. Although methylation of *SFRP1* lacks associations with clinical-pathological characteristics, it augments the diagnostic/prognostic value in combination with other genes.

To sum up, the selected genes are involved in various cellular processes and all together contribute to cell proliferation, differentiation, apoptosis inhibition, epithelial-mesenchymal transition, migration, invasion, and metastasis (**Fig. 4.1**). It is also nicely reflected by the fact that methylated status of even seven out of ten genes analyzed, particularly *ZNF677*, *PCDH8*,

TAC1, *FLRT2*, *ADAMTS19*, *BMP7*, and *SIM1*, was significantly related to larger tumor size, defined as a relevant prognostic parameter in numerous studies [362-364]. However, only a few genes showed significant associations with other highly predictive clinical-pathological parameters, such as tumor stage (*ZNF677* and *PCDH8*), WHO/ISUP grade (*PCDH8*, *ADAMTS19*, and *BMP7)*, Fuhrman grade, intravascular tumor invasion (*ADAMTS19*), and tumor necrosis (*ZNF677* and *BMP7*). Considering this, it is improbable that a single gene will be applied directly in the clinic and replace the clinical-pathological factors. On the other hand, the panels of biomarkers are generally recommended to improve the accuracy of diagnostic and/or prognostic tests; e.g., three genes DNA methylation test are used for other urological cancers such as prostate and bladder for a long time [13].

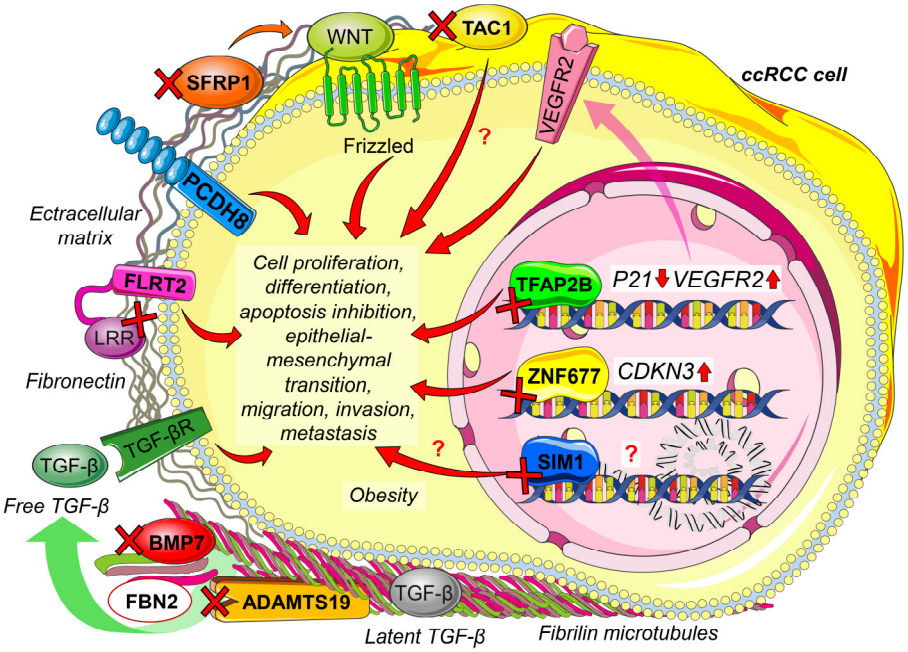

Fig. 4.1. The putative role of the selected genes methylation and/or downregulation in the ccRCC development and progression.

The superiority of gene combinations over a single biomarker was aptly reflected by survival analysis. Kaplan-Meier survival curves revealed a significant association of the methylated status of only two single genes, particularly *ZNF677* and *FBN2*, with patient's overall survival; although no associations with OS were observed for another single gene, various combinations of two-four biomarkers were significantly associated with the poorer overall survival of ccRCC patients. The multivariate Cox regression analysis revealed the panels of *ZNF677 & BMP7* and *ZNF677*, *PCDH8 &*

FLRT2 as the two best prognostic multimarker panels. However, none of them retained an independent prognostic value while adjustment according to demographic and clinical-pathological variables was done. Although the previous study presents a relatively high independent prognostic value of four biomarkers panel methylation in ccRCC tissues [265], tumor necrosis, an important prognostic factor for kidney cancer, was not considered in this study; in addition, the liquid biopsies that are particularly useful for timely cancer detection and follow-up were not analyzed.

4.2. The applicability of selected biomarkers for non-invasive ccRCC detection and prognosis

The histopathological assessment of tumor biopsy tissue and surgical resection specimens is the gold standard for the diagnosis of kidney cancers. However, such an approach has some important disadvantages, including the subjective evaluation by a pathologist, the need for tissue that is of a certain quality and representative of the tumor, and constraints on sampling frequency [306]. Considering these limitations, there is an urgent need to develop non-invasive methods that could provide clinicians with rapid, objective, and accurate routines for the detection of kidney cancer.

Among the ten genes analyzed in the ccRCC tissue samples, six genes with both the highest methylation frequencies and the most promising prognostic values, particularly *ZNF677*, *FBN2*, *PCDH8*, *TFAP2B*, *TAC1*, and *FLRT2*, were selected for further methylation analysis in the urine samples from 123 ccRCC patients and 92 cancer-free (asymptomatic controls) individuals.

The current study revealed for the first time significantly higher methylation levels of all selected genes in the urine sediments of ccRCC patients, compared to asymptomatic controls with sensitivity between 36.6 and 71.5 %; that is higher than most of the previously reported urine-based epigenetic biomarkers ([reviewed in [306]). The highest AUC value equal to 0.71 was identified for *PCDH8* with 68% sensitivity and 73% specificity. The multi-marker panels of two-four biomarkers showed even better characteristics; the highest diagnostic power (AUC = 0.78) was observed for a panel of *ZNF677 & PCDH8*, either with or without *FBN2* or *FLRT2*, with 69%-78% of sensitivity, which considerably outperformed the value of the previously reported two-biomarkers panel [17]. The specificity of that biomarker panels was also high and ranged between 69% and 80%. Although some previous studies established urine-based biomarker panels with better diagnostic characteristics [14,15,18], they used a considerably lower number (≤50) of quite heterogeneous samples; used classic tumor suppressor genes,

that applicability to ccRCC detection are very questionable; finally, the aforementioned studies lack the results verification in the validation cohort.

Survival analysis revealed that the methylated promoter status of *PCDH8* in the urine sediments was a significant predictor of ccRCC patients' overall survival. Moreover, the panel of *ZNF677 & PCDH8* showed even better prognostic power, and in the multivariate analysis, together with patients' age, gender, and tumor necrosis, retained an independent prognostic value for OS. There is only one report presenting urine-based prognostic DNA methylation biomarker of ccRCC thus far. Outeiro-Pinho *et al.* [19] described an association between higher levels of methylated urinary miR-30a and disease-specific survival in the multivariable analysis. However, no such associations were found in the independent study cohort, which perfectly reflects the necessity of validating such results. To sum up, the present study suggests the possibility of predicting ccRCC progression based on only two urinary biomarkers, namely *ZNF677 & PCDH8*, but further validation steps are crucial to transfer such panel to the clinical practice.

The inconsistency of the biomarkers methylation pattern in the tissue and urine samples is quite confusing and has been possibly occurred for several reasons. Firstly, in the present study, urine sediments were used for biomarker analysis, thus contaminating urinary bladder cells may have had an impact on the results [365]. Secondly, as renal tumors are highly heterogeneous, regional tissue samples of the tumor may not reflect that heterogeneity [9], while the analysis of body fluids may reflect a broader spectrum of (epi)genetic alterations. Thirdly, while DNA methylation may significantly vary between the regions in the same CpG island [266], and as the PCR primers for tissue and urine analysis are not fully overlapped, this can cause differences in methylation results between these two sources of samples as well. Finally, the differences in the sensitivity and specificity of MSP and QMSP methods [366] might also cause these variations. However, considering the ability of these biomarkers to discriminate patients with ccRCC from asymptomatic controls, it is very likely that such methylation differences mainly come from cancerous renal cells. To be more guaranteed, further DNA methylation investigations on the cell-free urine samples would be desirable.

4.3. The limitations of the selected biomarkers and study design

Along with the significant impact of the study in the search for novel ccRCC biomarkers, the investigation has important shortcomings as well.

The biomarkers selection was based on the genome-wide DNA methylation profile of only 11 pairs of ccRCC and NRT samples, producing

numerous methylation differences with only a small handful of them analyzed in more detail. Thus, it is obvious that there are more clinically significant biomarkers waiting for further investigations. In addition, the specificity of selected biomarkers for precisely kidney cancer was not established in the present study; thus, further cross-validations, at least in other urological cancers, are highly desirable. Moreover, the candidate DNA methylation biomarkers ideally should be differently expressed, particularly downregulated [13], which has not been confirmed for two of the biomarkers (*FBN2* and *PCDH8*) analyzed, while downregulation of other biomarkers has not been directly linked with DNA methylation, except *ZNF677*. Thus further investigations are needed to select precisely those CpGs, that would be especially clinically significant. The lack of knowledge about the exact biological function and role in carcinogenesis of ccRCC of the particular biomarkers is another major obstacle to their use in clinical settings; thus, further functional investigations would be desirable.

Among the study design limitations, the relatively small number of samples tested and lack of validation are the main downsides. Thus, considering the relatively short follow-up and a low number of deaths in the study cohort, the results of the multivariate analysis should be viewed with some reservation. In addition, only a patient's death as an endpoint was used for the survival analysis that has a lower power as compared to disease-free survival [367], for example. However, such data was not available in the present study. Nonetheless, the novelty of using DNA methylation biomarkers with presumable diagnostic and prognostic value in ccRCC, susceptible for non-invasive urine-based detection, will undoubtedly stimulate the design of validation studies in more extensive series with more detailed monitoring data.

Despite these limitations, this study makes a valuable contribution to the field of searching ccRCC-specific DNA methylation biomarkers. The methylation status of most biomarkers in the case of ccRCC has been investigated for the first time, and some of them showed auspicious results due to their association with numerous clinical-pathological parameters and patients' overall survival. Furthermore, some biomarkers, especially *ZNF677* and *PCDH8*, have a significant potential to serve for non-invasive urine-based ccRCC diagnostics and follow-up. However, navigation toward clinical utility is challenging, requiring representative, large, and preferably multiregional patient series as well as sufficient validations. Thus, further comprehensive verification of the current results on a large number of clinical samples is mandatory; considering the large mortality rates among patients diagnosed with ccRCC, it's very likely that provided genes will attract researchers' attention and may stimulate these validation studies.

CONCLUSIONS

1. Microarray-based DNA methylation and gene expression profiling revealed significant methylation differences (FC ≥ 1.5) in 367 genes and significant alterations (FC ≥ 2.0) in mRNA expression of 3942 genes comparing ccRCC and NRT samples. Deregulated genes were commonly enriched among biological and molecular processes related to cancer development and progression.

2. Methylation frequencies of *ZNF677*, *FBN2*, *PCDH8*, *TFAP2B*, *TAC1*, *FLRT2*, *SFRP1*, *ADAMTS19*, *BMP7*, and *SIM1* was significantly higher in ccRCC tissue samples as compared to NRT and reached 18-60%. The combined sensitivity for ccRCC of *ZNF677*, *FBN2*, *PCDH8*, *TFAP2B*, *TAC1 & SFRP1* was 85.4%, while specificity - 95.6%.

3. Hypermethylation of most (7 out of 10) genes was significantly related to at least one clinical-pathological parameter, including larger tumor size, higher stage, grade, intravascular invasion, and necrosis. Moreover, the methylated status of *ZNF677*, *FBN2*, and various two-four gene panels in ccRCC tissues showed significant associations with shorter patients OS.

4. The lower expression levels of *ZNF677*, *TFAP2B*, *TAC1*, and *FLRT2* and a higher level of *PCDH8* is characteristic for ccRCC tissues compared to NRT. The downregulation of *ZNF677* was significantly related to methylated promoter status, numerous clinical-pathological tumors parameters, and patients' OS.

5. Significantly higher methylation levels of *ZNF677*, *FBN2*, *PCDH8*, *TFAP2B*, *TAC1*, and *FLRT2* was detected in ccRCC patients urine samples compared to ASC, and a panel of *ZNF677 & PCDH8*, either with or without *FBN2* or *FLRT2*, produced moderate to high sensitivities and specificities equal to 69-78% and 69-80% respectively.

6. Methylated status of *PCDH8* was related to higher tumor stage and fat invasion and independently predicts patient's OS with HR: 5.7, which considerably increased in combination with *ZNF677* (HR: 12.5).

BIBLIOGRAPHY

[1] Siegel RL, Miller KD, Jemal A. Cancer statistics, 2015. *CA Cancer J Clin*, 2015;65:5-29.

[2] Chow WH, Dong LM, Devesa SS. Epidemiology and risk factors for kidney cancer. *Nat. Rev. Urol.* 2010;7,245–257.

[3] Hsieh JJ, Purdue MP, Signoretti S, Swanton Ch, Albiges L, Schmidinger M, Heng DY, Larkin J, Ficarra V. Renal cell carcinoma. *Nat Rev Dis Primers.* 2017; 3:17009.

[4] Dabestani S, Thorstenson A, Lindblad P, Harmenberg U, Ljungberg B, Lundstam S. Renal cell carcinoma recurrences and metastases in primary non-metastatic patients: a population-based study. *World J Urol* 2016;34:1081-1086.

[5] Linehan W, Bratslavsky G, Pinto PA, Schmidt LS, Neckers L, Bottaro DP, Srinivasan R. Molecular diagnosis and therapy of kidney cancer. *Annu Rev Med.* 2010;61:329–43.

[6] Mitchell TJ, Turajlic S, Rowan A, Nicol D, Farmery JHR, O'Brien T, Martincorena I, Tarpey P, Angelopoulos N, Yates LR, Butler AP, Raine K, Stewart GD, Challacombe B, Fernando A, Lopez JI, Hazell S, Chandra A, Chowdhury S, Rudman S, Soultati A, Stamp G, Fotiadis N, Pickering L, Au L, Spain L, Lynch J, Stares M, Teague J, Maura F, Wedge DC, Horswell S, Chambers T, Litchfield K, Xu H, Stewart A, Elaidi R, Oudard S, McGranahan N, Csabai I, Gore M, Futreal PA, Larkin J, Lynch AG, Szallasi Z, Swanton C, Campbell PJ; TRACERx Renal Consortium. Timing the Landmark Events in the Evolution of Clear Cell Renal Cell Cancer: TRACERx Renal. *Cell.* 2018;173(3):611-623.e17.

[7] Gerlinger M, Horswell S, Larkin J, Rowan AJ, Salm MP, Varela I, Fisher R, McGranahan N, Matthews N, Santos CR, Martinez P, Phillimore B, Begum S, Rabinowitz A, Spencer-Dene B, Gulati S, Bates PA, Stamp G, Pickering L, Gore M, Nicol DL, Hazell S, Futreal PA, Stewart A, Swanton C. Genomic architecture and evolution of clear cell renal cell carcinomas defined by multiregion sequencing. *Nat Genet.* 2014;46(3):225-233.

[8] Turajlic S, Xu H, Litchfield K, Rowan A, Chambers T, Lopez JI, Nicol D, O'Brien T, Larkin J, Horswell S, Stares M, Au L, Jamal-Hanjani M, Challacombe B, Chandra A, Hazell S, Eichler-Jonsson C, Soultati A, Chowdhury S, Rudman S, Lynch J, Fernando A, Stamp G, Nye E, Jabbar F, Spain L, Lall S, Guarch R, Falzon M, Proctor I, Pickering L, Gore M, Watkins TBK, Ward S, Stewart A, DiNatale R, Becerra MF, Reznik E, Hsieh JJ, Richmond TA, Mayhew GF, Hill SM, McNally CD, Jones C, Rosenbaum H, Stanislaw S, Burgess DL, Alexander NR, Swanton C; PEACE; TRACERx Renal Consortium. Tracking Cancer Evolution

Reveals Constrained Routes to Metastases: TRACERx Renal. Cell. 2018;173(3):581-594.e12.

[9] Turajlic S, Xu H, Litchfield K, Rowan A, Horswell S, Chambers T, O'Brien T, Lopez JI, Watkins TBK, Nicol D, Stares M, Challacombe B, Hazell S, Chandra A, Mitchell TJ, Au L, Eichler-Jonsson C, Jabbar F, Soultati A, Chowdhury S, Rudman S, Lynch J, Fernando A, Stamp G, Nye E, Stewart A, Xing W, Smith JC, Escudero M, Huffman A, Matthews N, Elgar G, Phillimore B, Costa M, Begum S, Ward S, Salm M, Boeing S, Fisher R, Spain L, Navas C, Grönroos E, Hobor S, Sharma S, Aurangzeb I, Lall S, Polson A, Varia M, Horsfield C, Fotiadis N, Pickering L, Schwarz RF, Silva B, Herrero J, Luscombe NM, Jamal-Hanjani M, Rosenthal R, Birkbak NJ, Wilson GA, Pipek O, Ribli D, Krzystanek M, Csabai I, Szallasi Z, Gore M, McGranahan N, Van Loo P, Campbell P, Larkin J, Swanton C; TRACERx Renal Consortium. Deterministic Evolutionary Trajectories Influence Primary Tumor Growth: TRACERx Renal. Cell. 2018;173(3):595-610.e11.

[10] Arai E, Kanai Y. Genetic and epigenetic alterations during renal carcinogenesis. *Int J Clin Exp Pathol.* 2010;4(1):58-73. PMID: 21228928

[11] Chen W, Zhuang J, Wang PP, Jiang J, Lin C, Zeng P, Liang Y, Zhang X, Dai Y, Diao H. DNA methylation-based classification and identification of renal cell carcinoma prognosis-subgroups. *Cancer Cell Int.* 2019;19:185.

[12] Ricketts CJ, De Cubas AA, Fan H, Smith CC, Lang M, Reznik E, Bowlby R, Gibb EA, Akbani R, Beroukhim R, Bottaro DP, Choueiri TK, Gibbs RA, Godwin AK, Haake S, Hakimi AA, Henske EP, Hsieh JJ, Ho TH, Kanchi RS, Krishnan B, Kwiatkowski DJ, Lui W, Merino MJ, Mills GB, Myers J, Nickerson ML, Reuter VE, Schmidt LS, Shelley CS, Shen H, Shuch B, Signoretti S, Srinivasan R, Tamboli P, Thomas G, Vincent BG, Vocke CD, Wheeler DA, Yang L, Kim WY, Robertson AG; Cancer Genome Atlas Research Network, Spellman PT, Rathmell WK, Linehan WM. The Cancer Genome Atlas. Comprehensive Molecular Characterization of Renal Cell Carcinoma. *Cell Rep.* 2018;23(1):313-326.e5.

[13] Koch A, Joosten SC, Feng Z, de Ruijter TC, Draht MX, Melotte V, Smits KM, Veeck J, Herman JG, Van Neste L, Van Criekinge W, De Meyer T, van Engeland M. Analysis of DNA methylation in cancer: location revisited. *Nat Rev Clin Oncol.* 2018;15(7):459-466.

[14] Battagli C, Uzzo RG, Dulaimi E, Ibanez de Caceres I, Krassenstein R, Al-Saleem T, Greenberg RE, Cairns P. Promoter hypermethylation of tumor suppressor genes in urine from kidney cancer patients. *Cancer Res.* 2003;63(24):8695-9.

[15] Hoque MO, Begum S, Topaloglu O, Jeronimo C, Mambo E, Westra WH, Califano JA, Sidransky D. Quantitative detection of promoter

hypermethylation of multiple genes in the tumor, urine, and serum DNA of patients with renal cancer. *Cancer Res.* 2004;64(15):5511-7.

[16] Costa VL, Henrique R, Danielsen SA, Duarte-Pereira S, Eknaes M, Skotheim RI, Rodrigues A, Magalhães JS, Oliveira J, Lothe RA, Teixeira MR, Jerónimo C, Lind GE. Three epigenetic biomarkers, GDF15, TMEFF2, and VIM, accurately predict bladder cancer from DNA-based analyses of urine samples. *Clin Cancer Res.* 2010;16(23):5842-51.

[17] Costa VL, Henrique R, Danielsen SA, Eknaes M, Patrício P, Morais A, Oliveira J, Lothe RA, Teixeira MR, Lind GE, Jerónimo C. TCF21 and PCDH17 methylation: An innovative panel of biomarkers for a simultaneous detection of urological cancers. *Epigenetics.* 2011;6(9):1120-30.

[18] Xin J, Xu R, Lin S, Xin M, Cai W, Zhou J, Fu C, Zhen G, Lai J, Li Y, Zhang P. Clinical potential of TCF21 methylation in the diagnosis of renal cell carcinoma. *Oncol Lett.* 2016;12(2):1265-1270.

[19] Outeiro-Pinho G, Barros-Silva D, Aznar E, Sousa AI, Vieira-Coimbra M, Oliveira J, Gonçalves CS, Costa BM, Junker K, Henrique R, Jerónimo C. MicroRNA-30a-5p(me): a novel diagnostic and prognostic biomarker for clear cell renal cell carcinoma in tissue and urine samples. *J Exp Clin Cancer Res.* 2020;39(1):98.

[20] Nuzzo PV, Berchuck JE, Korthauer K, Spisak S, Nassar AH, Abou Alaiwi S, Chakravarthy A, Shen SY, Bakouny Z, Boccardo F, Steinharter J, Bouchard G, Curran CR, Pan W, Baca SC, Seo JH, Lee GM, Michaelson MD, Chang SL, Waikar SS, Sonpavde G, Irizarry RA, Pomerantz M, De Carvalho DD, Choueiri TK, Freedman ML. Detection of renal cell carcinoma using plasma and urine cell-free DNA methylomes. *Nat Med.* 2020;26(7):1041-1043.

[21] Sampaio FJ. Renal anatomy. Endourologic considerations. *Urol Clin North Am.* 2000;27(4):585-607.

[22] Koeppen BA, Stanton BA. Berne and Levy's Physiology. *Elsevier.* 2010.

[23] Lemley KV, Kriz W. Anatomy of the renal interstitium. *Kidney Int.* 1991;39:370–381.

[24] Takahashi-Iwanaga H. The three-dimensional cytoarchitecture of the interstitial tissue in the rat kidney. *Cell Tissue Res.* 1991;264: 269–281.

[25] Kriz W, Napiwotzky P. Structural and functional aspects of the renal interstitium. *Contrib Nephrol*. 1979;16:104–108.

[26] Knepper MA, Danielson RA, Saidel GM, Post RS. Quantitative analysis of renal medullary anatomy in rats and rabbits. *Kidney Int*. 1977;12:313–323.

[27] Zeisberg M, Kalluri R. Physiology of the Renal Interstitium. *Clin J Am Soc Nephrol.* 2015;10(10):1831-40.

[28] Fried W, Kilbridge T, Krantz S, McDonald TP, Lange RD. Studies on extrarenal erythropoietin. *J Lab Clin Med.* 1969;73(2):244-8.

[29] Betts JG, Desaix P, Johnson E, Johnson JE, Korol O, Kruse D, Poe B, Wise JA, Womble M, Young KA. Anatomy & Physiology. *Rice University, Houston, Texas*. 2017.

[30] Johns EJ, Ahmeda AF. Renal circulation. Reference Module in Biomedical Sciences. 2014.

[31] Little MH. Growing Kidney Tissue from Stem Cells: How Far from "Party Trick" to Medical Application? *Cell Stem Cell.* 2016;18(6):695-698.

[32] Moch H, Cubilla AL, Humphrey PA, Reuter VE, Ulbright TM. The 2016 WHO Classification of Tumours of the Urinary System and Male Genital Organs-Part A: Renal, Penile, and Testicular Tumours. *Eur Urol.* 2016;70(1):93-105.

[33] Cheville JC, Lohse CM, Zincke H, Weaver AL, Blute ML. Comparisons of outcome and prognostic features among histologic subtypes of renal cell carcinoma. *Am. J. Surg. Pathol.* 2003;27; 612–624.

[34] Sanganeria BS, Misra R, Shukla KK. Molecular Diagnostics in Renal Cancer. In: Shukla K., Sharma P., Misra S. (eds) Molecular Diagnostics in Cancer Patients. Springer, Singapore. 2019.

[35] Lindgren D, Sjölund J, Axelson H. Tracing Renal Cell Carcinomas back to the Nephron. *Trends Cancer.* 2018;4(7):472-484.

[36] Ayerbes MV, Gallego GA, Prado SD, Fonseca PJ, Campelo RG, Aparicio LMA. Origin of renal cell carcinomas. *Clin Transl Oncol.* 2008;10:697-712.

[37] Lindgren D, Boström AK, Nilsson K, Hansson J, Sjölund J, Möller C, Jirström K, Nilsson E, Landberg G, Axelson H, Johansson ME. Isolation and characterization of progenitor-like cells from human renal proximal tubules. *Am J Pathol.* 2011;178(2):828-37.

[38] Lombardi D, Becherucci F, Romagnani P. How much can the tubule regenerate and who does it? An open question. *Nephrol Dial Transplant.* 2016;31(8):1243-50.

[39] El-Nahas AM. Plasticity of kidney cells: role in kidney remodeling and scarring. *Kidney Int.* 2003;64(5):1553-63.

[40] Fan JM, Ng YY, Hill PA, Nikolic-Paterson DJ, Mu W, Atkins RC, Lan HY. Transforming growth factor-beta regulates tubular epithelial-myofibroblast transdifferentiation *in vitro*. *Kidney Int.* 1999;56(4):1455-67.

[41] Zeisberg M, Strutz F, Muller GA. Renal fibrosis: an update. *Curr Opin Nephrol Hypert*. 2001;10:315–320.

[42] Liu X, Fan D. The epithelial-mesenchymal transition and cancer stem cells: functional and mechanistic links. *Curr Pharm Des.* 2015;21(10):1279-91.

[43] Landolt L, Eikrem Ø, Strauss P, Scherer A, Lovett DH, Beisland C, Finne K, Osman T, Ibrahim MM, Gausdal G, Ahmed L, Lorens JB, Thiery JP, Tan TZ, Sekulic M, Marti HP. Clear Cell Renal Cell Carcinoma is linked to Epithelial-to-Mesenchymal Transition and to Fibrosis. *Physiol Rep.* 2017;5(11):e13305.

[44] Sheng L, Zhuang S. New Insights Into the Role and Mechanism of Partial Epithelial-Mesenchymal Transition in Kidney Fibrosis. *Front Physiol.* 2020;11:569322.

[45] Lichner Z, Saleh C, Subramaniam V, Seivwright A, Prud'homme GJ, Yousef GM. miR-17 inhibition enhances the formation of kidney cancer spheres with stem cell/ tumor initiating cell properties. *Oncotarget.* 2015; 6(8):5567-81.

[46] Piva F, Giulietti M, Santoni M, Occhipinti G, Scarpelli M, Lopez-Beltran A, Cheng L, Principato G, Montironi R. Epithelial to Mesenchymal Transition in Renal Cell Carcinoma: Implications for Cancer Therapy. *Mol Diagn Ther.* 2016;20(2):111-7.

[47] Simon N, Hertig A. Alteration of fatty acid oxidation in tubular epithelial cells: from acute kidney injury to renal fibrogenesis. *Front. Med.* 2015;2:52.

[48] Zhou D, Liu, Y. Renal fibrosis in 2015: Understanding the mechanisms of kidney fibrosis. *Nat. Rev. Nephrol.* 2016;12, 68–70.

[49] Kirkali Z, Yorukoglu K. Premalignant lesions in the kidney. *Scientific World Journal.* 2001;1:855-67.

[50] Yörükoğlu K, Aktaş S, Mungan U, Kõrkalõ Z. Tubular dysplasia and carcinoma in situ: precursors of renal cell carcinoma. *Urology.* 1999; 53:684-689.

[51] Mourad WA, Nestok BR, Saleh GY, Solez K, Power RF, Jewell LD. Dysplastic tubular epithelium in "normal" kidney associated with renal cell carcinoma. *Am. J. Surg. Pathol.* 1994;18:1117–1124.

[52] Goldfarb S, Pugh TD. Morphology and anatomic localization of renal microneoplasms and proximal tubule dysplasias induced by four different estrogens in the hamster. *Cancer Res.* 1990;50:113–119.

[53] Gudbjartsson T, Hardarson S, Petursdottir V, Thoroddsen A, Magnusson J, Einarsson GV. Histological subtyping and nuclear grading of renal cell carcinoma and their implications for survival: a retrospective nation-wide study of 629 patients. *Eur Urol* 2005;48(4):593-600.

[54] Grignon DJ, Che M. Clear cell renal cell carcinoma. Clin Lab Med. 2005;25(2):305-16.

[55] Novara G, Ficarra V, Antonelli A, Artibani W, Bertini R, Carini M, Cosciani Cunico S, Imbimbo C, Longo N, Martignoni G, Martorana G, Minervini A, Mirone V, Montorsi F, Schiavina R, Simeone C, Serni S, Simonato A, Siracusano S, Volpe A, Carmignani G; SATURN Project-LUNA Foundation. Validation of the 2009 TNM version in a large multi-institutional cohort of patients treated for renal cell carcinoma: are further improvements needed? *Eur Urol.* 2010;58(4):588-95.

[56] Jayson M, Sanders H. Increased incidence of serendipitously discovered renal cell carcinoma. *Urology.* 1998;51(2):203-5.

[57] Patard JJ, Leray E, Rodriguez A, Rioux-Leclercq N, Guillé F, Lobel B. Correlation between symptom graduation, tumor characteristics and survival in renal cell carcinoma. *Eur Urol.* 2003;44(2):226-32.

[58] Lee CT, Katz J, Fearn PA, Russo P. Mode of presentation of renal cell carcinoma provides prognostic information. *Urol Oncol.* 2002;7(4):135-40.

[59] Evelönn EA, Landfors M, Haider Z, Köhn L, Ljungberg B, Roos G, Degerman S. DNA Methylation Associates With Survival in Non-Metastatic Clear Cell Renal Cell Carcinoma. *BMC Cancer.* 2019;19(1):65.

[60] Rossi SH, Prezzi D, Kelly-Morland C, Goh V. Imaging for the diagnosis and response assessment of renal tumours. *World J Urol.* 2018;36(12):1927-1942.

[61] Choudhary S, Rajesh A, Mayer NJ, Mulcahy KA, Haroon A. Renal oncocytoma: CT features cannot reliably distinguish oncocytoma from other renal neoplasms *Clin Radiol.* 2009;64(5):517-22.

[62] Hindman N, Ngo L, Genega EM, Melamed J, Wei J, Braza JM, Rofsky NM, Pedrosa I. Angiomyolipoma with minimal fat: can it be differentiated from clear cell renal cell carcinoma by using standard MR techniques? *Radiology.* 2012;265(2):468-77.

[63] Motzer RJ, Jonasch E, Agarwal N, Bhayani S, Bro WP, Chang SS, Choueiri TK, Costello BA, Derweesh IH, Fishman M, Gallagher TH, Gore JL, Hancock SL, Harrison MR, Kim W, Kyriakopoulos C, LaGrange C, Lam ET, Lau C, Michaelson MD, Olencki T, Pierorazio PM, Plimack ER, Redman BG, Shuch B, Somer B, Sonpavde G, Sosman J, Dwyer M, Kumar R. Kidney Cancer, Version 2.2017, NCCN Clinical Practice Guidelines in Oncology. *J Natl Compr Canc Netw.* 2017;15(6):804-834.

[64] Montironi R, Cheng L, Scarpelli M, Lopez-Beltran A. Pathology and Genetics: Tumours of the Urinary System and Male Genital System: Clinical Implications of the 4th Edition of the WHO Classification and Beyond. *Eur Urol.* 2016;70(1):120-123.

[65] Brierley JD, Gospodarowicz MK, Wittekind C. TNM classification of malignant tumours, 8th edn. Wiley-Blackwell, Hoboken. 2017.

[66] Amin MB, Edge S, Greene F, Byrd DR, Brookland RK, Washington MK, Gershenwald JE, Compton CC, Hess KR, Sullivan DC, Jessup JM, Brierley JD, Gaspar LE, Schilsky RL, Balch CM, Winchester DP, Asare EA, Madera M, Gress DM, Meyer LR. AJCC cancer staging manual, 8th edn. Springer, New York. 2016.

[67] Fuhrman SA, Lasky LC, Limas C. Prognostic significance of morphologic parameters in renal cell carcinoma. *Am. J. Surg. Pathol.* 1982;6:655–663.

[68] Delahunt B, Eble JN, Egevad L, Samaratunga H. Grading of renal cell carcinoma. *Histopathology.* 2019;74(1):4-17.

[69] Delahunt B. Advances and controversies in grading and staging of renal cell carcinoma. *Mod Pathol.* 2009;22:S24–S36.

[70] Delahunt B, Sika-Paotonu D, Bethwaite PB, William Jordan T, Magi-Galluzzi C, Zhou M, Samaratunga H, Srigley JR. Grading of clear cell renal cell carcinoma should be based on nucleolar prominence. *Am J Surg Pathol.* 2011;35(8):1134-9.

[71] Nazeer T, Amin MB, Delahunt B *et al*. Interobserver variability of nuclear grading (NG) in renal cell carcinoma. *Mod. Pathol.*1998;11:91A.

[72] Al-Aynati M, Chen V, Salama S, Shuhaibar H, Treleaven D, Vincic L. Interobserver and intraobserver variability using the Fuhrman grading system for renal cell carcinoma. *Arch Pathol Lab Med.* 2003;127(5):593-6.

[73] Lang H, Linder V, de Fromont M, Molinié V, Letourneux H, Meyer N, Martin M, Jacqmin D. Multicentric determination of optimal interobserver agreement using Fuhrman grading system for renal cell carcinoma:

assessment of 241 patients with >15-year follow-up. *Cancer* 2005; 103; 625–629.

[74] International Agency for Research on Cancer. WHO classification of tumours of the urinary system and male genital organs (IARC WHO classification of tumours), 4th edn. WHO/ IARC Press, Lyon. 2016.

[75] Delahunt B, Cheville JC, Martignoni G, Humphrey PA, Magi-Galluzzi C, McKenney J, Egevad L, Algaba F, Moch H, Grignon DJ, Montironi R, Srigley JR; Members of the ISUP Renal Tumor Panel. The International Society of Urological Pathology (ISUP) grading system for renal cell carcinoma and other prognostic parameters. *Am J Surg Pathol.* 2013;37(10):1490-504.

[76] Humphrey PA, Moch H, Reuter VE, Ulbright TM. World Health Organisation (WHO) Classification of tumours. Pathology and genetics of the urinary system and male genital organs. Lyon, France: IARC Press, 2016.

[77] Dagher J, Delahunt B, Rioux-Leclercq N, Egevad L, Srigley JR, Coughlin G, Dunglinson N, Gianduzzo T, Kua B, Malone G, Martin B, Preston J, Pokorny M, Wood S, Yaxley J, Samaratunga H. Clear cell renal cell carcinoma: validation of World Health Organization/International Society of Urological Pathology grading. *Histopathology.* 2017;71(6):918-925.

[78] Ljungberg B, Albiges L, Abu-Ghanem Y, Bensalah K, Dabestani S, Fernández-Pello S, Giles RH, Hofmann F, Hora M, Kuczyk MA, Kuusk T, Lam TB, Marconi L, Merseburger AS, Powles T, Staehler M, Tahbaz R, Volpe A, Bex A. European association of urology guidelines on renal cell carcinoma: the 2019 update. *Eur Urol.* 2019;75(5):799-810.

[79] Delahunt B, McKenney JK, Lohse CM, Leibovich BC, Thompson RH, Boorjian SA, Cheville JC. A novel grading system for clear cell renal cell carcinoma incorporating tumor necrosis. *Am J Surg Pathol.* 2013;37(3):311-22.

[80] Khor LY, Dhakal HP, Jia X, Reynolds JP, McKenney JK, Rini BI, Magi-Galluzzi C, Przybycin CG. Tumor Necrosis Adds Prognostically Significant Information to Grade in Clear Cell Renal Cell Carcinoma: A Study of 842 Consecutive Cases From a Single Institution. *Am J Surg Pathol.* 2016;40(9):1224-31.

[81] Dagher J, Delahunt B, Rioux-Leclercq N, Egevad L, Coughlin G, Dunglison N, Gianduzzo T, Kua B, Malone G, Martin B, Preston J, Pokorny M, Wood S, Samaratunga H. Assessment of tumour-associated necrosis provides prognostic information additional to World Health Organization/International Society of Urological Pathology grading for clear cell renal cell carcinoma. *Histopathology*. 2019;74(2):284-290.

[82] Lohse CM, Gupta S, Cheville JC. Outcome prediction for patients with renal cell carcinoma. *Semin. Diagn. Pathol.* 2015;32:172–183.

[83] Sengupta S, Lohse CM, Leibovich BC, Frank I, Thompson RH, Webster WS, Zincke H, Blute ML, Cheville JC, Kwon ED. Histologic coagulative tumor necrosis as a prognostic indicator of renal cell carcinoma aggressiveness. *Cancer.* 2005;104(3):511-20.

[84] Leibovich BC, Lohse CM, Crispen PL, Boorjian SA, Thompson RH, Blute ML, Cheville JC. Histological subtype is an independent predictor of outcome for patients with renal cell carcinoma. *J Urol.* 2010;183(4):1309-15.

[85] Steffens S, Roos FC, Janssen M, Becker F, Steinestel J, Abbas M, Steinestel K, Wegener G, Siemer S, Thüroff JW, Hofmann R, Stöckle M, Schrader M, Hartmann A, Junker K, Kuczyk MA, Schrader AJ; German Renal Cell Cancer Network. Clinical behavior of chromophobe renal cell carcinoma is less aggressive than that of clear cell renal cell carcinoma, independent of Fuhrman grade or tumor size. *Virchows Arch.* 2014;465(4):439-44.

[86] Wagener N, Edelmann D, Benner A, Zigeuner R, Borgmann H, Wolff I, Krabbe LM, Musquera M, Dell'Oglio P, Capitanio U, Klatte T, Cindolo L, May M, Brookman-May SD; European Association of Urology (EAU) Young Academic Urologists (YAU) Kidney Cancer Group. Outcome of papillary versus clear cell renal cell carcinoma varies significantly in non-metastatic disease. PLoS One. 2017;12(9):e0184173.

[87] Cheville JC, Lohse CM, Zincke H, Weaver AL, Leibovich BC, Frank I, Blute ML. Sarcomatoid renal cell carcinoma: an examination of underlying histologic subtype and an analysis of associations with patient outcome. *Am J Surg Pathol.* 2004;28(4):435-41.

[88] Przybycin CG, McKenney JK, Reynolds JP, Campbell S, Zhou M, Karafa MT, Magi-Galluzzi C. Rhabdoid differentiation is associated with aggressive behaviour in renal cell carcinoma: a clinicopathological analysis of 76 cases with clinical follow-up. Am J Surg Pathol 2014;38(9):1260–1265.

[89] Leroy X, Zini L, Buob D, Ballereau C, Villers A, Aubert S. Renal cell carcinoma with rhabdoid features: an aggressive neoplasm with overexpression of p53. *Arch Pathol Lab Med.* 2007;131(1):102-6.

[90] Mohamed AH, Mohamud HA. Renal cell carcinoma with rhabdoid features: A rare aggressive and fatal variant. *Urol Case Rep.* 2020;32:101244.

[91] Zhang BY, Cheville JC, Thompson RH, Lohse CM, Boojian SA, Leibovich BC, Costello BA. Impact of rhabdoid differentiation on prognosis for patients with grade four renal cell carcinoma. *Eur Urol.* 2015;68:5–7.

[92] Parker WP, Cheville JC, Frank I, Zaid HB, Lohse CM, Boorjian SA, Leibovich BC, Thompson RH. Application of the Stage, Size, Grade, and Necrosis (SSIGN) Score for Clear Cell Renal Cell Carcinoma in Contemporary Patients. *Eur Urol.* 2017;71(4):665-673.

[93] Zisman A, Pantuck AJ, Wieder J, Chao DH, Dorey F, Said JW, deKernion JB, Figlin RA, Belldegrun AS. Risk group assessment and clinical outcome algorithm to predict the natural history of patients with surgically resected renal cell carcinoma. *J Clin Oncol.* 2002;20(23):4559-66.

[94] Klatte T, Rossi SH, Stewart GD. Prognostic factors and prognostic models for renal cell carcinoma: a literature review. *World J Urol.* 2018;36(12):1943-1952.

[95] Scosyrev E, Messing EM, Sylvester R, Campbell S, Van Poppel, H. Renal function after nephron-sparing surgery versus radical nephrectomy: results from EORTC randomized trial 30904. *Eur. Urol.* 2014;65:372–377.

[96] Pignot G, Bigot P, Bernhard JC, Bouliere F, Bessede T, Bensalah K, Salomon L, Mottet N, Bellec L, Soulié M, Ferrière JM, Pfister C, Drai J, Colombel M, Villers A, Rigaud J, Bouchot O, Montorsi F, Bertini R, Belldegrun AS, Pantuck AJ, Patard JJ. Nephron-sparing surgery is superior to radical nephrectomy in preserving renal function benefit even when expanding indications beyond the traditional 4-cm cutoff. *Urol Oncol.* 2014;32(7):1024-30.

[97] Gordetsky J, Eich ML, Garapati M, Del Carmen Rodriguez Pena M, Rais-Bahrami S. Active Surveillance of Small Renal Masses. *Urology.* 2019;123:157-166.

[98] Gray RE, Harris GT. Renal Cell Carcinoma: Diagnosis and Management. *Am Fam Physician.* 2019;99(3):179-184. PMID: 30702258

[99] Lane BR, Tobert CM, Riedinger CB. Growth kinetics and active surveillance for small renal masses. *Curr. Opin. Urol.* 2012;22,353–359.

[100] Pierorazio PM, Johnson MH, Ball MW, Gorin MA, Trock BJ, Chang P, Wagner AA, McKiernan JM, Allaf ME. Five-year analysis of a multi-institutional prospective clinical trial of delayed intervention and surveillance for small renal masses: the DISSRM registry. *Eur Urol.* 2015;68(3):408-15.

[101] Dabestani S, Thorstenson A, Lindblad P, Harmenberg U, Ljungberg B, Lundstam S. Renal cell carcinoma recurrences and metastases in primary

non-metastatic patients: a population-based study. *World J Urol.* 2016;34:1081-1086.

[102] Makhov P, Joshi S, Ghatalia P, Kutikov A, Uzzo RG, Kolenko VM. Resistance to Systemic Therapies in Clear Cell Renal Cell Carcinoma: Mechanisms and Management Strategies. *Mol Cancer Ther.* 2018;17(7):1355-1364.

[103] Motzer RJ, McCann L, Deen K. Pazopanib versus sunitinib in renal cancer. *N. Engl. J. Med.* 2013;369:1970.

[104] Rini BI, Escudier B, Tomczak P, Kaprin A, Szczylik C, Hutson TE, Michaelson MD, Gorbunova VA, Gore ME, Rusakov IG, Negrier S, Ou YC, Castellano D, Lim HY, Uemura H, Tarazi J, Cella D, Chen C, Rosbrook B, Kim S, Motzer RJ.Comparative effectiveness of axitinib versus sorafenib in advanced renal cell carcinoma (AXIS): a randomised phase 3 trial. *Lancet.* 2011;378(9807):1931-9.

[105] Motzer RJ, Hutson TE, Glen H, Michaelson MD, Molina A, Eisen T, Jassem J, Zolnierek J, Maroto JP, Mellado B, Melichar B, Tomasek J, Kremer A, Kim HJ, Wood K, Dutcus C, Larkin J. Lenvatinib, everolimus, and the combination in patients with metastatic renal cell carcinoma: a randomised, phase 2, open-label, multicentre trial. *Lancet Oncol.* 2015;16(15):1473-1482.

[106] Choueiri TK, Escudier B, Powles T, Mainwaring PN, Rini BI, Donskov F, Hammers H, Hutson TE, Lee JL, Peltola K, Roth BJ, Bjarnason GA, Géczi L, Keam B, Maroto P, Heng DY, Schmidinger M, Kantoff PW, Borgman-Hagey A, Hessel C, Scheffold C, Schwab GM, Tannir NM, Motzer RJ; METEOR Investigators. Cabozantinib versus Everolimus in Advanced Renal-Cell Carcinoma. *N Engl J Med.* 2015;373(19):1814-23.

[107] Motzer RJ, Escudier B, Oudard S, Hutson TE, Porta C, Bracarda S, Grünwald V, Thompson JA, Figlin RA, Hollaender N, Urbanowitz G, Berg WJ, Kay A, Lebwohl D, Ravaud A; RECORD-1 Study Group. Efficacy of everolimus in advanced renal cell carcinoma: a double-blind, randomised, placebo-controlled phase III trial. *Lancet.* 2008;372(9637):449-56.

[108] Hudes G, Carducci M, Tomczak P, Dutcher J, Figlin R, Kapoor A, Staroslawska E, Sosman J, McDermott D, Bodrogi I, Kovacevic Z, Lesovoy V, Schmidt-Wolf IG, Barbarash O, Gokmen E, O'Toole T, Lustgarten S, Moore L, Motzer RJ; Global ARCC Trial. Temsirolimus, interferon alfa, or both for advanced renal-cell carcinoma. *N Engl J Med.* 2007;356(22):2271-81.

[109] McDermott DF, Regan MM, Clark JI, Flaherty LE, Weiss GR, Logan TF, Kirkwood JM, Gordon MS, Sosman JA, Ernstoff MS, Tretter CP, Urba WJ, Smith JW, Margolin KA, Mier JW, Gollob JA, Dutcher JP, Atkins MB. Randomized phase III trial of high-dose interleukin-2 versus

subcutaneous interleukin-2 and interferon in patients with metastatic renal cell carcinoma. *J Clin Oncol.* 2005;23(1):133-41.

[110] Motzer RJ, Escudier B, McDermott DF, George S, Hammers HJ, Srinivas S, Tykodi SS, Sosman JA, Procopio G, Plimack ER, Castellano D, Choueiri TK, Gurney H, Donskov F, Bono P, Wagstaff J, Gauler TC, Ueda T, Tomita Y, Schutz FA, Kollmannsberger C, Larkin J, Ravaud A, Simon JS, Xu LA, Waxman IM, Sharma P; CheckMate 025 Investigators.Nivolumab versus Everolimus in Advanced Renal-Cell Carcinoma. N Engl J Med. 2015;373(19):1803-13.

[111] Hanna N, Sun M, Meyer CP, Nguyen PL, Pal SK, Chang SL, de Velasco G, Trinh QD, Choueiri TK. Survival Analyses of Patients With Metastatic Renal Cancer Treated With Targeted Therapy With or Without Cytoreductive Nephrectomy: A National Cancer Data Base Study. *J Clin Oncol.* 2016;34(27):3267-75.

[112] Rodriguez-Vida A, Hutson TE, Bellmunt J, Strijbos MH. New treatment options for metastatic renal cell carcinoma. *ESMO Open.* 2017;2(2):e000185.

[113] Gupta K, Miller JD, Li JZ, Russell MW, Charbonneau C. Epidemiologic and socioeconomic burden of metastatic renal cell carcinoma (mRCC): a literature review. *Cancer Treat Rev.* 2008;34(3):193–205.

[114] Capitanio U, Montorsi F. Renal cancer. *Lancet* 2016;387:894–906.

[115] Padala SA, Barsouk A, Thandra KC, Saginala K, Mohammed A, Vakiti A, Rawla P, Barsouk A. Epidemiology of Renal Cell Carcinoma. *World J Oncol.* 2020;11(3):79-87.

[116] Zhang GM, Zhu Y, Ye DW. Metabolic syndrome and renal cell carcinoma. *World J Surg Oncol.* 2014;12:236.

[117] Howlader N, Noone AM, Krapcho M, Miller D, Brest A, Yu M, Ruhl J, Tatalovich Z, Mariotto A, Lewis DR, Chen HS, Feuer EJ, Cronin KA (eds). SEER Cancer Statistics Review, 1975-2018, National Cancer Institute. Bethesda, MD, https://seer.cancer.gov/csr/1975_2018/.

[118] Taccoen X, Valeri A, Descotes JL, Morin V, Stindel E, Doucet L, Joulin V, Bocqueraz F, Coulange C, Rambeaud JJ, Fournier G, Mejean A; Oncology Committee of the Association Française d'Urologie. Renal cell carcinoma in adults 40 years old or less: young age is an independent prognostic factor for cancer-specific survival. *Eur Urol.* 2007;51(4):980-7.

[119] Bray F, Ferlay J, Soerjomataram I, Siegel RL, Torre LA, Jemal A. Global cancer statistics 2018: GLOBOCAN estimates of incidence and mortality worldwide for 36 cancers in 185 countries. *CA Cancer J Clin.* 2018;68(6):394-424.

[120] Mancini M, Righetto M, Baggio G. Gender-Related Approach to Kidney Cancer Management: Moving Forward. *Int J Mol Sci.* 2020;21(9):3378.

[121] May M, Aziz A, Zigeuner R, Chromecki T, Cindolo L, Schips L, De Cobelli O, Rocco B, De Nunzio C, Tubaro A, Coman I, Truss M, Dalpiaz O, Hoschke B, Gilfrich C, Feciche B, Stoltze A, Fenske F, Fritsche HM, Figenshau RS, Madison K, Sánchez-Chapado M, Martin Mdel C, Salzano L, Lotrecchiano G, Joniau S, Waidelich R, Stief C, Brookman-May S, Members of the CORONA project the Young Academic Urologists Renal Cancer Group. Gender differences in clinicopathological features and survival in surgically treated patients with renal cell carcinoma: an analysis of the multicenter CORONA database. *World J Urol.* 2013;31(5):1073-80.

[122] Aron M, Nguyen MM, Stein RJ, Gill IS. Impact of gender in renal cell carcinoma: an analysis of the SEER database. *Eur Urol.* 2008;54(1):133-40.

[123] Marchioni M, Martel T, Bandini M, Pompe RS, Tian Z, Kapoor A, Cindolo L, Autorino R, Briganti A, Shariat SF, Schips L, Karakiewicz PI. Marital status and gender affect stage, tumor grade, treatment type and cancer specific mortality in T 1-2 N 0 M 0 renal cell carcinoma. *World J Urol.* 2017;35(12):1899-1905.

[124] Noh SJ, Kang MJ, Kim KM, Bae JS, Park HS, Moon WS, Chung MJ, Lee H, Lee DG, Jang KY. Acetylation status of P53 and the expression of DBC1, SIRT1, and androgen receptor are associated with survival in clear cell renal cell carcinoma patients. *Pathology.* 2013;45(6):574-80.

[125] Chen Y, Sun Y, Rao Q, Xu H, Li L, Chang C. Androgen receptor (AR) suppresses miRNA-145 to promote renal cell carcinoma (RCC) progression independent of VHL status. *Oncotarget.* 2015; 6(31):31203-15.

[126] Tsivian M, Moreira DM, Caso JR, Mouraviev V, Polascik TJ. Cigarette smoking is associated with advanced renal cell carcinoma. *J Clin Oncol.* 2011;29(15):2027-2031.

[127] Keizman D, Gottfried M, Ish-Shalom M, Maimon N, Peer A, Neumann A, Hammers H, Eisenberger MA, Sinibaldi V, Pili R, Hayat H, Kovel S, Sella A, Boursi B, Weitzen R, Mermershtain W, Rouvinov K, Berger R, Carducci MA. Active smoking may negatively affect response rate, progression-free survival, and overall survival of patients with metastatic renal cell carcinoma treated with sunitinib. *Oncologist.* 2014;19(1):51-60.

[128] Wozniak MB, Brennan P, Brenner DR, Overvad K, Olsen A, Tjønneland A, Boutron-Ruault MC, Clavel-Chapelon F, Fagherazzi G, Katzke V, Kühn T, Boeing H, Bergmann MM, Steffen A, Naska A, Trichopoulou A, Trichopoulos D, Saieva C, Grioni S, Panico S, Tumino R, Vineis P, Bueno-de-Mesquita HB, Peeters PH, Hjartåker A, Weiderpass E, Arriola L, Molina-Montes E, Duell EJ, Santiuste C, Alonso de la Torre R, Barricarte

Gurrea A, Stocks T, Johansson M, Ljungberg B, Wareham N, Khaw KT, Travis RC, Cross AJ, Murphy N, Riboli E, Scelo G. Alcohol consumption and the risk of renal cancers in the European prospective investigation into cancer and nutrition (EPIC). *Int J Cancer.* 2015;137(8):1953-66.

[129] Xu X, Zhu Y, Zheng X, Xie L. Does beer, wine or liquor consumption correlate with the risk of renal cell carcinoma? A dose-response meta-analysis of prospective cohort studies. *Oncotarget* 2015;6:13347–58.

[130] Lew JQ, Chow WH, Hollenbeck AR, Schatzkin A, Park Y. Alcohol consumption and risk of renal cell cancer: the NIH-AARP diet and health study. *Br J Cancer.* 2011;104(3):537-541.

[131] Koppes LL, Dekker JM, Hendriks HF, Bouter LM, Heine RJ. Moderate alcohol consumption lowers the risk of type 2 diabetes: a meta-analysis of prospective observational studies. *Diabetes Care.* 2005;28(3):719-25.

[132] Chow WH, Gridley G, Fraumeni JF Jr, Jarvholm B: Obesity, hypertension, and the risk of kidney cancer in men. *N Engl J Med* 2000, 343:1305–1311.

[133] Bergström A, Hsieh CC, Lindblad P, Lu CM, Cook NR,Wolk A. Obesity and renal cell cancer—a quantitative review. *Br J Cancer* 2001;85:984–90.

[134] Pollak M. The insulin and insulin-like growth factor receptor family in neoplasia: an update. *Nat Rev Cancer* 2012;12(3):159-69.

[135] Macleod LC, Hotaling JM, Wright JL, Davenport MT, Gore JL, Harper J, White E. Risk factors for renal cell carcinoma in the VITAL study. *J Urol.* 2013;190(5):1657-1661.

[136] Waalkes S, Merseburger AS, Kramer MW, Herrmann TR, Wegener G, Rustemeier J, Hofmann R, Schrader M, Kuczyk MA, Schrader AJ. Obesity is associated with improved survival in patients with organ-confined clear-cell kidney cancer. *Cancer Causes Control* 2010;21:1905–1910.

[137] Behrens G, Leitzmann MF. The association between physical activity and renal cancer: systematic review and meta-analysis. *Br J Cancer* 2013;108:798–811.

[138] Hidayat K, Du X, Zou S-Y, Shi BM. Blood pressure and kidney cancer risk. *J Hypertens*. 2017;35:1333–44.

[139] Capitanio U, Bensalah K, Bex A, Boorjian SA, Bray F, Coleman J, Gore JL, Sun M, Wood C, Russo P. Epidemiology of Renal Cell Carcinoma. *Eur Urol.* 2019;75(1):74-84.

[140] Colt JS, Schwartz K, Graubard BI, Davis F, Ruterbusch J, DiGaetano R, Purdue M, et al. Hypertension and risk of renal cell carcinoma among white and black Americans. *Epidemiology.* 2011;22(6):797-804.

[141] Schmidt LS, Linehan WM. Genetic predisposition to kidney cancer. *Semin Oncol.* 2016 Oct;43(5):566-574.

[142] Nordstrom-O'Brien M, van der Luijt RB, van Rooijen E, van den Ouweland AM, Majoor-Krakauer DF, Lolkema MP, van Brussel A, Voest EE, Giles RH.Genetic analysis of von Hippel-Lindau disease. *Hum Mutat.* 2010;31(5):521-37.

[143] Walther MM, Lubensky IA, Venzon D, Zbar B, Linehan WM. Prevalence of microscopic lesions in grossly normal renal parenchyma from patients with von Hippel-Lindau disease, sporadic renal cell carcinoma and no renal disease: clinical implications. *J Urol.* 1995;154:2010–4.

[144] Popova T, Hebert L, Jacquemin V, Gad S, Caux-Moncoutier V, Dubois-d'Enghien C, Richaudeau B, Renaudin X, Sellers J, Nicolas A, Sastre-Garau X, Desjardins L, Gyapay G, Raynal V, Sinilnikova OM, Andrieu N, Manié E, de Pauw A, Gesta P, Bonadona V, Maugard CM, Penet C, Avril MF, Barillot E, Cabaret O, Delattre O, Richard S, Caron O, Benfodda M, Hu HH, Soufir N, Bressac-de Paillerets B, Stoppa-Lyonnet D, Stern MH. Germline BAP1 mutations predispose to renal cell carcinomas. *Am J Hum Genet.* 2013;92(6):974-80.

[145] Farley MN, Schmidt LS, Mester JL, Pena-Llopis S, Pavia-Jimenez A, Christie A, Vocke CD, Ricketts CJ, Peterson J, Middelton L, Kinch L, Grishin N, Merino MJ, Metwalli AR, Xing C, Xie XJ, Dahia PLM, Eng C, Linehan WM, Brugarolas J. A novel germline mutation in BAP1 predisposes to familial clear-cell renal cell carcinoma. *Mol Cancer Res.* 2013;11(9):1061-1071.

[146] Schmidt L, Duh FM, Chen F, Kishida T, Glenn G, Choyke P, Scherer SW, Zhuang Z, Lubensky I, Dean M, Allikmets R, Chidambaram A, Bergerheim UR, Feltis JT, Casadevall C, Zamarron A, Bernues M, Richard S, Lips CJ, Walther MM, Tsui LC, Geil L, Orcutt ML, Stackhouse T, Lipan J, Slife L, Brauch H, Decker J, Niehans G, Hughson MD, Moch H, Storkel S, Lerman MI, Linehan WM, Zbar B. Germline and somatic mutations in the tyrosine kinase domain of the MET proto-oncogene in papillary renal carcinomas. *Nat Genet.* 1997;16(1):68-73.

[147] Hasumi Y, Baba M, Ajima R, Hasumi H, Valera VA, Klein ME, Haines DC, Merino MJ, Hong SB, Yamaguchi TP, Schmidt LS, Linehan WM. Homozygous loss of BHD causes early embryonic lethality and kidney tumor development with activation of mTORC1 and mTORC2. *Proc Natl Acad Sci U S A.* 2009;106(44):18722-7.

[148] Tomlinson IP, Alam NA, Rowan AJ, Barclay E, Jaeger EE, Kelsell D, Leigh I, Gorman P, Lamlum H, Rahman S, Roylance RR, Olpin S, Bevan S, Barker K, Hearle N, Houlston RS, Kiuru M, Lehtonen R, Karhu A, Vilkki S, Laiho P, Eklund C, Vierimaa O, Aittomäki K, Hietala M, Sistonen P, Paetau A, Salovaara R, Herva R, Launonen V, Aaltonen LA;

Multiple Leiomyoma Consortium. Germline mutations in FH predispose to dominantly inherited uterine fibroids, skin leiomyomata and papillary renal cell cancer. *Nat Genet.* 2002 Apr;30(4):406-10.

[149] Ricketts C, Woodward ER, Killick P, Morris MR, Astuti D, Latif F, Maher ER. Germline SDHB mutations and familial renal cell carcinoma. *J Natl Cancer Inst.* 2008;100(17):1260-2.

[150] Cheungpasitporn W, Thongprayoon C, O'Corragain OA, Edmonds PJ, Ungprasert P, Kittanamongkolchai W, Erickson SB. The risk of kidney cancer in patients with kidney stones: a systematic review and meta-analysis. *QJM.* 2015;108(3):205-12.

[151] Joh H-K, WillettWC, Cho E. Type 2 diabetes and the risk of renal cell cancer in women. *Diabetes Care* 2011;34:1552–6.

[152] Christensson A, Savage C, Sjoberg DD, Cronin AM, O'Brien MF, Lowrance W, Nilsson PM, Vickers AJ, Russo P, Lilja H. Association of cancer with moderately impaired renal function at baseline in a large, representative, population-based cohort followed for up to 30 years. *Int J Cancer.* 2013;133(6):1452-8.

[153] Choueiri TK, Je Y, Cho E. Analgesic use and the risk of kidney cancer: a meta-analysis of epidemiologic studies. *Int J Cancer.* 2014;134(2):384-96.

[154] International Agency for Research on Cancer. Trichloroethylene, tetrachloroethylene, and some other chlorinated agents. 2014;106:35-217.

[155] Tahbaz R, Schmid M, Merseburger AS. Prevention of kidney cancer incidence and recurrence: lifestyle, medication and nutrition. *Curr Opin Urol.* 2018;28(1):62-79.

[156] Cancer Genome Atlas Research Network. Comprehensive molecular characterization of clear cell renal cell carcinoma. *Nature* 2013;499,43–49.

[157] Sato Y, Yoshizato T, Shiraishi Y, Maekawa S, Okuno Y, Kamura T, Shimamura T, Sato-Otsubo A, Nagae G, Suzuki H, Nagata Y, Yoshida K, Kon A, Suzuki Y, Chiba K, Tanaka H, Niida A, Fujimoto A, Tsunoda T, Morikawa T, Maeda D, Kume H, Sugano S, Fukayama M, Aburatani H, Sanada M, Miyano S, Homma Y, Ogawa S. Integrated molecular analysis of clear-cell renal cell carcinoma. *Nat Genet.* 2013;45(8):860-7.

[158] Beroukhim R, Brunet JP, Di Napoli A, Mertz KD, Seeley A, Pires MM, Linhart D, Worrell RA, Moch H, Rubin MA, Sellers WR, Meyerson M, Linehan WM, Kaelin WG Jr, Signoretti S. Patterns of gene expression and copy-number alterations in von-hippel lindau disease-associated and sporadic clear cell carcinoma of the kidney. *Cancer Res.* 2009;69(11):4674-81.

[159] Moore LE, Jaeger E, Nickerson ML, Brennan P, De Vries S, Roy R, Toro J, Li H, Karami S, Lenz P, Zaridze D, Janout V, Bencko V, Navratilova M, Szeszenia-Dabrowska N, Mates D, Linehan WM, Merino M, Simko J, Pfeiffer R, Boffetta P, Hewitt S, Rothman N, Chow WH, Waldman FM. Genomic copy number alterations in clear cell renal carcinoma: associations with case characteristics and mechanisms of VHL gene inactivation. *Oncogenesis.* 2012;1(6):e14.

[160] Hakimi AA, Pham CG, Hsieh JJ. A clear picture of renal cell carcinoma. *Nat. Genet.* 2013;45,849–850.

[161] Wei EY, Hsieh JJ. A river model to map convergent cancer evolution and guide therapy in RCC. *Nat. Rev. Urol.* 2015;12:706–712.

[162] Varela I, Tarpey P, Raine K, Huang D, Ong CK, Stephens P, Davies H, Jones D, Lin ML, Teague J, Bignell G, Butler A, Cho J, Dalgliesh GL, Galappaththige D, Greenman C, Hardy C, Jia M, Latimer C, Lau KW, Marshall J, McLaren S, Menzies A, Mudie L, Stebbings L, Largaespada DA, Wessels LF, Richard S, Kahnoski RJ, Anema J, Tuveson DA, Perez-Mancera PA, Mustonen V, Fischer A, Adams DJ, Rust A, Chan-on W, Subimerb C, Dykema K, Furge K, Campbell PJ, Teh BT, Stratton MR, Futreal PA. Exome sequencing identifies frequent mutation of the SWI/SNF complex gene PBRM1 in renal carcinoma. *Nature.* 2011;469(7331):539-42.

[163] Guo G, Gui Y, Gao S, Tang A, Hu X, Huang Y, Jia W, Li Z, He M, Sun L, Song P, Sun X, Zhao X, Yang S, Liang C, Wan S, Zhou F, Chen C, Zhu J, Li X, Jian M, Zhou L, Ye R, Huang P, Chen J, Jiang T, Liu X, Wang Y, Zou J, Jiang Z, Wu R, Wu S, Fan F, Zhang Z, Liu L, Yang R, Liu X, Wu H, Yin W, Zhao X, Liu Y, Peng H, Jiang B, Feng Q, Li C, Xie J, Lu J, Kristiansen K, Li Y, Zhang X, Li S, Wang J, Yang H, Cai Z, Wang J. Frequent mutations of genes encoding ubiquitin-mediated proteolysis pathway components in clear cell renal cell carcinoma. *Nat Genet.* 2011;44(1):17-9.

[164] Hakimi AA, Chen YB, Wren J, Gonen M, Abdel-Wahab O, Heguy A, Liu H, Takeda S, Tickoo SK, Reuter VE, Voss MH, Motzer RJ, Coleman JA, Cheng EH, Russo P, Hsieh JJ. Clinical and pathologic impact of select chromatin-modulating tumor suppressors in clear cell renal cell carcinoma. *Eur Urol.* 2013;63(5):848-54.

[165] Dalgliesh GL, Furge K, Greenman C, Chen L, Bignell G, Butler A, Davies H, Edkins S, Hardy C, Latimer C, Teague J, Andrews J, Barthorpe S, Beare D, Buck G, Campbell PJ, Forbes S, Jia M, Jones D, Knott H, Kok CY, Lau KW, Leroy C, Lin ML, McBride DJ, Maddison M, Maguire S, McLay K, Menzies A, Mironenko T, Mulderrig L, Mudie L, O'Meara S, Pleasance E, Rajasingham A, Shepherd R, Smith R, Stebbings L, Stephens P, Tang G, Tarpey PS, Turrell K, Dykema KJ, Khoo SK, Petillo D, Wondergem B, Anema J, Kahnoski RJ, Teh BT, Stratton MR, Futreal PA. Systematic

sequencing of renal carcinoma reveals inactivation of histone modifying genes. *Nature.* 2010;463(7279):360-3.

[166] Nickerson ML, Jaeger E, Shi Y, Durocher JA, Mahurkar S, Zaridze D, Matveev V, Janout V, Kollarova H, Bencko V, Navratilova M, Szeszenia-Dabrowska N, Mates D, Mukeria A, Holcatova I, Schmidt LS, Toro JR, Karami S, Hung R, Gerard GF, Linehan WM, Merino M, Zbar B, Boffetta P, Brennan P, Rothman N, Chow WH, Waldman FM, Moore LE. Improved identification of von Hippel-Lindau gene alterations in clear cell renal tumors. *Clin Cancer Res.* 2008;14(15):4726-34.

[167] Young AC, Craven RA, Cohen D, Taylor C, Booth C, Harnden P, Cairns DA, Astuti D, Gregory W, Maher ER, Knowles MA, Joyce A, Selby PJ, Banks RE. Analysis of VHL Gene Alterations and their Relationship to Clinical Parameters in Sporadic Conventional Renal Cell Carcinoma. *Clin Cancer Res.* 2009;15(24):7582-7592.

[168] Shen C, Kaelin WG Jr. The VHL/HIF axis in clear cell renal carcinoma. *Semin Cancer Biol.* 2013;23(1):18-25.

[169] Semenza GL. Oxygen sensing, homeostasis, and disease. *N Engl J Med.* 2011;365:537–547.

[170] Schito L, Semenza GL. Hypoxia-Inducible Factors: Master Regulators of Cancer Progression. *Trends Cancer.* 2016;2(12):758-770.

[171] Braga EA, Fridman MV, Loginov VI, Dmitriev AA, Morozov SG. Molecular Mechanisms in Clear Cell Renal Cell Carcinoma: Role of miRNAs and Hypermethylated miRNA Genes in Crucial Oncogenic Pathways and Processes. *Front Genet.* 2019;10:320.

[172] Reuter VE, Tickoo SK. Differential diagnosis of renal tumours with clear cell histology. *Pathology.* 2010;42(4):374-83.

[173] Roskoski RJr. Vascular endothelial growth factor (VEGF) and VEGF receptor inhibitors in the treatment of renal cell carcinomas. *Pharmacol. Res.* 2017;120:116–132.

[174] Pantuck AJ, An J, Liu H, Rettig MB. NF-kappaB-dependent plasticity of the epithelial to mesenchymal transition induced by Von Hippel-Lindau inactivation in renal cell carcinomas. *Cancer Res.* 2010;70(2):752-61.

[175] Esteban MA, Tran MG, Harten SK, Hill P, Castellanos MC, Chandra A, Raval R, O'brien TS, Maxwell PH. Regulation of E-cadherin expression by VHL and hypoxia-inducible factor. *Cancer Res.* 2006;66(7):3567-75.

[176] Evans AJ, Russell RC, Roche O, Burry TN, Fish JE, Chow VW, Kim WY, Saravanan A, Maynard MA, Gervais ML, Sufan RI, Roberts AM, Wilson LA, Betten M, Vandewalle C, Berx G, Marsden PA, Irwin MS, Teh BT, Jewett MA, Ohh M. VHL promotes E2 box-dependent E-cadherin

transcription by HIF-mediated regulation of SIP1 and snail. *Mol Cell Biol.* 2007;27(1):157-69.

[177] Pescador N, Villar D, Cifuentes D, Garcia-Rocha M, Ortiz-Barahona A, Vazquez S, Ordoñez A, Cuevas Y, Saez-Morales D, Garcia-Bermejo ML, Landazuri MO, Guinovart J, del Peso L. Hypoxia promotes glycogen accumulation through hypoxia inducible factor (HIF)-mediated induction of glycogen synthase 1. *PLoS One.* 2010;5(3):e9644.

[178] Semenza GL. HIF-1 mediates metabolic responses to intratumoral hypoxia and oncogenic mutations. *J Clin Invest.* 2013;123(9):3664-71.

[179] Wise DR, Ward PS, Shay JE, Cross JR, Gruber JJ, Sachdeva UM, Platt JM, DeMatteo RG, Simon MC, Thompson CB. Hypoxia promotes isocitrate dehydrogenase-dependent carboxylation of alpha-ketoglutarate to citrate to support cell growth and viability. *Proc Natl Acad Sci U S A.* 2011;108(49):19611-6.

[180] Hanahan D, Weinberg RA. Hallmarks of Cancer: The Next Generation. *Cell*. 2011;144:646–674.

[181] Pavlova NN, Thompson CB. The Emerging Hallmarks of Cancer Metabolism. *Cell Metabolism*. 2016;23:27–47.

[182] Hakimi AA, Reznik E, Lee CH, Creighton CJ, Brannon AR, Luna A, Aksoy BA, Liu EM, Shen R, Lee W, Chen Y, Stirdivant SM, Russo P, Chen YB, Tickoo SK, Reuter VE, Cheng EH, Sander C, Hsieh JJ. An integrated metabolic atlas of clear cell renal cell carcinoma. *Cancer Cell.* 2016;29:104–116.

[183] Wettersten HI, Hakimi AA, Morin D, Bianchi C, Johnstone ME, Donohoe DR, Trott JF, Aboud OA,Stirdivant S, Neri B, Wolfert R, Stewart B, Perego R, Hsieh JJ, Weiss RH. Grade-dependent metabolic reprogramming in kidney cancer revealed by combined proteomics and metabolomics analysis. *Cancer Res*. 2015;75:2541–2552.

[184] Hu SL, Chang A, Perazella MA, Okusa MD, Jaimes EA, Weiss RH. American Society of Nephrology Onco-Nephrology Forum. The nephrologist's tumor: basic biology and management of renal cell carcinoma. *J. Am. Soc. Nephrol*. 2016;27:2227–2237.

[185] Linehan WM, Ricketts CJ. The metabolic basis of kidney cancer. *Semin. Cancer Biol*. 2013;23:46–55.

[186] Linehan WM, Srinivasan R, Schmidt LS. The genetic basis of kidney cancer: a metabolic disease. *Nat. Rev. Urol*. 2010;7:277–285.

[187] Ozcan A, Shen SS, Zhai QJ, Truong LD. Expression of GLUT1 in primary renal tumors: morphologic and biologic implications. *Am. J. Clin. Pathol*. 2017;128: 245–254.

[188] Shelar S, Shim EH, Brinkley GJ, Kundu A, Carobbio F, Poston T, Tan J, Parekh V, Benson D, Crossman DK, Buckhaults PJ, Rakheja D, Kirkman R, Sato Y, Ogawa S, Dutta S, Velu SE, Emberley E, Pan A, Chen J, Huang T, Absher D, Becker A, Kunick C, Sudarshan S. Biochemical and Epigenetic Insights into L-2-Hydroxyglutarate, a Potential Therapeutic Target in Renal Cancer. *Clin Cancer Res*. 2018; 24(24):6433-6446.

[189] Sciacovelli M, Gonçalves E, Johnson TI, Zecchini VR, da Costa AS, Gaude E, Drubbel AV, Theobald SJ, Abbo SR, Tran MG, Rajeeve V, Cardaci S, Foster S, Yun H, Cutillas P, Warren A, Gnanapragasam V, Gottlieb E, Franze K, Huntly B, Maher ER, Maxwell PH, Saez-Rodriguez J, Frezza C. Fumarate is an epigenetic modifier that elicits epithelial-to-mesenchymal transition. *Nature*. 2016;537(7621):544-547.

[190] Lucarelli G, Loizzo D, Franzin R, Battaglia S, Ferro M, Cantiello F, Castellano G, Bettocchi C, Ditonno P, Battaglia M. Metabolomic insights into pathophysiological mechanisms and biomarker discovery in clear cell renal cell carcinoma. *Expert Rev Mol Diagn*. 2019;19(5):397-407.

[191] Shanmugasundaram K, Block K. Renal Carcinogenesis, Tumor Heterogeneity, and Reactive Oxygen Species: Tactics Evolved. *Antioxid Redox Signal*. 2016;25(12):685-701.

[192] Wettersten HI, Aboud OA, Lara PN Jr, Weiss RH. Metabolic reprogramming in clear cell renal cell carcinoma. *Nat Rev Nephrol*. 2017;13(7):410-419.

[193] Sanchez DJ, Simon MC. Genetic and metabolic hallmarks of clear cell renal cell carcinoma. *Biochim Biophys Acta Rev Cancer*. 2018;1870(1):23–31.

[194] Yong C, Stewart GD, Frezza C. Oncometabolites in renal cancer. *Nat Rev Nephrol*. 2020;16(3):156-172.

[195] Chitalia VC, Foy RL, Bachschmid MM, Zeng L, Panchenko MV, Zhou MI, Bharti A, Seldin DC, Lecker SH, Dominguez I, Cohen HT. Jade-1 inhibits Wnt signalling by ubiquitylating β-catenin and mediates Wnt pathway inhibition by pVHL. *Nat. Cell Biol*. 2008;10;1208–1216.

[196] Wang Y, Zhou CJ, Liu Y. Wnt Signaling in Kidney Development and Disease. *Prog Mol Biol Transl Sci*. 2018;153:181-207.

[197] Valenta T, Hausmann G, Basler K. The many faces and functions of β-catenin *EMBO J*. 2012; 31(12):, 2714–2736.

[198] Kaelin, W. G. Von Hippel–Lindau disease. *Annu. Rev. Pathol*. 2007;2:145–173.

[199] Burrows AE, Smogorzewska A, Elledge SJ. Polybromo-associated BRG1-associated factor components BRD7 and BAF180 are critical regulators of p53 required for induction of replicative senescence. *Proc Natl Acad Sci USA.* 2010; 107(32):14280-5.

[200] Kakarougkas A, Ismail A, Chambers AL, Riballo E, Herbert AD, Künzel J, Löbrich M, Jeggo PA, Downs JA. Requirement for PBAF in transcriptional repression and repair at DNA breaks in actively transcribed regions of chromatin. *Mol Cell.* 2014; 55(5):723-32.

[201] Brownlee PM, Chambers AL, Cloney R, Bianchi A, Downs JA. BAF180 promotes cohesion and prevents genome instability and aneuploidy. *Cell Rep*. 2014;6(6):973–981.

[202] Su D, Singer EA, Srinivasan R. Molecular pathways in renal cell carcinoma: recent advances in genetics and molecular biology. *Curr Opin Oncol* 2015;27(3):217-23.

[203] Yan HB, Wang XF, Zhang Q, Tang ZQ, Jiang YH, Fan HZ, Sun YH, Yang PY, Liu F. Reduced expression of the chromatin remodeling gene ARID1A enhances gastric cancer cell migration and invasion via downregulation of E-cadherin transcription. *Carcinogenesis*. 2014;35(4):867–876.

[204] Chowdhury B, Porter EG, Stewart JC, Ferreira CR, Schipma MJ, Dykhuizen EC. PBRM1 regulates the expression of genes involved in metabolism and cell adhesion in renal clear cell carcinoma. *PLoS ONE*. 2016;11(4):e0153718.

[205] Gao W, Li W, Xiao T, Liu XS, Kaelin WG Jr. Inactivation of the PBRM1 tumor suppressor gene amplifies the HIF-response in VHL−/− clear cell renal carcinoma. *Proc Natl Acad Sci U S A.* 2017;114(5):1027–1032.

[206] Sun XJ, Wei J, Wu XY, Hu M, Wang L, Wang HH, Zhang QH, Chen SJ, Huang QH, Chen Z. Identification and characterization of a novel human histone H3 lysine 36-specific methyltransferase. *J. Biol. Chem*. 2005;280(42), 35261–35271.

[207] Al Sarakbi W, Sasi W, Jiang WG, Roberts T, Newbold RF, Mokbel K. The mRNA expression of SETD2 in human breast cancer: correlation with clinico-pathological parameters. *BMC Cancer.* 2009;9:290.

[208] Zhang J, Ding L, Holmfeldt L, Wu G, Heatley SL, Payne-Turner D, Easton J, Chen X, Wang J, Rusch M, Lu C, Chen SC, Wei L, Collins-Underwood JR, Ma J, Roberts KG, Pounds SB, Ulyanov A, Becksfort J, Gupta P, Huether R, Kriwacki RW, Parker M, McGoldrick DJ, Zhao D, Alford D, Espy S, Bobba KC, Song G, Pei D, Cheng C, Roberts S, Barbato MI, Campana D, Coustan-Smith E, Shurtleff SA, Raimondi SC, Kleppe M, Cools J, Shimano KA, Hermiston ML, Doulatov S, Eppert K, Laurenti E, Notta F, Dick JE, Basso G, Hunger SP, Loh ML, Devidas M, Wood B,

Winter S, Dunsmore KP, Fulton RS, Fulton LL, Hong X, Harris CC, Dooling DJ, Ochoa K, Johnson KJ, Obenauer JC, Evans WE, Pui CH, Naeve CW, Ley TJ, Mardis ER, Wilson RK, Downing JR, Mullighan CG. The genetic basis of early T-cell precursor acute lymphoblastic leukaemia. *Nature.* 2012;481(7380):157-63.

[209] Kanu N, Grönroos E, Martinez P, Burrell RA, Yi Goh X, Bartkova J, Maya-Mendoza A, Mistrík M, Rowan AJ, Patel H, Rabinowitz A, East P, Wilson G, Santos CR, McGranahan N, Gulati S, Gerlinger M, Birkbak NJ, Joshi T, Alexandrov LB, Stratton MR, Powles T, Matthews N, Bates PA, Stewart A, Szallasi Z, Larkin J, Bartek J, Swanton C. SETD2 loss-offunction promotes renal cancer branched evolution through replication stress and impaired DNA repair. *Oncogene* 2015;34(46):5699-5708.

[210] Li J, Kluiver J, Osinga J, Westers H, van Werkhoven MB, Seelen MA, Sijmons RH, van den Berg A, and Kok K. Functional studies on primary tubular epithelial cells indicate a tumor suppressor role of SETD2 in clear cell renal cell carcinoma. *Neoplasia*. 2016;18(6):339–346.

[211] Li F, Mao G, Tong D, Huang J, Gu L, Yang W, Li GM. The histone mark H3K36me3 regulates human DNA mismatch repair through its interaction with MutSalpha. *Cell*. 2013;153:590-600.

[212] Carvalho S, Vítor AC, Sridhara SC, Martins FB, Raposo AC, Desterro JM, Ferreira J, de Almeida SF. SETD2 is required for DNA double-strand break repair and activation of the p53-mediated checkpoint. *Elife.* 2014;3:e02482.

[213] Pfister SX, Ahrabi S, Zalmas LP, Sarkar S, Aymard F, Bachrati CZ, Helleday T, Legube G, La Thangue NB, Porter AC, Humphrey TC. SETD2-dependent histone H3K36 trimethylation is required for homologous recombination repair and genome stability. *Cell Rep.* 2014;7:2006-2018.

[214] Cancer Genome Atlas Research Network. Comprehensive molecular characterization of clear cell renal cell carcinoma. *Nature.* 2013;499:43-49.

[215] Chantalat S, Depaux A, Héry P, Barral S, Thuret JY, Dimitrov S, Gérard M. Histone H3 trimethylation at lysine 36 is associated with constitutive and facultative heterochromatin. *Genome Res*. 2011;21(9):1426–1437.

[216] Simon JM, Hacker KE, Singh D, Brannon AR, Parker JS, Weiser M, Ho TH, Kuan PF, Jonasch E, Furey TS, Prins JF, Lieb JD, Rathmell WK, Davis IJ. Variation in chromatin accessibility in human kidney cancer links H3K36 methyltransferase loss with widespread RNA processing defects. *Genome Res*. 2014;24(2):241–250.

[217] Nishikawa H, Wu W, Koike A, Kojima R, Gomi H, Fukuda M, Ohta T. BRCA1-associated protein 1 interferes with BRCA1/BARD1 RING heterodimer activity. *Cancer Res.* 2009;69(1):111-119.

[218] Pan H, Jia R, Zhang L, Xu S, Wu Q, Song X, Zhang H, Ge S, Xu XL, Fan X.BAP1 regulates cell cycle progression through E2F1 target genes and mediates transcriptional silencing via H2A monoubiquitination in uveal melanoma cells. *Int. J. Biochem. Cell Biol*. 2015;60:176–184.

[219] Piva F, Santoni M, Matrana MR, Satti S, Giulietti M, Occhipinti G, Massari F, Cheng L, Lopez-Beltran A, Scarpelli M, Principato G, Cascinu S, Montironi R.BAP1, PBRM1 and SETD2 in clear-cell renal cell carcinoma: molecular diagnostics and possible targets for personalized therapies. *Expert Rev Mol Diagn*. 2015;15(9):1201-1210.

[220] Peng J, Ma J, Li W, Mo R, Zhang P, Gao K, Jin X, Xiao J, Wang C, Fan J. Stabilization of MCRS1 by BAP1 prevents chromosome instability in renal cell carcinoma. *Cancer Lett*. 2015;369(1):167–174.

[221] Bott M, Brevet M, Taylor BS, Shimizu S, Ito T, Wang L, Creaney J, Lake RA, Zakowski MF, Reva B, Sander C, Delsite R, Powell S, Zhou Q, Shen R, Olshen A, Rusch V, Ladanyi M. The nuclear deubiquitinase BAP1 is commonly inactivated by somatic mutations and 3p21.1 losses in malignant pleural mesothelioma. *Nat Genet.* 2011;43(7):668-72.

[222] Nargund AM, Pham CG, Dong Y, Wang PI, Osmangeyoglu HU, Xie Y, Aras O, Han S, Oyama T, Takeda S, Ray CE, Dong Z, Berge M, Hakimi AA, Monette S, Lekaye CL, Koutcher JA, Leslie CS, Creighton CJ, Weinhold N, Lee W, Tickoo SK, Wang Z, Cheng EH, Hsieh JJ. The SWI/SNF protein PBRM1 restrains VHL- loss-driven clear cell renal cell carcinoma. *Cell Rep*. 2017;18(12):2893–2906.

[223] Ricketts CJ, De Cubas AA, Fan H, Smith CC, Lang M, Reznik E, Bowlby R, Gibb EA, Akbani R, Beroukhim R, Bottaro DP, Choueiri TK, Gibbs RA, Godwin AK, Haake S, Hakimi AA, Henske EP, Hsieh JJ, Ho TH, Kanchi RS, Krishnan B, Kwiatkowski DJ, Lui W, Merino MJ, Mills GB, Myers J, Nickerson ML, Reuter VE, Schmidt LS, Shelley CS, Shen H, Shuch B, Signoretti S, Srinivasan R, Tamboli P, Thomas G, Vincent BG, Vocke CD, Wheeler DA, Yang L, Kim WY, Robertson AG; Cancer Genome Atlas Research Network, Spellman PT, Rathmell WK, Linehan WM. The Cancer Genome Atlas Comprehensive Molecular Characterization of Renal Cell Carcinoma. *Cell Rep*. 2018;23(1):313-326.e5.

[224] Hakimi AA, Ostrovnaya I, Reva B, Schultz N, Chen YB, Gonen M, Liu H, Takeda S, Voss MH, Tickoo SK, Reuter VE, Russo P, Cheng EH, Sander C, Motzer RJ, Hsieh JJ; ccRCC Cancer Genome Atlas (KIRC TCGA) Research Network investigators. Adverse outcomes in clear cell renal cell carcinoma with mutations of 3p21 epigenetic regulators BAP1 and SETD2:

a report by MSKCC and the KIRC TCGA Research Network. *Clin. Cancer Res*. 2013;19(12):3259–3267.

[225] Manley BJ, Zabor EC, Casuscelli J, Tennenbaum DM, Redzematovic A, Becerra MF, Benfante N, Sato Y, Morikawa T, Kume H, Fukayama M, Homma Y, Ogawa S, Arcila ME, Voss MH, Feldman DR, Coleman JA, Reuter VE, Motzer RJ, Russo P, Hsieh JJ, Hakimi AA. Integration of recurrent somatic mutations with clinical outcomes: a pooled analysis of 1049 patients with clear cell renal cell carcinoma. *Eur. Urol. Focus*. 2017;3(4-5):421-427.

[226] de Cubas AA, Rathmell WK.Epigenetic modifiers: activities in renal cell carcinoma. *Nat Rev Urol*. 2018;15(10):599-614.

[227] Niu X, Zhang T, Liao L, Zhou L, Lindner DJ, Zhou M, Rini B, Yan Q, Yang H. The von Hippel- Lindau tumor suppressor protein regulates gene expression and tumor growth through histone demethylase JARID1C. *Oncogene.* 2012;31:76–786.

[228] Rondinelli B, Rosano D, Antonini E, Frenquelli M, Montanini L, Huang D, Segalla S, Yoshihara K, Amin SB, Lazarevic D, The BT, Verhaak RG, Futreal PA, Di Croce L, Chin L, Cittaro D, Tonon G. Histone demethylase JARID1C inactivation triggers genomic instability in sporadic renal cancer. *J. Clin. Invest*. 2015;125:4625–4637.

[229] Tumkur Sitaram R, Landström M, Roos G, Ljungberg B. Significance of PI3K signalling pathway in clear cell renal cell carcinoma in relation to VHL and HIF status. *J Clin Pathol*. 2020;74(4):216-222.

[230] Kwiatkowski DJ, Choueiri TK, Fay AP, Rini BI, Thorner AR, de Velasco G, Tyburczy ME, Hamieh L, Albiges L, Agarwal N, Ho TH, Song J, Pignon JC, Barrios PM, Michaelson MD, Van Allen E, Krajewski KM, Porta C, Pal S, Bellmunt J, McDermott DF, Heng DYC, Gray KP, Signoretti S. Mutations in TSC1, TSC2, and Mtor are associated with response to rapalogs in patients with metastatic renal cell carcinoma. *Clin Cancer Res.* 2016;22:2445–52.

[231] Fan C, Zhao C, Wang F, Li S, Wang J. Significance of PTEN mutation in cellular process, prognosis, and drug selection in clear cell renal cell carcinoma. *Front Oncol.* 2019;9:357.

[232] Tang L, Li X, Gao Y, Chen L, Gu L, Chen J, Lyu X, Zhang Y, Zhang X. Phosphatase and tensin homolog (PTEN) expression on oncologic outcome in renal cell carcinoma: a systematic review and meta-analysis. *PLoS One* 2017; 12(7):e0179437.

[233] Gerlinger M, Rowan AJ, Horswell S, Math M, Larkin J, Endesfelder D, Gronroos E, Martinez P, Matthews N, Stewart A, Tarpey P, Varela I, Phillimore B, Begum S, McDonald NQ, Butler A, Jones D, Raine K, Latimer C, Santos CR, Nohadani M, Eklund AC, Spencer-Dene B, Clark

G, Pickering L, Stamp G, Gore M, Szallasi Z, Downward J, Futreal PA, Swanton C. Intratumor heterogeneity and branched evolution revealed by multiregion sequencing. *N. Engl. J. Med*. 2012;366(10):883–892.

[234] Sankin A, Hakimi AA, Mikkilineni N, Ostrovnaya I, Silk MT, Liang Y, Mano R, Chevinsky M, Motzer RJ, Solomon SB, Cheng EH, Durack JC, Coleman JA, Russo P, Hsieh JJ. The impact of genetic heterogeneity on biomarker development in kidney cancer assessed by multiregional sampling. *Cancer Med*. 2014;3(6):1485–1492.

[235] Hsieh JJ, Manley BJ, Khan N, Gao J, Carlo MI, Cheng EH. Overcome tumor heterogeneity-imposed therapeutic barriers through convergent genomic biomarker discovery: a braided cancer river model of kidney cancer. *Semin. Cell Dev. Biol*. 2017;64:98-106.

[236] Venkatesan S, Swanton C. Tumor evolutionary principles: how intratumor heterogeneity influences cancer treatment and outcome. *Am. Soc. Clin. Oncol*. 2016;35:e141–e149.

[237] Stirzaker C, Taberlay PC, Statham AL, Clark SJ. Mining cancer methylomes: prospects and challenges. *Trends Genet*. 2014;30(2):75-84.

[238] Jones, P A. Functions of DNA methylation: islands, start sites, gene bodies and beyond. *Nat Rev Genet*. 2012;13(7):484-492.

[239] Lin RK, Wang YC. Dysregulated transcriptional and post-translational control of DNA methyltransferases in cancer. *Cell Biosci*. 2014;4:46.

[240] Watson CJ, Collier P, Tea I, Neary R, Watson JA, Robinson C, Phelan D, Ledwidge MT, McDonald KM, McCann A, Sharaf O, Baugh JA. Hypoxia-induced epigenetic modifications are associated with cardiac tissue fibrosis and the development of a myofibroblast- like phenotype. *Hum. Mol. Genet*. 2014;23:2176–2188.

[241] Klutstein M, Nejman D, Greenfield R, Cedar H. DNA Methylation in Cancer and *Aging. Cancer Res*. 2016;76(12):3446-50.

[242] McMahon KW, Karunasena E, Ahuja N. The roles of DNA methylation in the stages of cancer. *Cancer J*. 2017;23(5):257-261.

[243] Lasseigne BN, Brooks JD. The role of DNA methylation in renal cell carcinoma. *Mol Diagn Ther*. 2018;22(4):431-442.

[244] Hu CY, Mohtat D, Yu Y, Ko YA, Shenoy N, Bhattacharya S, Izquierdo MC, Park AS, Giricz O, Vallumsetla N, Gundabolu K, Ware K, Bhagat TD, Suzuki M, Pullman J, Liu XS, Greally JM, Susztak K, Verma A.. Kidney cancer is characterized by aberrant methylation of tissue-specific enhancers that are prognostic for overall survival. *Clin. Cancer Res*. 2014;20(16):4349-60.

[245] Wu P , Cao Z , Wu S . New Progress of Epigenetic Biomarkers in Urological *Cancer. Dis. Markers*. 2016;2016:9864047.

[246] Minardi D, Lucarini G, Filosa A, Milanese G, Zizzi A, Di Primio R, Montironi R, Muzzonigro G. Prognostic role of global DNA-methylation and histone acetylation in pT1a clear cell renal carcinoma in partial nephrectomy specimens. *J Cell Mol Med*. 2009;13(8B):2115-2121.

[247] Delpu Y, Cordelier P, Cho WC, Torrisani J. DNA methylation and cancer diagnosis. *Int J Mol Sci* 2013;14(7):15029-58.

[248] Shenoy N, Vallumsetla N, Zou Y, Galeas JN, Shrivastava M, Hu C, Susztak K, Verma A. Role of DNA methylation in renal cell carcinoma. *J Hematol Oncol*. 2015;8:88.

[249] Joosten SC, Smits KM, Aarts MJ, Melotte V, Koch A, Tjan-Heijnen VC, van Engeland M. Epigenetics in renal cell cancer: mechanisms and clinical applications. *Nat Rev Urol*. 2018;15(7):430-451.

[250] Qi JH, Ebrahem Q, Moore N, Murphy G, Claesson-Welsh L, Bond M, Baker A, Anand-Apte B. A novel function for tissue inhibitor of metalloproteinases-3 (TIMP3): inhibition of angiogenesis by blockage of VEGF binding to VEGF receptor-2. *Nat. Med*. 2003;9(4):407-15.

[251] Lamouille S, Xu J, Derynck R. Molecular mechanisms of epithelial-mesenchymal transition. *Nat. Rev. Mol. Cell Biol*. 2014;15:178–196.

[252] Banks RE, Tirukonda P, Taylor C, Hornigold N, Astuti D, Cohen D, Maher ER, Stanley AJ, Harnden P, Joyce A, Knowles M, Selby PJ. Genetic and epigenetic analysis of von Hippel- Lindau (VHL) gene alterations and relationship with clinical variables in sporadic renal cancer. *Cancer Res*. 2006;66(4):2000-11.

[253] Dulaimi E, Ibanez de Caceres I, Uzzo RG, Al-Saleem T, Greenberg RE, Polascik TJ, Babb JS, Grizzle WE, Cairns P. Promoter hypermethylation profile of kidney cancer. *Clin. Cancer Res*. 2004;10(12 Pt 1):3972-9.

[254] Hori Y, Oda Y, Kiyoshima K, Yamada Y, Nakashima Y, Naito S, Tsuneyoshi M. Oxidative stress and DNA hypermethylation status in renal cell carcinoma arising in patients on dialysis. *J. Pathol*. 2007;212(2):218-26.

[255] Arai E, Kanai Y, Ushijima S, Fujimoto H, Mukai K, Hirohashi S. Regional DNA hypermethylation and DNA methyltransferase (DNMT) 1 protein overexpression in both renal tumors and corresponding nontumorous renal tissues. *Int. J. Cancer.* 2006;119(2):288-96.

[256] Schouten LJ, Deckers IA, van den Brandt PA, Baldewijns MM, van Engeland M, M. Alcohol and dietary folate intake and promoter CpG island methylation in clear- cell renal cell cancer. *Nutr. Cancer.*2016;68(7):1097-107.

[257] Kim JH, Jung CW, Cho YH, Lee J, Lee SH, Kim HY, Park J, Park JO, Kim K, Kim WS, Park YS, Im YH, Kang WK, Park K. Somatic VHL alteration and its impact on prognosis in patients with clear cell renal cell carcinoma. *Oncol. Rep*. 2005;13(5):859-64.

[258] Smits KM, Schouten LJ, van Dijk BA, Hulsbergen-van de Kaa CA, Wouters KA, Oosterwijk E, van Engeland M, van den Brandt PA. Genetic and epigenetic alterations in the von hippel- lindau gene: the influence on renal cancer prognosis. *Clin. Cancer Res*. 2008;14(3):782-7.

[259] Patard JJ, Rioux-Leclercq N, Masson D, Zerrouki S, Jouan F, Collet N, Dubourg C, Lobel B, Denis M, Fergelot P. Absence of VHL gene alteration and high VEGF expression are associated with tumour aggressiveness and poor survival of renal- cell carcinoma. *Br. J. Cancer.* 2009;101(8):1417-24.

[260] Young AC, Craven RA, Cohen D, Taylor C, Booth C, Harnden P, Cairns DA, Astuti D, Gregory W, Maher ER, Knowles MA, Joyce A, Selby PJ, Banks RE. Analysis of VHL gene alterations and their relationship to clinical parameters in sporadic conventional renal cell carcinoma. *Clin. Cancer Res*. 2009;15(24):7582-7592.

[261] Moore LE, Nickerson ML, Brennan P, Toro JR, Jaeger E, Rinsky J, Han SS, Zaridze D, Matveev V, Janout V, Kollarova H, Bencko V, Navratilova M, Szeszenia-Dabrowska N, Mates D, Schmidt LS, Lenz P, Karami S, Linehan WM, Merino M, Chanock S, Boffetta P, Chow WH, Waldman FM, Rothman N. Von Hippel- Lindau (VHL) inactivation in sporadic clear cell renal cancer: associations with germline VHL polymorphisms and etiologic risk factors. *PLoS Genet*. 2011;7(10):e1002312.

[262] Gossage L, Murtaza M, Slatter AF, Lichtenstein CP, Warren A, Haynes B, Marass F, Roberts I, Shanahan SJ, Claas A, Dunham A, May AP, Rosenfeld N, Forshew T, Eisen T. Clinical and pathological impact of VHL, PBRM1, BAP1, SETD2, KDM6A, and JARID1c in clear cell renal cell carcinoma. *Genes Chromosomes Cancer.* 2014;53(1):38-51.

[263] Lessi F, Mazzanti CM, Tomei S, Di Cristofano C, Minervini A, Menicagli M, Apollo A, Masieri L, Collecchi P, Minervini R, Carini M, Bevilacqua G. VHL and HIF-1alpha: gene variations and prognosis in early- stage clear cell renal cell carcinoma. *Med. Oncol*. 2014;31(3):840.

[264] Morris MR, Ricketts C, Gentle D, Abdulrahman M, Clarke N, Brown M, Kishida T, Yao M, Latif F, Maher ER. Identification of candidate tumour

suppressor genes frequently methylated in renal cell carcinoma. *Oncogene.* 2010;29(14):2104-17.

[265] van Vlodrop IJH, Joosten SC, De Meyer T, Smits KM, Van Neste L, Melotte V, Baldewijns MMLL, Schouten LJ, van den Brandt PA, Jeschke J, Yi JM, Schuebel KE, Ahuja N, Herman JG, Aarts MJ, Bosman FT, Van Criekinge W, van Engeland M. A four- gene promoter methylation marker panel consisting of GREM1, NEURL, LAD1, and NEFH predicts survival of clear cell renal cell cancer patients. *Clin. Cancer Res*. 2017;23(8):2006-2018.

[266] van Vlodrop IJ, Baldewijns MM, Smits KM, Schouten LJ, van Neste L, van Criekinge W, van Poppel H, Lerut E, Schuebel KE, Ahuja N, Herman JG, de Bruïne AP, van Engeland M. Prognostic significance of Gremlin1 (GREM1) promoter CpG island hypermethylation in clear cell renal cell carcinoma. *Am. J. Pathol*. 2010;176(2):575-84.

[267] Costa VL, Henrique R, Ribeiro FR, Pinto M, Oliveira J, Lobo F, Teixeira MR, Jerónimo C. Quantitative promoter methylation analysis of multiple cancer- related genes in renal cell tumors. *BMC Cancer.* 2007;7:133.

[268] Onay H, Pehlivan S, Koyuncuoglu M, Kirkali Z, Ozkinay F. Multigene methylation analysis of conventional renal cell carcinoma. *Urol. Int*. 2009;83(1):107-12.

[269] Masson D, Rioux-Leclercq N, Fergelot P, Jouan F, Mottier S, Théoleyre S, Bach-Ngohou K, Patard JJ, Denis MG. Loss of expression of TIMP3 in clear cell renal cell carcinoma. *Eur. J. Cancer*. 2010;46(8):1430-7.

[270] Morris MR, Ricketts CJ, Gentle D, McRonald F, Carli N, Khalili H, Brown M, Kishida T, Yao M, Banks RE, Clarke N, Latif F, Maher ER. Genome-wide methylation analysis identifies epigenetically inactivated candidate tumour suppressor genes in renal cell carcinoma. *Oncogene.* 2011;30(12):1390-401.

[271] Ricketts CJ, Morris MR, Gentle D, Brown M, Wake N, Woodward ER, Clarke N, Latif F, Maher ER. Genome- wide CpG island methylation analysis implicates novel genes in the pathogenesis of renal cell carcinoma. *Epigenetics.* 2012;7(3):278-90.

[272] Lin YL, Wang YL, Fu XL, Ma JG. Aberrant methylation of PCDH8 is a potential prognostic biomarker for patients with clear cell renal cell carcinoma. *Med. Sci. Monit*. 2014;20:2380-5.

[273] Dubrowinskaja N, Gebauer K, Peters I, Hennenlotter J, Abbas M, Scherer R, Tezval H, Merseburger AS, Stenzl A, Grünwald V, Kuczyk MA, Serth J. Neurofilament heavy polypeptide CpG island methylation associates with prognosis of renal cell carcinoma and prediction of antivascular endothelial growth factor therapy response. *Cancer Med*. 2014;3(2):300-9.

[274] Mitsui Y, Hirata H, Arichi N, Hiraki M, Yasumoto H, Chang I, Fukuhara S, Yamamura S, Shahryari V, Deng G, Saini S, Majid S, Dahiya R, Tanaka Y, Shiina H. Inactivation of bone morphogenetic protein 2 may predict clinical outcome and poor overall survival for renal cell carcinoma through epigenetic pathways. *Oncotarget.* 2015;6(11):9577-91.

[275] Urakami S, Shiina H, Enokida H, Hirata H, Kawamoto K, Kawakami T, Kikuno N, Tanaka Y, Majid S, Nakagawa M, Igawa M, Dahiya R. Wnt antagonist family genes as biomarkers for diagnosis, staging, and prognosis of renal cell carcinoma using tumor and serum DNA. *Clin. Cancer Res*. 2006;12(23):6989-97.

[276] Dahl E, Wiesmann F, Woenckhaus M, Stoehr R, Wild PJ, Veeck J, Knüchel R, Klopocki E, Sauter G, Simon R, Wieland WF, Walter B, Denzinger S, Hartmann A, Hammerschmied CG. Frequent loss of SFRP1 expression in multiple human solid tumours: association with aberrant promoter methylation in renal cell carcinoma. *Oncogene.* 2007;26(38):5680-91.

[277] Awakura Y, Nakamura E, Ito N, Kamoto T, Ogawa O. Methylation-associated silencing of SFRP1 in renal cell carcinoma. *Oncol. Rep*. 2008;20(5):1257-63.

[278] Hirata H, Hinoda Y, Nakajima K, Kawamoto K, Kikuno N, Ueno K, Yamamura S, Zaman MS, Khatri G, Chen Y, Saini S, Majid S, Deng G, Ishii N, Dahiya R. Wnt antagonist DKK1 acts as a tumor suppressor gene that induces apoptosis and inhibits proliferation in human renal cell carcinoma. *Int. J. Cancer.* 2011;128(8):1793-803.

[279] Okuda H, Toyota M, Ishida W, Furihata M, Tsuchiya M, Kamada M, Tokino T, Shuin T. Epigenetic inactivation of the candidate tumor suppressor gene HOXB13 in human renal cell carcinoma. *Oncogene* 2006;25(12):1733-42.

[280] Sanz-Casla MT, Maestro ML, del Barco V, Zanna I, Moreno J, Vidaurreta M, Almansa I, Fernández C, Blanco J, Maestro C, Resel L. Loss of heterozygosity and methylation of p16 in renal cell carcinoma. *Urol. Res*. 2003;31(3):159-62.

[281] Vidaurreta M, Maestro ML, Sanz-Casla MT, Maestro C, Rafael S, Veganzones S, Moreno J, Blanco J, Silmi A, Arroyo M. Inactivation of p16 by CpG hypermethylation in renal cell carcinoma. *Urol. Oncol*. 2008;26(3):239-45.

[282] Morrissey C, Martinez A, Zatyka M, Agathanggelou A, Honorio S, Astuti D, Morgan NV, Moch H, Richards FM, Kishida T, Yao M, Schraml P, Latif F, Maher ER. Epigenetic inactivation of the RASSF1A 3p21.3 tumor suppressor gene in both clear cell and papillary renal cell carcinoma. *Cancer Res*. 2001;61(19):7277-81.

[283] Tokinaga K, Okuda H, Nomura A, Ashida S, Furihata M, Shuin T. Hypermethylation of the RASSF1A tumor suppressor gene in Japanese clear cell renal cell carcinoma. *Oncol. Rep*. 2004;12(4):805-10.

[284] Gonzalgo ML, Yegnasubramanian S, Yan G, Rogers CG, Nicol TL, Nelson WG, Pavlovich CP. Molecular profiling and classification of sporadic renal cell carcinoma by quantitative methylation analysis. *Clin. Cancer Res*. 2004;10(21):7276-83.

[285] Kawai Y, Sakano S, Suehiro Y, Okada T, Korenaga Y, Hara T, Naito K, Matsuyama H, Hinoda Y. Methylation level of the RASSF1A promoter is an independent prognostic factor for clear- cell renal cell carcinoma. *Ann. Oncol*. 2010;21(8):1612-1617.

[286] Christoph F, Weikert S, Kempkensteffen C, Krause H, Schostak M, Köllermann J, Miller K, Schrader M. Promoter hypermethylation profile of kidney cancer with new proapoptotic p53 target genes and clinical implications. *Clin. Cancer Res*. 2006;12(17):5040-6.

[287] Christoph F, Hinz S, Kempkensteffen C, Schostak M, Schrader M, Miller K. mRNA expression profiles of methylated APAF-1 and DAPK-1 tumor suppressor genes uncover clear cell renal cell carcinomas with aggressive phenotype. *J. Urol*. 2007;178(6):2655-9.

[288] Christoph F, Hinz S, Weikert S, Kempkensteffen C, Schostak M, Miller K, Schrader M. Comparative promoter methylation analysis of p53 target genes in urogenital cancers. *Urol. Int*. 2008;80(4):398-404.

[289] Ahmad ST, Arjumand W, Seth A, Saini AK, Sultana S. Methylation of the APAF-1 and DAPK-1 promoter region correlates with progression of renal cell carcinoma in North Indian population. *Tumour Biol*. 2012;33(2):395-402.

[290] Deckers IA, Schouten LJ, Van Neste L, van Vlodrop IJ, Soetekouw PM, Baldewijns MM, Jeschke J, Ahuja N, Herman JG, van den Brandt PA, van Engeland M. Promoter methylation of CDO1 identifies clear- cell renal cell cancer patients with poor survival outcome. *Clin. Cancer Res*. 2015;21(15):3492-500.

[291] Dongre A, Weinberg RA. New insights into the mechanisms of epithelial-mesenchymal transition and implications for cancer. *Nat Rev Mol Cell Biol.* 2019;20(2):69-84.

[292] van Roy, F. Beyond E-cadherin: roles of other cadherin superfamily members in cancer. *Nat. Rev. Cancer.* 2014;14(2):121-34.

[293] Ricketts CJ, Hill VK, Linehan WM. Tumorspecific hypermethylation of epigenetic biomarkers, including SFRP1, predicts for poorer survival in

patients from the TCGA Kidney Renal Clear Cell Carcinoma (KIRC) project. *PLoS One*. 2014;9(1):e85621.

[294] Samavarchi-Tehrani P, Golipour A, David L, Sung HK, Beyer TA, Datti A, Woltjen K, Nagy A, Wrana JL. Functional genomics reveals a BMP-driven mesenchymal-to-epithelial transition in the initiation of somatic cell reprogramming. *Cell Stem Cell*. 2010;7(1):64-77.

[295] Kruck S, Eyrich C, Scharpf M, Sievert KD, Fend F, Stenzl A, Bedke J. Impact of an altered Wnt1/β-catenin expression on clinicopathology and prognosis in clear cell renal cell carcinoma. *Int. J. Mol. Sci*. 2013;14(6):10944-57.

[296] Cruciat CM, Niehrs C. Secreted and transmembrane wnt inhibitors and activators. *Cold Spring Harb Perspect Biol*. 2013;5(3):a015081.

[297] Ibragimova I, Slifker MJ, Maradeo ME, Banumathy G, Dulaimi E, Uzzo RG, Cairns P. Genome-wide promoter methylome of small renal masses. *PLoS One*. 2013;8(10):e77309.

[298] Evelönn EA, Degerman S, Köhn L, Landfors M, Ljungberg B, Roos G. DNA methylation status defines clinicopathological parameters including survival for patients with clear cell renal cell carcinoma (ccRCC). *Tumour Biol*. 2016;37(8):10219-28.

[299] Kang HW, Park H, Seo SP, Byun YJ, Piao XM, Kim SM, Kim WT, Yun SJ, Jang W, Shon HS, Ryu KH, Lee SC, Kim WJ, Kim YJ. Methylation Signature for Prediction of Progression Free Survival in Surgically Treated Clear Cell Renal Cell Carcinoma. *J Korean Med Sci*. 2019;34(19):e144.

[300] Kim YJ, Jang W, Piao XM, Yoon HY, Byun YJ, Kim JS, Kim SM, Lee SK, Seo SP, Kang HW, Kim WT, Yun SJ, Shon HS, Ryu KH, Kim SW, Ha YS, Yoon GS, Lee SC, Kwon TG, Kim WJ. ZNF492 and GPR149 methylation patterns as prognostic markers for clear cell renal cell carcinoma: Array-based DNA methylation profiling. *Oncol Rep*. 2019;42(1):453-460.

[301] Yoo KH, Park YK, Kim HS, Jung WW, Chang SG. Epigenetic inactivation of HOXA5 and MSH2 gene in clear cell renal cell carcinoma. *Pathol Int*. 2010;60(10):661-6.

[302] Hauser S, Zahalka T, Fechner G, Müller SC, Ellinger J. Serum DNA hypermethylation in patients with kidney cancer: results of a prospective study. Anticancer Res. 2013;33(10):4651-6.

[303] de Martino M, Klatte T, Haitel A, Marberger M. Serum cell-free DNA in renal cell carcinoma: a diagnostic and prognostic marker. Cancer. *Cancer*. 2012;118(1):82-90.

[304] Skrypkina I, Tsyba L, Onyshchenko K, Morderer D, Kashparova O, Nikolaienko O, Panasenko G, Vozianov S, Romanenko A, Rynditch A. Concentration and Methylation of Cell-Free DNA from Blood Plasma as Diagnostic Markers of Renal Cancer. *Dis Markers*. 2016;2016:3693096.

[305] Jung M, Ellinger J, Gevensleben H, Syring I, Lüders C, de Vos L, Pützer S, Bootz F, Landsberg J, Kristiansen G, Dietrich D. Cell-Free SHOX2 DNA Methylation in Blood as a Molecular Staging Parameter for Risk Stratification in Renal Cell Carcinoma Patients: A Prospective Observational Cohort Study. *Clin Chem*. 2019;65(4):559-568.

[306] Larsen LK, Lind GE, Guldberg P, Dahl Ch. DNA-Methylation-Based Detection of Urological Cancer in Urine: Overview of Biomarkers and Considerations on Biomarker Design, Source of DNA, and Detection Technologies. *Int J Mol Sci*. 2019;20(11):2657.

[307] Maleckaite R, Zalimas A, Bakavicius A, Jankevicius F, Jarmalaite S, Daniunaite K. DNA methylation of metallothionein genes is associated with the clinical features of renal cell carcinoma. *Oncol Rep*. 2019;41(6):3535-3544.

[308] Lehmann U, Langer F, Feist H, Glöckner S, Hasemeier B, Kreipe H. Quantitative assessment of promoter hypermethylation during breast cancer development. *Am J Pathol*. 2002;160(2):605-12.

[309] Kubiliūtė R, Žukauskaitė K, Žalimas A, Ulys A, Sabaliauskaitė R, Bakavičius A, Želvys A, Jankevičius F, Jarmalaitė S. Clinical significance of novel DNA methylation biomarkers for renal clear cell carcinoma. *J Cancer Res Clin Oncol.* 2021. Online ahead of print.

[310] Kubiliute R, Zalimas A, Bakavicius A, Ulys A, Jankevicius F, Jarmalaite S. Clinical Significance of ADAMTS19, BMP7, SIM1, and SFRP1 Promoter Methylation in Renal Clear Cell Carcinoma. *Onco Targets Ther*. 2021;14:4979-4990.

[311] Richard PO, Lavallée LT, Pouliot F, Komisarenko M, Martin L, Lattouf JB, Finelli A. Is Routine Renal Tumor Biopsy Associated with Lower Rates of Benign Histology following Nephrectomy for Small Renal Masses? *J Urol*. 2018;200(4):731-736.

[312] Morris MR, Latif F. The epigenetic landscape of renal cancer. *Nat. Rev. Nephrol*. 2017;13(1):47-60.

[313] Atschekzei F, Hennenlotter J, Jänisch S, Großhennig A, Tränkenschuh W, Waalkes S, Peters I, Dörk T, Merseburger AS, Stenzl A, Kuczyk MA, Serth J. SFRP1 CpG island methylation locus is associated with renal cell cancer susceptibility and disease recurrence. *Epigenetics.* 2012;7(5):447-57.

[314] Jen J, Wang YC. Zinc finger proteins in cancer progression. *J Biomed Sci.* 2016;23(1):53.

[315] Heller G, Altenberger C, Schmid B, Marhold M, Tomasich E, Ziegler B, Müllauer L, Minichsdorfer C, Lang G, End-Pfützenreuter A, Döme B, Arns BM, Fong KM, Wright CM, Yang IA, Klepetko W, Zielinski CC, Zöchbauer-Müller S. DNA methylation transcriptionally regulates the putative tumor cell growth suppressor ZNF677 in non-small cell lung cancers. *Oncotarget.* 2015;6(1):394-408.

[316] Li Y, Yang Q, Guan H, Shi B, Ji M, Hou P. ZNF677 Suppresses Akt Phosphorylation and Tumorigenesis in Thyroid Cancer. *Cancer Res*. 2018;78(18):5216-5228.

[317] Dai Y, Lv Q, Qi T, Qu J, Ni H, Liao Y, Liu P, Qu Q. Identification of hub methylated-CpG sites and associated genes in oral squamous cell carcinoma. *Cancer Med*. 2020;9(9):3174-3187.

[318] van Loon K, Yemelyanenko-Lyalenko J, Margadant C, Griffioen AW, Huijbers EJM. Role of fibrillin-2 in the control of TGF-β activation in tumor angiogenesis and connective tissue disorders. *Biochim Biophys Acta Rev Cancer*. 2020;1873(2):188354.

[319] Kahr I, Vandepoele K, van Roy F. Delta-protocadherins in health and disease. *Prog Mol Biol Transl Sci*. 2013;116:169-92.

[320] He D, Zeng Q, Ren G, Xiang T, Qian Y, Hu Q, Zhu J, Hong S, Hu G. Protocadherin8 is a functional tumor suppressor frequently inactivated by promoter methylation in nasopharyngeal carcinoma. *Eur J Cancer Prev*. 2012;21(6):569-75.

[321] Yu JS, Koujak S, Nagase S, Li CM, Su T, Wang X, Keniry M, Memeo L, Rojtman A, Mansukhani M, Hibshoosh H, Tycko B, Parsons R. PCDH8, the human homolog of PAPC, is a candidate tumor suppressor of breast cancer. *Oncogene*. 2008;27(34):4657-65.

[322] Zhang D, Zhao W, Liao X, Bi T, Li H, Che X. Frequent silencing of protocadherin 8 by promoter methylation, a candidate tumor suppressor for human gastric cancer. *Oncol Rep*. 2012;28(5):1785-91.

[323] Li Z, Gou J, Jia J, Zhao X. MicroRNA-429 functions as a regulator of epithelial-mesenchymal transition by targeting Pcdh8 during murine embryo implantation. *Hum Reprod*. 2015;30(3):507-18.

[324] Lin Y, Ge X, Zhang X, Wu Z, Liu K, Lin F, Dai C, Guo W, Li J. Protocadherin-8 promotes invasion and metastasis via laminin subunit γ2 in gastric cancer. *Cancer Sci*. 2018;109(3):732-740.

[325] Eckert D, Buhl S, Weber S, Jäger R, Schorle H. The AP-2 family of transcription factors. *Genome Biol*. 2005;6(13):246.

[326] Moser M, Pscherer A, Roth C, Becker J, Mücher G, Zerres K, Dixkens C, Weis J, Guay-Woodford L, Buettner R, Fässler R. Enhanced apoptotic cell death of renal epithelial cells in mice lacking transcription factor AP-2beta. *Genes Dev*. 1997;11(15):1938-48.

[327] Ikram F, Ackermann S, Kahlert Y, Volland R, Roels F, Engesser A, Hertwig F, Kocak H, Hero B, Dreidax D, Henrich KO, Berthold F, Nürnberg P, Westermann F, Fischer M. Transcription factor activating protein 2 beta (TFAP2B) mediates noradrenergic neuronal differentiation in neuroblastoma. *Mol Oncol*. 2016;10(2):344-59.

[328] Yoldi G, Pellegrini P, Trinidad EM, Cordero A, Gomez-Miragaya J, Serra-Musach J, Dougall WC, Muñoz P, Pujana MA, Planelles L, González-Suárez E. RANK Signaling Blockade Reduces Breast Cancer Recurrence by Inducing Tumor Cell Differentiation. *Cancer Res*. 2016;76(19):5857-5869.

[329] Wang L, Wang C, Wu T, Sun F. Long non-coding RNA TP73-AS1 promotes TFAP2B-mediated proliferation, metastasis and invasion in retinoblastoma via decoying of miRNA-874-3p. *J Cell Commun Signal*. 2020;14(2):193-205.

[330] Liang S, Deng H. Dual role of transcription factor AP-2 in carcinogenesis. *Zhejiang Da Xue Xue Bao Yi Xue Ban*. 2010;39(4):430-5.

[331] Oya M, Mikami S, Mizuno R, Miyajima A, Horiguchi Y, Nakashima J, Marumo K, Mukai M, Murai M. Differential expression of activator protein-2 isoforms in renal cell carcinoma. *Urology*. 2004;64(1):162-7.

[332] Wang Y, Hoeppner LH, Angom RS, Wang E, Dutta S, Doeppler HR, Wang F, Shen T, Scarisbrick IA, Guha S, Storz P, Bhattacharya R, Mukhopadhyay D. Protein kinase D up-regulates transcription of VEGF receptor-2 in endothelial cells by suppressing nuclear localization of the transcription factor AP2β. *J Biol Chem*. 2019;294(43):15759-15767.

[333] Tun HW, Marlow LA, von Roemeling CA, Cooper SJ, Kreinest P, Wu K, Luxon BA, Sinha M, Anastasiadis PZ, Copland JA. Pathway signature and cellular differentiation in clear cell renal cell carcinoma. *PLoS One*. 2010;5(5):e10696.

[334] Rameshwar P, Gascón P. Induction of negative hematopoietic regulators by neurokinin-A in bone marrow stroma. *Blood*. 1996 Jul 1;88(1):98-106.

[335] Steinhoff MS, von Mentzer B, Geppetti P, Pothoulakis C, Bunnett NW. Tachykinins and Their Receptors: Contributions to Physiological Control

and the Mechanisms of Disease. *Physiological Reviews.* 2014;94(1):265-301.

[336] Chevrier S, Levine JH, Zanotelli VRT, Silina K, Schulz D, Bacac M, Ries CH, Ailles L, Jewett MAS, Moch H, van den Broek M, Beisel C, Stadler MB, Gedye C, Reis B, Pe'er D, Bodenmiller B. An Immune Atlas of Clear Cell Renal Cell Carcinoma. *Cell*. 2017;169(4):736-749.e18.

[337] Díaz-Montero CM, Rini BI, Finke JH. The immunology of renal cell carcinoma. *Nat Rev Nephrol*. 2020;16(12):721-735.

[338] Wrangle J, Machida EO, Danilova L, Hulbert A, Franco N, Zhang W, Glöckner SC, Tessema M, Van Neste L, Easwaran H, Schuebel KE, Licchesi J, Hooker CM, Ahuja N, Amano J, Belinsky SA, Baylin SB, Herman JG, Brock MV. Functional identification of cancer-specific methylation of CDO1, HOXA9, and TAC1 for the diagnosis of lung cancer. *Clin Cancer Res*. 2014;20(7):1856-64.

[339] Tham C, Chew M, Soong R, Lim J, Ang M, Tang C, Zhao Y, Ong SY, Liu Y. Postoperative serum methylation levels of TAC1 and SEPT9 are independent predictors of recurrence and survival of patients with colorectal cancer. *Cancer*. 2014;120(20):3131-41.

[340] Misawa K, Mochizuki D, Imai A, Endo S, Mima M, Misawa Y, Kanazawa T, Carey TE, Mineta H. Prognostic value of aberrant promoter hypermethylation of tumor-related genes in early-stage head and neck cancer. *Oncotarget*. 2016;7(18):26087-98.

[341] Henriksen SD, Madsen PH, Larsen AC, Johansen MB, Pedersen IS, Krarup H, Thorlacius-Ussing O. Promoter hypermethylation in plasma-derived cell-free DNA as a prognostic marker for pancreatic adenocarcinoma staging. *Int J Cancer*. 2017;141(12):2489-2497.

[342] Jin Z, Olaru A, Yang J, Sato F, Cheng Y, Kan T, Mori Y, Mantzur C, Paun B, Hamilton JP, Ito T, Wang S, David S, Agarwal R, Beer DG, Abraham JM, Meltzer SJ. Hypermethylation of tachykinin-1 is a potential biomarker in human esophageal cancer. *Clin Cancer Res*. 2007;13(21):6293-300.

[343] Jeschke J, Van Neste L, Glöckner SC, Dhir M, Calmon MF, Deregowski V, Van Criekinge W, Vlassenbroeck I, Koch A, Chan TA, Cope L, Hooker CM, Schuebel KE, Gabrielson E, Winterpacht A, Baylin SB, Herman JG, Ahuja N. Biomarkers for detection and prognosis of breast cancer identified by a functional hypermethylome screen. *Epigenetics*. 2012;7(7):701–709.

[344] Lacy SE, Bönnemann CG, Buzney EA, Kunkel LM. Identification of FLRT1, FLRT2, and FLRT3: a novel family of transmembrane leucine-rich repeat proteins. *Genomics*. 1999;62(3):417-26.

[345] Flintoff KA, Arudchelvan Y, Gong SG. FLRT2 interacts with fibronectin in the ATDC5 chondroprogenitor cells. *J Cell Physiol*. 2014;229(10):1538-47.

[346] Bae H, Kim B, Lee H, Lee S, Kang HS, Kim SJ. Epigenetically regulated Fibronectin leucine rich transmembrane protein 2 (FLRT2) shows tumor suppressor activity in breast cancer cells. *Sci Rep*. 2017;7(1):272.

[347] Cal S, López-Otín C. ADAMTS proteases and cancer. *Matrix Biol*. 2015;44-46:77-85.

[348] Hubmacher D, Apte SS. Genetic and functional linkage between ADAMTS superfamily proteins and fibrillin-1: a novel mechanism influencing microfibril assembly and function. *Cell Mol Life Sci*. 2011;68(19):3137-48.

[349] Zeisberg M. Bone morphogenic protein-7 and the kidney: current concepts and open questions. *Nephrol Dial Transplant*. 2006;21(3):568-73.

[350] Gregory KE, Ono RN, Charbonneau NL, Kuo CL, Keene DR, Bächinger HP, Sakai LY. The prodomain of BMP-7 targets the BMP-7 complex to the extracellular matrix. *J Biol Chem*. 2005;280(30):27970-80.

[351] Wang Z, Zhao J, Zhang J, Wei J, Huang Y. Protective effect of BMP-7 against aristolochic acid-induced renal tubular epithelial cell injury. *Toxicol Lett*. 2010;198(3):348-57.

[352] Gould SE, Day M, Jones SS, Dorai H. BMP-7 regulates chemokine, cytokine, and hemodynamic gene expression in proximal tubule cells. *Kidney Int* 2002;61(1):51-60.

[353] Basic-Jukic N, Hudolin T, Radic-Antolic M, Coric M, Zadro R, Kastelan Z, Pasini J, Bandic-Pavlovic D, Kes P. Bone morphogenetic protein-7 expression is down-regulated in human clear cell renal carcinoma. *J Nephrol*. 2011;24(1):91-7.

[354] Markić D, Celić T, Spanjol J, Grsković A, Bobinac D, Fuckar Z. Expression of bone morphogenetic protein-7, its receptors and Smad1/5/8 in normal human kidney and renal cell cancer. *Coll Antropol*. 2010;34 Suppl 2:149-53.

[355] Michaud JL, Rosenquist T, May NR, Fan CM. Development of neuroendocrine lineages requires the bHLH-PAS transcription factor SIM1. *Genes Dev* 1998;12:3264–3275.

[356] Kim MJ, Oksenberg N, Hoffmann TJ, Vaisse C, Ahituv N. Functional characterization of SIM1-associated enhancers. *Hum Mol Genet*. 2014;23(7):1700-8.

[357] Sidaway P. Kidney cancer: Methylation of obesity-related genes is associated with prognosis. *Nat Rev Urol*. 2017;14(8):452.

[358] Faryna M, Konermann C, Aulmann S, Bermejo JL, Brugger M, Diederichs S, Rom J, Weichenhan D, Claus R, Rehli M, Schirmacher P, Sinn HP, Plass C, Gerhauser C. Genome-wide methylation screen in low-grade breast cancer identifies novel epigenetically altered genes as potential biomarkers for tumor diagnosis. *FASEB J*. 2012;26(12):4937-50.

[359] Daugaard I, Dominguez D, Kjeldsen TE, Kristensen LS, Hager H, Wojdacz TK, Hansen LL. Identification and validation of candidate epigenetic biomarkers in lung adenocarcinoma. *Sci Rep.* 201626;6:35807.

[360] Kim HJ, Kim CY, Jin J, Bae MK, Kim YH, Ju W, Kim YH, Kim SC. Aberrant single-minded homolog 1 methylation as a potential biomarker for cervical cancer. *Diagn Cytopathol.* 2018;46(1):15-21.

[361] Mo S, Su Z, Heng B, Chen W, Shi L, Du X, Lai C. SFRP1 Promoter Methylation and Renal Carcinoma Risk: A Systematic Review and Meta-Analysis. *J Nippon Med Sch*. 2018;85(2):78-86.

[362] Schiavina R, Borghesi M, Chessa F, Dababneh H, Bianchi L, Della Mora L, Del Prete C, Longhi B, Rizzi S, Fiorentino M, Martorana G, Brunocilla E. The Prognostic Impact of Tumor Size on Cancer-Specific and Overall Survival Among Patients With Pathologic T3a Renal Cell Carcinoma. *Clin Genitourin Cancer*. 2015;13(4):e235-e241.

[363] Chen L, Ma X, Li H, Gu L, Li X, Gao Y, Xie Y, Zhang X. Influence of tumor size on oncological outcomes of pathological T3aN0M0 renal cell carcinoma treated by radical nephrectomy. *PLoS One*. 2017;12(3):e0173953.

[364] Li L, Shi L, Zhang J, Fan Y, Li Q. The critical impact of tumor size in predicting cancer special survival for T3aM0M0 renal cell carcinoma: A proposal of an alternative T3aN0M0 stage. *Cancer Med*. 2021;10(2):605-614.

[365] Lu T, Li J. Clinical applications of urinary cell-free DNA in cancer: current insights and promising future. *Am J Cancer Res*. 2017;7(11):2318-2332.

[366] Daniūnaitė K, Jarmalaitė S, Kriukienė E. Epigenomic technologies for deciphering circulating tumor DNA. *Curr Opin Biotechnol*. 2019;55:23-29.

[367] Sauerbrei W, Taube SE, McShane LM, Cavenagh MM, Altman DG. Reporting Recommendations for Tumor Marker Prognostic Studies (REMARK): An Abridged Explanation and Elaboration. J Natl Cancer Inst. 2018;110(8):803-811.

SUPPLEMENTARY MATERIAL

Table S1. Demographic and clinical-pathological characteristics of the patients with clear cell renal cell carcinoma (ccRCC) and asymptomatic controls (ASCs).

Parameter	**Genome-wide DNA methylation analysis**		**Global gene expression analysis**		**DNA Methylation analysis using MSP or qMSP**			**Survival analysis****	
Group composition	ccRCC (N=11)	NRT (N=11)	ccRCC (N=4)	NRT (N=4)	ccRCC* (N=123)	NRT* (N=45)	ASC (N=92)	Survived (N=86)	Dead (N=21)
Age, years									
Mean ±SD, [min; max]	61±4 [55; 66]	61±4 [55; 66]	62±4 [57; 66]	62±4 [57; 66]	63±12 [21; 85]	63±15 [21; 85]	60±9 [27; 82]	61±12 [21; 84]	72±9 [50; 85]
Gender									
Male	6 (55%)	6 (55%)	3 (75%)	3 (75%)	64 (52%)	20 (44%)	49 (53%)	40 (47%)	15 (71%)
Female	5 (45%)	5 (45%)	1 (25%)	1 (25%)	59 (48%)	25 (56%)	43 (47%)	46 (53%)	6 (29%)
Stage									
pT1	4 (36%)	na	na	na	52 (42%)	na	na	44 (51%)	4 (19%)
pT2	-	na	na	na	5 (4%)	na	na	5 (6%)	na
pT3	4 (36%)	na	1 (25%)	na	61 (50%)	na	na	36 (42%)	15 (71%)
pT4	3 (28%)	na	3 (75%)	na	5 (4%)	na	na	1 (1%)	2 (10%)
Tumor size, mm									
Mean ±SD, [min; max]	48±29 [20; 95]	na	80±23 [45; 95]	na	57±29 [20; 180]	na	na	51±27 [20; 180]	64±29 [25; 130]
WHO/ISUP grade									
1	na	na	na	na	6 (5%)	na	na	4 (5%)	na
2	6 (55%)	na	na	na	71 (58%)	na	na	57 (66%)	9 (43%)
3	5 (45%)	na	4 (100%)	na	46 (37%)	na	na	25 (29%)	12 (57%)

Table S1. Continued.

Parameter	Genome-wide DNA methylation analysis		Global gene expression analysis		DNA Methylation analysis using MSP or qMSP			Survival analysis**	
Group composition	ccRCC (N=11)	NRT (N=11)	ccRCC (N=4)	NRT (N=4)	ccRCC* (N=123)	NRT* (N=45)	ASC (N=92)	Survived (N=86)	Dead (N=21)
Fuhrman grade									
1	na	na	na	na	4 (3%)	na	na	na	na
2	4 (36%)	na	na	na	46 (37%)	na	na	3 (3%)	8 (38%)
3	6 (55%)	na	3 (75%)	na	64 (52%)	na	na	35 (41%)	10 (48%)
4	1 (9%)	na	1 (25%)	na	6 (5%)	na	na	45 (53%)	3 (14%)
Unknown	na	na	na	na	3 (3%)	na	na	3 (3%)	na
Intravascular invasion									
No	6 (55%)	na	1 (25%)	na	83 (67%)	na	na	66 (77%)	12 (57%)
Yes	5 (45%)	na	3 (75%)	na	40 (33%)	na	na	20 (23%)	9 (43%)
Fat invasion									
No	7 (64%)	na	2 (50%)	na	73 (59%)	na	na	59 (69%)	7 (33%)
Yes	4 (36%)	na	2 (50%)	na	50 (41%)	na	na	27 (31%)	14 (67%)
Tumor necrosis									
No	8 (72%)	na	2 (50%)	na	94 (76%)	na	na	73 (85%)	10 (48%)
Yes	3 (28%)	na	2 (50%)	na	29 (24%)	na	na	13 (15%)	11 (52%)

ccRCC – clear cell renal cell carcinoma; NRT – non-cancerous renal tissues; ASC – asymptomatic control; MSP – methylation-specific PCR; qMSP – quantitative MSP; WHO/ISUP – World Health Organisation/Internation Society of Urological Pathology; pT – pathological tumor stage; na – not applicable.

* – tissue samples were also included in gene expression analysis.

** – survival data last updated in February 2020 was used for the analysis.

Table S2. Primers used for methylation-specific PCR analysis (MSP) and amplification conditions.

Assay	Primer type	Primer/probe sequence (5‘→3‘)	Amplicon size, nt	Amplicon location from TSS	Primer annealing t °C	Number of MSP cycles
ZNF677	M-F	TCGCGGGTTATAGGTTTTTAC	156	+74/+230	58	37
	M-R	AATCCGAAATAAACGCAAATCTC				
	U-F	GTTTTGTGGGTTATAGGTTTTTATG	162	+71/+233	58	
	U-R	TTTAATCCAAAATAAACACAAATCTCT				
FBN2	M-F	TTTAATATTCGTTTTCGGAGCG	182	+206/+388	58	37
	M-R	CCGAACGATACACGTTACATAA				
	U-F	GTAGTTTTTTAATATTTGTTTTTGGAGTG	192	+199/+391	58	
	U-R	ACCCCAAACAATACACATTACATAA				
PCDH8	M-F	TTTAGAGTTCGTTGGAGGTTC	146	+50/+196	58	37
	M-R	CCTCAAATACGATCCGAAAAAC				
	U-F	GTTTTTAGAGTTTGTTGGAGGTTT	152	+47/+199	58	
	U-R	CAACCTCAAATACAATCCAAAAAAC				
TFAP2B	M-F	TTCGAAGATTTTAAGAGTGGGC	90	+1414/+1504	58	35
	M-R	AAACGCTACCTATAAACGCTCG				
	U-F	GTTTTGAAGATTTTAAGAGTGGGT	94	+1412/+1506	58	
	U-R	CCAAACACTACCTATAAACACTCA				
TAC1	M-F	GGTATTGAGTAGGCGAAAGAGC	139	-17/+122	65	35
	M-R	GCGAACACTTACTACGACGAAC				
	U-F	TAAGGTATTGAGTAGGTGAAAGAGT	143	-20/+123	63	
	U-R	CACAAACACTTACTACAACAAACAAT				

Table S2. Continued.

Assay	Primer type	Primer/probe sequence (5‘→3‘)	Amplicon size, nt	Amplicon location from TSS	Primer annealing t °C	Number of MSP cycles
FLRT2	M-F	TAGTATTTGGAGCGAGTTTTGC	277	+44/+321	63	38
	M-R	CACTTTCTCTTAACTTCGACCG				
	U-F	GTAGTATTTGGAGTGAGTTTTGTGT	279	+43/+322	63	
	U-R	CCACTTTCTCTTAACTTCAACCA				
ADAMTS19	M-F	AAAGGGTTTGGGTAAATTCGTC	157	-9/+148	58	36
	M-R	AAATATAAATCAAACGCATCTCGC				
	U-F	TAAAGGGTTTGGGTAAATTTGTTG	160	+10/+150	58	
	U-R	ACAAATATAAATCAAACACATCTCAC				
BMP7	M-F	GTTTTTTAAGTTTTGCGGTGCG	161	+275/+436	61	35
	M-R	GCCGCTCGATCACTTACTAC				
	U-F	GTTGTTTTTTAAGTTTTGTGGTGT	165	+272/+437	61	
	U-R	CACCACTCAATCACTTACTACA				
SIM1	M-F	GTGAAGTAGAAGACGTTTCGC	130	+320/+450	62	34
	M-R	AAATTAACAAATAACGCGCTCG				
	U-F	TAGGTGAAGTAGAAGATGTTTTGT	135	+317/+452	62	
	U-R	CCAAATTAACAAATAACACACTCAC				
SFRP1	M-F	TCGCGTTTGGTTTTAGTAAATC	156	-149/+7	58	36
	M-R	AATACGCGAAACTCCTACGAC				
	U-F	GAGTTGTGTTTGGTTTTAGTAAATT	161	-152/+9	58	
	U-R	AAAATACACAAAACTCCTACAACC				

M-F/R – methylated forward/ reverse; U-F/R – unmethylated forward/ reverse; nt – nucleotides.

Table S3. Primers used for quantitative methylation-specific PCR analysis (qMSP).

Assay	Primer type	Primer/probe sequence (5'→3')	Amplicon size, nt	Amplicon location from TSS
ZNF677	M-F	GGCGTTTTCGGGTGAGTTTTC	96	+29/+125
	M-R	CAAAACGACCCCAAAACCCG		
	M-P	FAM-GAAACGTAAAAACCTATAACCCGCGAAACG-BHQ-1		
FBN2	M-F	TGACGGTTTTGGAGTCGTTC	102	+331/+433
	M-R	TAACGCAATAAACGACGAAACG		
	M-P	FAM-CGACAACCCCGAACGATACACGTTACA-BHQ-1		
PCDH8	M-F	TAGAGTGAGGGCGGGTTC	91	+25/+116
	M-R	CTCTTTACGAACCCTATACGAA		
	M-P	FAM-CGAACCTCCAACGAACTCTAAAAACGCG-BHQ-1		
TFAP2B	M-F	CGGGATAGTTTTTGAAAGTTCG	118	+1380/ +1498
	M-R	TACCTATAAACGCTCGTCCG		
	M-P	FAM-GAGTCGTTTCGAAGATTTTAAGAGTGGGCG-BHQ-1		
TAC1	M-F	GAGCGATTAGCGTGCGTTC	107	+46/+153
	M-R	AAATAACCCGAACAACCGCGA		
	M-P	FAM-TTGTTCGTCGTAGTAAGTGTTCGCGC-BHQ-1		
FLRT2	M-F	AGTTTTTAGATTTACGTCGGGC	92	+17/+109
	M-R	GAACAACTCGAAACCGAACG		
	M-P	FAM-GCGAGTTTTGCGTTCGTTTTCGCG-BHQ-1		
ACTB	M-F	TGGTGATGGAGGAGGTTTAGTAAGT	133	-1629/-1497
	M-R	AACCAATAAAACCTACTCCTCCCTTAA		
	M-P	FAM-ACCACCACCCAACACACAATAACAAACACA-BHQ-1		

M-F/R/P – methylated forward/reverse/probe; nt – nucleotides.

Table S4. The analyzed sequences of fully methylated DNA (after modification by bisulfite) and MSP as well as QMSP primers and probes arrangement on there. Light gray depicts MSP primers, dark gray – QMSP primers, and turquoise – QMSP probes.

Assay	Analyzed sequence	Amplicon location from TSS
ZNF677	GGCGTTTTCGGGTGAGTTTTCGTTTTTCGGGTTTAAGTTTGCGTTTCGCGGGTTATAG GTTTTTACGTTTCGTTGTCGGGTTTTGGGGTCGTTTTGTAGGTTAAAATTTCGAATTTG TTTATTTTTTTCGCGGCGTGGTTTTAAGACGTTTTTAGTTTCGTCGTTTCGAGAGGGTT TAGAGATTTGCGTTTATTTCGGATT	+74/+230 +29/+125
FBN2	TTTAATATTCGTTTTCGGAGCGTACGGGAATTCGTCGAGTTTTGCGTGTAGGTTTTTT TTTTTTTTGAGGTTTATATTTTTTGAAATTTTACGTTAGGGTTTTTGTAATTTTTTTTTT CGTTCGTTGACGGTTTTGGAGTCGTTCGGGGTTTTAGGTCGGTTATGTAACGTGTATC GTTCGGGGTTGTCGGTTGTATTTTCGTCGCGTTTCGTCGTTTATTGCGTTA	+206/+388 +331/+433
PCDH8	TAGAGTGAGGGCGGGTTCGCGCGTTTTTAGAGTTCGTTGGAGGTTCGGAGTTGTTAT TCGTAGATTTTTTTCGTATAGGGTTCGTAAAGAGCGTGATTTCGAGAGTTTGAGATTG ACGTTCGATTTGGAAATTAGAGAAGATTTTTTTAGTTTTTCGGATCGTATTTGAGG	+50/+196 +25/+116
TFAP2B	CGGGATAGTTTTTGAAAGTTCGGCGTAGAGTCGTTTCGAAGATTTTAAGAGTGGGCG ATTTATAGGCGCGGTCGGTAAGTTTTTGGGGGATTCGGGTTCGGACGAGCGTTTATA GGTAGCGTTT	+1414/+1504 +1380/+1498
TAC1	GGTATTGAGTAGGCGAAAGAGCGCGTTCGGATTTTTTTTTCGGCGGTAGTTATCGAG AGTGCGGAGCGATTAGCGTGCGTTCGGAGGAATTAGAGAAATTTAGTATTTCGCGGG ATTGTTCGTCGTAGTAAGTGTTCGCGCGGTGTTGGTCGCGGTTGTTCGGGTTATTT	-17/+122 +46/+153
FLRT2	AGTTTTTAGATTTACGTCGGGCGGGCGTAGTATTTGGAGCGAGTTTTGCGTTCGTTTT CGCGTAGCGTCGTACGTTCGGTTTCGAGTTGTTCGTATATACGCGTCGGAGGAGAGT TCGTTTAGTTTTTTCGTCGAGTTTCGGGATTTTTTAAATTCGAGGAGTTTCGGCGTCG CGGGGTAGTTTTTTGTCGTTTTTTTCGTTCGTTGTATTTTTTTTGGGGTTCGTTGGTTT GGCGAAGCGGAGAGGGGGAGGCGGAGGAGGAGAGAAGGCGGGGGTCGCGGCGGTC GAAGTTAAGAGAAAGTG	+44/+321 +17/+109

TSS – transcription start site; MSP – methylation-specific PCR; QMSP – quantitative MSP.

Table S5. The list of 175 hypermethylated genes in ccRCC tissue samples, while compared to adjacent non-cancerous tissue and their methylation levels in group comparisons. FC and P values are given for the most hypermethylated probe per gene.

No.	Gene symbol	Hypermethylated probes								
		ccRCC *vs.* NRT			pT1 *vs.* NRT			pT3-4 *vs.* NRT		
		N	FC	P-value*	N	FC	P-value	N	FC	P-value
1	*MIR124-2*	12	1.8	0.016	11	1.8	0.010	12	2.0	<0.001
2	***FBN2***	**8**	**1.8**	**0.018**	**8**	**2.0**	**0.017**	**8**	**1.8**	**0.006**
3	*HCN1*	2	1.8	0.015	3	1.9	0.006	2	1.7	0.001
4	*NETO1*	13	1.8	0.017	14	2.0	0.009	10	1.8	0.004
5	*11-Mar*	2	1.8	0.016	2	1.9	0.002	2	1.7	0.003
6	*GALNTL6*	4	1.8	0.018	2	1.6	0.007	4	1.8	0.005
7	*SNAP91*	4	1.8	0.020	2	1.7	0.014	4	1.8	0.010
8	*IRX2*	5	1.7	0.016	6	1.7	0.018	6	1.7	0.009
9	*CHODL*	4	1.7	0.018	4	1.8	0.006	4	1.7	0.008
10	*ELAVL2*	7	1.7	0.016	9	2.1	0.005	2	1.6	0.002
11	*ADAMTS20*	4	1.7	0.017	4	1.6	0.010	5	1.8	0.003
12	*NXPH1*	15	1.7	0.018	19	1.9	0.006	5	1.6	0.010
13	*HTR2C*	3	1.7	0.024	4	1.8	0.021	2	1.6	0.019
14	*PENK*	4	1.7	0.018	5	1.7	0.004	4	1.7	0.002
15	*KCNA4*	4	1.7	0.017	4	1.7	0.004	4	1.6	0.007
16	*SYT10*	3	1.7	0.020	3	1.7	0.005	4	1.8	0.010
17	*CA10*	4	1.7	0.019	3	1.6	0.005	5	1.9	0.003
18	*A2BP1*	3	1.7	0.016	2	1.6	<0.001	3	1.8	0.003
19	***PCDH8***	**4**	**1.7**	**0.021**	**7**	**2.0**	**0.003**	**3**	**1.6**	**0.022**
20	***SIM1***	**3**	**1.7**	**0.018**	**3**	**1.7**	**0.002**	**5**	**1.7**	**0.009**
21	*CDH8*	4	1.7	0.016	4	1.8	0.001	4	1.7	0.002
22	*KCNC2*	5	1.7	0.024	2	1.6	0.011	5	1.8	0.009
23	***FLRT2***	**2**	**1.7**	**0.018**	**2**	**1.7**	**0.003**	**2**	**1.7**	**0.009**
24	*STMN2*	2	1.7	0.016	1	1.7	0.004	4	1.7	<0.001
25	*PHACTR1*	4	1.7	0.019	4	1.7	0.002	4	1.7	0.017

Table S5. Continued.

No.	Gene symbol	Hypermethylated probes								
		ccRCC *vs.* NRT			pT1 *vs.* NRT			pT3-4 *vs.* NRT		
		N	FC	P-value*	N	FC	P-value	N	FC	P-value
26	*ANKS1B*	1	1.7	0.016	3	1.6	0.009	1	1.7	0.002
27	*ISL1*	4	1.6	0.024	2	1.6	0.030	6	1.7	0.011
28	*ONECUT2*	2	1.6	0.021	3	1.9	0.005	-	-	-
29	*MIR137*	3	1.6	0.034	1	1.5	0.044	3	1.6	0.019
30	*FOXG1*	4	1.6	0.018	7	1.8	0.008	1	1.5	0.009
31	*SYT14*	1	1.6	0.020	2	1.7	0.005	-	-	-
32	*ACTA1*	4	1.6	0.019	3	1.7	0.008	2	1.6	0.012
33	*KCTD1*	2	1.6	0.024	5	1.7	0.016	-	-	-
34	*TFAP2C*	4	1.6	0.016	5	1.7	0.014	2	1.6	0.003
35	*NPTX2*	3	1.6	0.018	7	1.8	0.005	1	1.6	0.010
36	*ZIC1*	4	1.6	0.022	7	2.0	0.022	-	-	-
37	*SRRM4*	4	1.6	0.016	3	1.7	<0.001	3	1.6	0.001
38	*ZIC3*	2	1.6	0.025	3	1.7	0.009	-	-	-
39	*HS3ST3A1*	3	1.6	0.016	4	1.6	0.001	3	1.6	0.002
40	*GALNT13*	2	1.6	0.019	1	1.7	0.012	1	1.7	0.007
41	*POU4F2*	5	1.6	0.018	8	1.7	0.037	2	1.6	0.006
42	*KCNA1*	3	1.6	0.021	2	1.5	0.043	5	1.6	0.008
43	*TBX18*	2	1.6	0.019	2	1.6	0.017	4	1.6	0.010
44	*NKX2-1*	1	1.6	0.016	1	1.6	0.002	1	1.6	0.004
45	*SOX17*	2	1.6	0.017	3	1.6	0.025	5	1.6	0.007
46	*PCDH7*	5	1.6	0.017	8	1.8	0.012	3	1.6	0.006
47	*CBLN1*	2	1.6	0.021	2	1.6	0.045	2	1.5	0.008
48	*DPP6*	6	1.6	0.018	4	1.7	0.015	8	1.7	0.003
49	*USP44*	4	1.6	0.019	2	1.6	0.029	6	1.7	0.006
50	*TBX20*	8	1.6	0.016	8	1.8	0.008	9	1.7	0.001
51	*FERD3L*	7	1.6	0.018	1	1.6	0.009	7	1.6	0.002

Table S5. Continued.

No.	Gene symbol	Hypermethylated probes								
		ccRCC *vs.* NRT			pT1 *vs.* NRT			pT3-4 *vs.* NRT		
		N	FC	P-value*	N	FC	P-value	N	FC	P-value
52	*KLF14*	4	1.6	0.022	9	1.9	0.014	2	1.5	0.029
53	*TRPC6*	4	1.6	0.023	4	1.6	0.019	7	1.6	0.016
54	*DPP10*	3	1.6	0.016	2	1.7	0.003	4	1.6	0.003
55	*HTR1A*	6	1.6	0.018	7	1.8	0.013	6	1.6	0.010
56	*SOX11*	2	1.6	0.018	5	1.7	0.012	2	1.6	0.002
57	*MIR935*	1	1.6	0.016	2	1.8	0.003	2	1.6	<0.001
58	*TRIM64*	1	1.6	0.023	2	1.7	0.018	-	-	-
59	*NCAM2*	2	1.6	0.018	2	1.5	0.015	2	1.6	0.004
60	***ZNF677***	**1**	**1.6**	**0.016**	**1**	**1.6**	**0.006**	**2**	**1.6**	**0.002**
61	*ST8SIA3*	3	1.6	0.016	6	1.7	0.007	1	1.5	0.004
62	***TFAP2B***	**1**	**1.6**	**0.022**	**1**	**1.6**	**0.042**	**1**	**1.5**	**0.015**
63	*GREM1*	1	1.6	0.023	1	1.6	0.019	1	1.6	0.016
64	*IRX1*	3	1.6	0.018	7	1.6	0.037	2	1.5	0.006
65	*BRUNOL4*	3	1.6	0.020	4	1.6	0.009	3	1.6	0.011
66	*SIX6*	2	1.6	0.019	3	1.7	0.012	2	1.5	0.010
67	*CLVS2*	2	1.6	0.041	-	-	-	3	1.8	0.011
68	*ADCY2*	1	1.6	0.021	1	1.6	0.015	1	1.5	0.015
69	*FEZF1*	1	1.6	0.019	1	1.7	0.024	-	-	-
70	*ZIC4*	2	1.6	0.017	5	1.6	0.041	2	1.6	0.002
71	*CPEB1*	1	1.6	0.025	6	1.9	0.004	-	-	-
72	***ADAMTS19***	**4**	**1.6**	**0.022**	**3**	**1.6**	**0.003**	**3**	**1.6**	**0.012**
73	*TMEM132C*	2	1.6	0.019	3	1.6	0.029	3	1.6	0.007
74	*TLX3*	3	1.6	0.020	10	1.7	0.010	1	1.6	0.008
75	*GPR149*	2	1.6	0.019	-	-	-	2	1.7	0.007
76	*NEUROD6*	1	1.6	0.019	2	1.6	0.019	1	1.5	0.009
77	*LHX8*	2	1.6	0.021	2	1.6	0.015	2	1.6	0.012

Table S5. Continued.

No.	Gene symbol	Hypermethylated probes								
		ccRCC *vs.* NRT			pT1 *vs.* NRT			pT3-4 *vs.* NRT		
		N	FC	P-value*	N	FC	P-value	N	FC	P-value
78	*FZD10*	2	1.6	0.018	4	1.6	0.019	3	1.6	0.006
79	*DCHS2*	2	1.6	0.020	2	1.6	0.007	2	1.6	0.012
80	*VWC2*	1	1.6	0.024	2	1.7	0.007	1	1.6	0.018
81	*LOC200726*	1	1.6	0.016	-	-	-	2	1.6	<0.001
82	*TCERG1L*	1	1.6	0.017	1	1.7	0.005	-	-	-
83	*SLITRK3*	1	1.6	0.028	1	1.7	0.016	1	1.5	0.032
84	*FAM123A*	1	1.6	0.020	3	1.8	0.012	-	-	-
85	*VSTM2A*	2	1.6	0.018	1	1.5	0.007	2	1.7	0.003
86	*FOXB1*	1	1.6	0.017	5	1.7	0.013	-	-	-
87	*DBX1*	2	1.6	0.016	4	1.7	0.011	4	1.6	0.003
88	*GSX1*	3	1.6	0.016	7	1.8	0.019	2	1.5	0.002
89	*OTP*	2	1.6	0.016	3	1.6	0.014	2	1.5	0.003
90	*CYP4X1*	2	1.6	0.019	-	-	-	2	1.7	0.001
91	*RIMS2*	1	1.6	0.024	1	1.6	0.002	1	1.5	0.022
92	*RGS22*	1	1.6	0.018	1	1.6	0.014	1	1.6	0.006
93	*ABCC9*	1	1.6	0.022	1	1.6	0.009	1	1.5	0.019
94	*TCHH*	3	1.6	0.018	2	1.6	0.011	4	1.6	0.008
95	*MDGA2*	1	1.6	0.036	1	1.5	0.037	1	1.6	0.023
96	*PCDH19*	1	1.6	0.036	-	-	-	1	1.7	0.017
97	*FOXA1*	1	1.6	0.016	3	1.7	0.005	1	1.6	0.004
98	*CYYR1*	1	1.6	0.017	-	-	-	1	1.6	0.003
99	*MCHR2*	1	1.6	0.019	-	-	-	1	1.6	0.001
100	*D4S234E*	1	1.5	0.016	1	1.5	0.031	-	-	-
101	*PCDH17*	4	1.5	0.017	10	1.7	0.018	1	1.5	0.009
102	*ADRA2A*	3	1.5	0.024	4	1.7	0.030	-	-	-
103	*AVPR1A*	1	1.5	0.018	-	-	-	1	1.5	0.006

Table S5. Continued.

No.	Gene symbol	Hypermethylated probes								
		ccRCC *vs.* NRT			pT1 *vs.* NRT			pT3-4 *vs.* NRT		
		N	FC	P-value*	N	FC	P-value	N	FC	P-value
104	*GRIN3A*	1	1.5	0.020	2	1.7	0.008	1	1.5	0.006
105	*TRIM64B*	1	1.5	0.021	3	1.7	0.014	-	-	-
106	*BEND4*	1	1.5	0.017	2	1.6	0.029	-	-	-
107	*GFI1*	2	1.5	0.017	1	1.5	0.035	2	1.5	0.003
108	*PRRX1*	1	1.5	0.026	-	-	-	3	1.6	0.009
109	*FOXD3*	1	1.5	0.016	7	1.6	0.016	-	-	-
110	*GAS7*	1	1.5	0.018	1	1.6	0.017	2	1.6	0.006
111	*ANKRD30B*	1	1.5	0.020	2	1.6	0.027	-	-	-
112	*PROX1*	1	1.5	0.017	3	1.6	0.004	-	-	-
113	*RIMS4*	1	1.5	0.028	1	1.7	0.015	-	-	-
114	*ZNF98*	1	1.5	0.018	1	1.6	0.016	2	1.5	0.008
115	*SOX1*	2	1.5	0.019	2	1.7	0.013	2	1.5	0.009
116	*TWIST1*	5	1.5	0.020	3	1.6	0.015	8	1.6	0.010
117	*CALN1*	4	1.5	0.024	2	1.5	0.003	5	1.6	0.014
118	*ULBP1*	2	1.5	0.020	-	-	-	4	1.6	0.011
119	*C20orf56*	2	1.5	0.017	3	1.7	0.023	1	1.6	0.002
120	*TIAM1*	1	1.5	0.018	-	-	-	1	1.5	0.004
121	*RASAL3*	1	1.5	0.017	1	1.6	0.001	1	1.5	0.008
122	*OTX2*	1	1.5	0.028	2	1.8	0.016	-	-	-
123	*OPRK1*	1	1.5	0.023	-	-	-	2	1.5	0.016
124	*MIR1247*	1	1.5	0.028	1	1.6	0.010	-	-	-
125	*ALX1*	1	1.5	0.019	1	1.5	0.018	3	1.5	0.007
126	*FOXI2*	1	1.5	0.016	2	1.8	<0.001	1	1.5	0.002
127	*FLJ42875*	1	1.5	0.016	-	-	-	4	1.6	<0.001
128	*HTR1B*	1	1.5	0.022	-	-	-	1	1.6	0.008
129	*GRIA2*	2	1.5	0.018	2	1.6	0.020	1	1.5	0.030

Table S5. Continued.

No.	Gene symbol	Hypermethylated probes								
		ccRCC *vs.* NRT			pT1 *vs.* NRT			pT3-4 *vs.* NRT		
		N	FC	P-value*	N	FC	P-value	N	FC	P-value
130	*LOC389333*	1	1.5	0.023	-	-	-	1	1.6	0.008
131	*NPY*	2	1.5	0.016	3	1.6	0.006	-	-	-
132	*GRHL2*	1	1.5	0.020	1	1.5	0.013	1	1.5	0.010
133	*IKZF1*	1	1.5	0.024	2	1.6	0.018	-	-	-
134	***TAC1***	**1**	**1.5**	**0.037**	**-**	**-**	**-**	**5**	**1.7**	**0.009**
135	*PRDM13*	1	1.5	0.016	1	1.6	0.005	1	1.6	0.001
136	*POU4F3*	1	1.5	0.021	3	1.7	0.007	4	1.6	0.014
137	*CACNA1B*	1	1.5	0.023	3	1.7	0.016	-	-	-
138	*TMEM215*	1	1.5	0.021	-	-	-	2	1.6	0.004
139	*WBSCR17*	1	1.5	0.021	1	1.6	0.018	2	1.5	0.008
140	*EBF1*	1	1.5	0.017	2	1.6	0.007	-	-	-
141	*ELAVL4*	1	1.5	0.016	1	1.7	0.003	-	-	-
142	*ZNF732*	1	1.5	0.030	-	-	-	1	1.7	0.004
143	*RGS20*	2	1.5	0.019	3	1.6	0.014	2	1.5	0.013
144	*TMEM108*	2	1.5	0.019	-	-	-	3	1.6	0.005
145	*CNGA3*	1	1.5	0.017	2	1.5	0.005	1	1.5	0.005
146	*NPY2R*	1	1.5	0.019	-	-	-	2	1.5	0.006
147	*NHLH2*	1	1.5	0.017	3	1.7	0.002	-	-	-
148	*CHRM2*	1	1.5	0.017	1	1.5	0.012	3	1.6	0.003
149	*GABRA2*	1	1.5	0.022	1	1.7	0.009	-	-	-
150	*PIWIL1*	1	1.5	0.017	1	1.5	0.003	1	1.6	0.005
151	*FOXE1*	1	1.5	0.027	2	1.7	0.006	-	-	-
152	***BMP7***	**2**	**1.5**	**0.020**	**2**	**1.5**	**0.005**	**1**	**1.6**	**0.008**
153	*CACNB2*	1	1.5	0.021	-	-	-	1	1.6	0.008
154	*CLIC6*	1	1.5	0.020	1	1.6	0.006	2	1.5	0.012
155	*DLX6AS*	1	1.5	0.017	-	-	-	2	1.6	0.012

Table S5. Continued.

No.	Gene symbol	Hypermethylated probes								
		ccRCC *vs.* NRT			pT1 *vs.* NRT			pT3-4 *vs.* NRT		
		N	FC	P-value*	N	FC	P-value	N	FC	P-value
156	*SP8*	1	1.5	0.025	1	1.6	0.012	1	1.6	0.009
157	*IRX4*	1	1.5	0.019	2	1.6	0.005	2	1.5	0.001
158	*psiTPTE22*	1	1.5	0.017	1	1.6	0.048	-	-	-
159	*DMRT2*	1	1.5	0.019	2	1.7	0.003	-	-	-
160	*HAND2*	1	1.5	0.021	1	1.8	0.003	-	-	-
161	*BARHL2*	2	1.5	0.022	5	1.8	0.033	-	-	-
162	*KCNH7*	1	1.5	0.019	-	-	-	1	1.5	0.007
163	*PCSK1*	1	1.5	0.017	-	-	-	1	1.6	0.002
164	*CSMD3*	1	1.5	0.016	1	1.6	0.002	-	-	-
165	*FAM155A*	1	1.5	0.019	2	1.7	0.003	-	-	-
166	*DSC3*	1	1.5	0.018	1	1.6	0.018	-	-	-
167	*SLC6A5*	1	1.5	0.017	2	1.6	0.022	2	1.6	<0.001
168	*VGLL2*	1	1.5	0.016	1	1.6	0.004	1	1.5	0.002
169	*PAX1*	2	1.5	0.016	1	1.6	0.012	2	1.6	0.003
170	*PLD5*	1	1.5	0.017	-	-	-	4	1.6	0.018
171	*OLIG3*	1	1.5	0.017	7	1.6	0.009	-	-	-
172	*PCDH11X*	1	1.5	0.016	1	1.7	0.013	-	-	-
173	*INSM1*	1	1.5	0.016	1	1.5	0.021	-	-	-
174	*ACAN*	1	1.5	0.016	-	-	-	1	1.6	0.002
175	*CRMP1*	1	1.5	0.024	-	-	-	4	1.6	0.013

ccRCC – clear cell renal cell carcinoma; NRT – non-cancerous renal tissues; pT – pathological stage; N – number of probes; FC – fold change. * Corrected (with Benjamini-Hochberg multiple testing correction) P-value.

Table S6. The amount of differentially methylated genes in various comparison groups.

Condition	Comparison groups	Differentially methylated genes, N (%)			Genes overlapped with entities (N=367) in ccRCC *vs.* NRT comparison group, N		
		Total	↑	↓	Total	↑	↓
TUMORS (N=11)							
Gender	Male (N=6) *vs.* Female (N=5)	273 (100%)	9 (3%)	264 (97%)	1	1	0
Age	> 60 yr. (N=6) *vs.* < 60 yr. (N=5)	278 (100%)	275 (99%)	3 (1%)	0	0	0
Tumor size	> 4 cm (N=4) *vs.* ≤ 4 cm (N=7)	124 (100%)	122 (98%)	2 (2%)	15	15	0
Fuhrman grade	G ≥ 3 (N=7) *vs.* G < 3 (N=4)	31 (100%)	29 (93%)	2 (7%)	3	3	0
WHO/ISUP grade	G = 3 (N=5) *vs.* G < 3 (N=6)	76 (100%)	74 (97%)	2 (3%)	10	10	0
Iv. invasion	Yes (N=5) *vs.* No (N=6)	15 (100%)	8 (53%)	7 (47%)	1	0	1
Fat invasion	Yes (N=4) *vs.* No (N=7)	11 (100%)	4 (36%)	7 (64%)	0	0	0
Tumor necrosis	Yes (N=3) *vs.* No (N=8)	39 (100%)	18 (46%)	21 (54%)	0	0	0
NON-TUMORS (N=11)							
Gender	Male (N=6) *vs.* Female (N=5)	1 (100%)	1 (100%)	0	0	0	0
Age	> 60 yr. (N=6) *vs.* < 60 yr. (N=5)	22 (100%)	19 (86%)	3 (14%)	0	0	0

WHO/ISUP – World Health Organisation/Internation Society of Urological Pathology; G – grade; yr. – years.
↑ – hypermethylated; ↓ – hypomethylated.

Table S7. The list of simultaneously down-regulated and hypermethylated genes in 4 ccRCC tissue samples while compared with paired NRT cases.

Gene	Down-regulated expression		Gene	Down-regulated expression		Gene	Down-regulated expression	
	FC	p-level		FC	p-level		FC	p-level
ESRP1	11.7	0.003	*KCNA4*	10.3	<0.001	*BMP4*	3.0	0.015
CHRM2	2.5	0.018	*KREMEN1*	2.0	0.043	*RASL11B*	52.4	<0.001
AVPR1A	2.6	0.008	*IRX2*	25.9	0.023	*TFAP2A*	6.8	0.033
ABCC8	3.6	0.025	*CRHBP*	42.1	0.012	*NPY5R*	4.1	0.006
FMN2	8.7	0.029	*CYP4X1*	3.1	0.015	*PDZRN3*	7.7	0.005
IRX1	688.1	<0.001	*TBC1D1*	3.1	0.002	*SORCS1*	2.1	0.035
SIM1	**18.5**	**0.015**	***BMP7***	**7.3**	**0.013**	*MDGA2*	2.6	0.011
TAC1	**7.7**	**0.003**	*UNC5D*	22.8	0.001	*RNF150*	10.2	0.007
KIAA1217	2.2	0.014	*GDNF*	10.0	0.006	*TCF21*	18.3	0.020
CA10	44.2	0.024	*TFCP2L1*	24.5	0.007	*ADAMTS16*	16.8	0.003
ADAMTS19	**2.1**	**0.030**	*SLIT2*	2.4	0.043	*VWA5B1*	16.9	<0.001
SHISA2	6.3	0.039	*OVOL2*	22.3	0.038	*ZNF577*	4.3	0.015
FAM83B	71.0	<0.001	***TFAP2B***	**349.5**	**<0.001**	*SH3YL1*	3.2	0.021
ZNF677	**10.0**	**0.015**	*ITGA8*	2.5	0.040	*CACNB2*	7.9	0.038
CDH3	6.2	0.023	*CDO1*	3.4	0.003	*SIM2*	13.4	0.007
RASSF10	12.4	0.011	*HECW1*	6.3	0.037	*PODXL*	8.6	0.010
MRAP2	19.1	0.007	*SLC26A4*	11.6	0.006	*NTRK3*	13.0	0.048
DACH1	19.1	0.014	*GSTM3*	25.7	<0.001	*FKBP1B*	3.9	0.025

FC – fold change.

Table S8. The list of top 50 most significant Gene Ontology (GO) Biological processes terms for all of the significantly deregulated genes in ccRCC tissues.

Gene set name	Genes, N	FDR q-value	Gene set name	Genes, N	FDR q-value
Down-regulated genes					
Regulation of immune system process	352	2.04e-146	Regulation of cell cell adhesion	119	1.19e-57
Defense response	359	8.54e-136	Mononuclear cell differentiation	115	4.82e-57
Immune effector process	292	2.18e-122	Regulation of defense response	147	2.29e-56
Positive regulation of immune system process	251	2.24e-110	Negative regulation of immune system process	111	2.99e-54
Regulation of immune response	243	3.9e-109	Positive regulation of cytokine production	114	4.55e-53
Lymphocyte activation	200	5.5e-97	Cell cell adhesion	160	7.16e-52
Response to cytokine	247	1.61e-94	Apoptotic process	247	4.74e-51
Innate immune response	226	5.14e-94	Activation of immune response	125	6.16e-50
Cytokine mediated signaling pathway	197	6.82e-88	Leukocyte proliferation	94	1.47e-49
T cell activation	153	3.44e-86	Cell population proliferation	246	1.54e-49
Regulation of cell activation	169	6.87e-82	Positive regulation of leukocyte cell cell adhesion	82	6.79e-49
Biological adhesion	246	7.05e-73	Immune response regulating signaling pathway	117	2.97e-48
Positive regulation of immune response	173	3.19e-72	Myeloid leukocyte mediated immunity	121	6.74e-48
Leukocyte mediated immunity	184	2.27e-70	Positive regulation of cell cell adhesion	87	1.21e-47
Immune system development	194	7.08e-69	Positive regulation of cell adhesion	106	2.51e-47
Regulation of lymphocyte activation	139	1.33e-68	Regulation of leukocyte differentiation	87	3.17e-47
Cytokine production	176	2.95e-68	Regulation of immune effector process	110	7.92e-47
Inflammatory response	168	3.97e-66	Regulation of leukocyte proliferation	81	9.66e-47
Leukocyte differentiation	139	8.28e-66	Locomotion	239	3.89e-45
Cell activation involved in immune response	161	5.63e-65	Cell migration	207	4.93e-43
Myeloid leukocyte activation	151	1.64e-62	Positive regulation of gene expression	163	3.15e-42
Regulation of cell adhesion	159	1.7e-62	Positive regulation of intracellular signal transduction	156	1.26e-41
Leukocyte cell cell adhesion	114	5.43e-62	Leukocyte migration	108	2.74e-41
Adaptive immune response	152	2.76e-60	Regulation of cell death	204	3.65e-39
Regulation of intracellular signal transduction	249	9.83e-59	T cell differentiation	74	6.44e-39

Table S8. Continued.

Gene set name	Genes, N	FDR q-value	Gene set name	Genes, N	FDR q-value
Up-regulated genes					
Regulation of immune system process	352	2.04e-146	Myeloid leukocyte activation	151	1.64e-62
Cell activation	337	5.63e-146	Regulation of cell adhesion	159	1.7e-62
Defense response	359	8.54e-136	Regulation of response to stress	224	2.76e-62
Immune effector process	292	2.18e-122	Leukocyte cell cell adhesion	114	5.43e-62
Positive regulation of immune system process	251	2.24e-110	Positive regulation of multicellular organismal process	220	1.18e-60
Regulation of immune response	243	3.9e-109	Adaptive immune response	152	2.76e-60
Response to biotic stimulus	306	3.9e-108	Regulation of intracellular signal transduction	249	9.83e-59
Defense response to other organism	257	6.38e-101	Regulation of cell cell adhesion	119	1.19e-57
Lymphocyte activation	200	5.5e-97	Mononuclear cell differentiation	115	4.82e-57
Response to cytokine	247	1.61e-94	Regulation of defense response	147	2.29e-56
Innate immune response	226	5.14e-94	Negative regulation of immune system process	111	2.99e-54
Cytokine mediated signaling pathway	197	6.82e-88	Positive regulation of cytokine production	114	4.55e-53
T-cell activation	153	3.44e-86	Positive regulation of signaling	234	1.1e-52
Regulation of cell activation	169	6.87e-82	Positive regulation of cell activation	109	3.6e-52
Biological adhesion	246	7.05e-73	Cell cell adhesion	160	7.16e-52
Positive regulation of immune response	173	3.19e-72	Apoptotic process	247	4.74e-51
Leukocyte mediated immunity	184	2.27e-70	Activation of immune response	125	6.16e-50
Immune system development	194	7.08e-69	Leukocyte proliferation	94	1.47e-49
Regulation of lymphocyte activation	139	1.33e-68	Cell population proliferation	246	1.54e-49
Cytokine production	176	2.95e-68	Secretion	207	3.62e-49
Inflammatory response	168	3.97e-66	Positive regulation of leukocyte cell cell adhesion	82	6.79e-49
Leukocyte differentiation	139	8.28e-66	Immune response regulating signaling pathway	117	2.97e-48
Cell activation involved in immune response	161	5.63e-65	Positive regulation of molecular function	227	6.42e-48
Regulation of T-cell activation	111	1.06e-64	Myeloid leukocyte mediated immunity	121	6.74e-48
Regulation of response to external stimulus	191	2.72e-63	Positive regulation of cell cell adhesion	87	1.21e-47

Table S9. Univariate and multivariate Cox proportional hazard analysis of overall survival according to molecular and/or clinicopathologic variables in ccRCC tissues samples.

Variables		UNIVARIATE ANALYSIS		MULTIVARIATE ANALYSIS (backward) Separetely		MULTIVARIATE ANALYSIS (backward) Altogether	
		P-value	HR [95% CI]	P-value	HR [95% CI]	P-value	HR [95% CI]
One gene	*ZNF677 (M vs. U)*	**0.029**	2.61 [1.10 - 6.17]		-		
	FBN2 (M vs. U)	**0.026**	2.96 [1.14 - 7.66]	**0.026**	2.96 [1.15 - 7.62]		-
Two genes	*ZNF677 & FBN2 (M vs. U)*	**0.047**	2.78 [1.02 - 7.58]		-		
	ZNF677 & SFRP1 (M vs. U)	**0.048**	2.76 [1.01 - 7.51]		-		
	ZNF677 & BMP7 (M vs. U)	**0.008**	3.28 [1.38 - 7.78]	**0.008**	3.27 [1.38 - 7.78]		-
	ZNF677 & SIM1 (M vs. U)	**0.026**	2.69 [1.13 - 6.37]		-		
	PCDH8 & FLRT2 (M vs. U)	**0.044**	2.82 [1.04 - 7.68]		-		
Three genes	*ZNF677, FBN2 & BMP7 (M vs. U)*	**0.047**	2.78 [1.02 - 7.58]		-		
	ZNF677, PCDH8 & FLRT2 (M vs. U)	**0.038**	3.18 [1.07 - 9.45]	**0.038**	3.18 [1.07 - 9.45]		-
	ZNF677, BMP7 & SIM1 (M vs. U)	0.050	2.39 [1.01 - 5.67]		-		
	PCDH8, SFRP1 & BMP7 (M vs. U)	**0.042**	3.11 [1.05 - 9.18]		-		
	FBN2, SFRP1 & ADAMTS19 (M vs. U)	**0.050**	4.29 [1.00 - 18.3]		-		
	PCDH8, FLRT2 & BMP7 (M vs. U)	0.051	2.73 [1.00 - 7.44]		-		
Four genes	*ZNF677, PCDH8, FLRT2 & BMP7 (M vs. U)*	**0.044**	3.08 [1.04 - 9.15]	**0.044**	3.08 [1.04 - 9.15]		-
	ZNF677, PCDH8 & FLRT2, SIM1 (M vs. U)	**0.046**	3.03 [1.02 - 9.00]		-		
Demographic and clinical-pathological	Age, years (cont.)	**<0.001**	1.09 [1.04 - 1.14]	**<0.001**	1.10 [1.04 - 1.16]	**<0.001**	1.10 [1.04 - 1.16]
	Gender (male vs. female)	**0.038**	2.73 [1.06 - 7.08]		-		
	Tumor size (cont.)	**0.036**	1.01 [1.00 - 1.02]	**0.004**	1.02 [1.01 - 1.03]	**0.004**	1.02 [1.01 - 1.03]
	Stage (pT3-4 *vs.* pT1-2)	**0.003**	5.12 [1.72 -15.24]		-		
	Fuhrman grade (G≥3 *vs.* G≤2)	0.433	1.42 [0.59 - 3.44]		-		
	WHO/ISUP grade (G=3 *vs.* G≤2)	**0.012**	3.04 [1.28 - 7.24]		-		
	Fat invasion (yes *vs.* no)	**0.001**	4.83 [1.87 -12.48]		-		
	Necrosis (yes *vs.* no)	**<0.001**	4.97 [2.10 -11.76]	**<0.001**	4.97 [2.10 - 11.8]	**0.010**	3.22 [1.32 - 7.84]

Table S10. The diagnostic test performance characteristics of the analyzed methylation biomarkers in urine samples (Receiver Operating Characteristic (ROC) analysis).

Biomarker	AUC	P-value	DSp, %	DSe, %	PPV, %	NPV, %	ACC, %
Single biomarker							
ZNF677	0.697	**<0.001**	95.7	43.9	95.9	42.2	59.4
FBN2	0.644	**<0.001**	92.4	36.6	91.8	38.4	53.3
PCDH8	0.709	**<0.001**	72.8	67.5	84.9	48.7	69.1
TFAP2B	0.597	**0.015**	53.3	67.5	77.1	41.2	63.2
TAC1	0.642	**0.001**	62.0	71.5	81.4	48.3	68.7
FLRT2	0.672	**<0.001**	89.2	46.3	90.9	41.6	59.2
Panel of two biomarkers							
ZNF677& FBN2	0.736	**<0.001**	88.0	58.5	92.0	47.6	67.4
ZNF677 & PCDH8	**0.778**	**<0.001**	**68.5**	**78.1**	**85.2**	**57.2**	**75.2**
ZNF677 & TFAP2B	0.720	**<0.001**	96.7	42.3	96.8	41.8	58.6
ZNF677 & TAC1	0.732	**<0.001**	62.0	77.2	82.6	53.8	72.7
ZNF677 & FLRT2	0.736	**<0.001**	85.9	60.2	90.9	48.0	67.9
FBN2 & PCDH8	0.728	**<0.001**	71.7	70.7	85.4	51.2	71.0
FBN2 & TFAP2B	0.659	**<0.001**	94.6	30.1	92.8	36.7	49.4
FBN2 & TAC1	0.696	**<0.001**	64.1	72.4	82.5	49.9	69.9
FBN2 & FLRT2	0.714	**<0.001**	84.8	58.5	90.0	46.7	66.4
PCDH8 & TFAP2B	0.690	**<0.001**	63.0	72.4	82.0	49.4	69.6
PCDH8 & TAC1	0.685	**<0.001**	56.5	80.5	81.2	55.4	73.3
PCDH8 & FLRT2	0.750	**<0.001**	78.3	68.3	88.0	51.4	71.3
TFAP2B & TAC1	0.604	**0.008**	40.2	79.7	75.5	44.9	67.8
TFAP2B & FLRT2	0.674	**<0.001**	81.5	47.2	85.6	39.8	57.5
TAC & FLRT2	0.713	**<0.001**	59.8	78.9	82.1	54.8	73.1
Panel of three biomarkers							
ZNF677, FBN2 & PCDH8	**0.778**	**<0.001**	**80.4**	**68.3**	**89.1**	**52.1**	**71.9**
ZNF677, FBN2 & TFAP2B	0.726	**<0.001**	88.0	58.5	92.0	47.6	67.4
ZNF677, FBN2 & TAC1	0.754	**<0.001**	81.5	62.6	88.8	48.3	68.3

Table S10. Continued.

Biomarker	AUC	P-value	DSp, %	DSe, %	PPV, %	NPV, %	ACC, %
Panel of three biomarkers							
ZNF677, FBN2 & FLRT2	0.752	**<0.001**	81.5	67.5	89.5	51.8	71.7
ZNF677, PCDH8 & TFAP2B	0.762	**<0.001**	80.4	64.2	88.5	49.1	69.1
ZNF677, PCDH8 & TAC1	0.740	**<0.001**	60.9	79.7	82.6	56.2	74.0
ZNF677, PCDH8 & FLRT2	**0.784**	**<0.001**	**75.0**	**76.4**	**87.7**	**57.7**	**76.0**
ZNF677, TFAP2B & TAC1	0.723	**<0.001**	85.9	49.6	89.1	42.2	60.5
ZNF677, TFAP2B & FLRT2	0.734	**<0.001**	88.0	55.3	91.5	45.8	65.1
ZNF677, TAC1 & FLRT2	0.750	**<0.001**	80.4	61.0	87.9	46.9	66.8
FBN2, PCDH8 & TFAP2B	0.712	**<0.001**	79.4	56.9	86.5	44.1	63.6
FBN2, PCDH8 & TAC1	0.710	**<0.001**	56.5	80.5	81.2	55.4	73.3
FBN2, PCDH8 & FLRT2	0.759	**<0.001**	75.0	74.0	87.4	55.3	74.3
FBN2, TFAP2B & TAC1	0.674	**<0.001**	81.5	48.0	85.8	40.2	58.0
FBN2, TFAP2B & FLRT2	0.711	**<0.001**	82.6	52.9	87.6	42.9	61.8
FBN2, TAC1 & FLRT2	0.738	**<0.001**	58.7	82.1	82.3	58.4	75.1
PCDH8, TFAP2B & TAC1	0.668	**<0.001**	52.2	79.7	79.5	52.4	71.4
PCDH8, TFAP2B & FLRT2	0.733	**<0.001**	77.2	62.6	86.5	46.9	67.0
PCDH8, TAC1 & FLRT2	0.735	**<0.001**	57.6	83.7	82.2	60.3	75.9
TFAP2B, TAC1 & FLRT2	0.675	**<0.001**	77.2	52.0	84.2	40.8	59.6
Panel of four biomarkers							
ZNF677, FBN2, PCDH8 & TFAP2B	0.754	**<0.001**	81.5	69.9	89.8	53.7	73.4
ZNF677, FBN2, PCDH8 & TAC1	0.753	**<0.001**	82.6	61.8	89.2	48.1	68.0
ZNF677, FBN2, PCDH8 & FLRT2	0.715	**<0.001**	81.5	66.7	89.4	51.2	71.1
ZNF677, FBN2, TFAP2B & TAC1	0.757	**<0.001**	81.5	62.6	88.8	48.3	68.3
ZNF677, FBN2, TFAP2B & FLRT2	0.750	**<0.001**	81.5	69.1	89.7	53.1	72.8
ZNF677, FBN2, TAC1 & FLRT2	0.759	**<0.001**	78.3	67.5	87.9	50.8	70.7
ZNF677, PCDH8, TFAP2B & TAC1	0.729	**<0.001**	58.7	79.7	81.8	55.3	73.4

Table S10. Continued.

Biomarker	AUC	P-value	DSp, %	DSe, %	PPV, %	NPV, %	ACC, %
Panel of four biomarkers							
ZNF677, PCDH8, TFAP2B & FLRT2	0.767	**<0.001**	76.1	68.3	87.0	50.7	70.6
ZNF677, PCDH8, TAC1 & FLRT2	0.754	**<0.001**	80.4	61.8	88.1	47.4	67.4
ZNF677, TFAP2B, TAC1 & FLRT2	0.741	**<0.001**	80.4	60.2	87.8	46.4	66.2
FBN2, PCDH8, TFAP2B & TAC1	0.696	**<0.001**	53.3	81.3	80.2	55.0	72.9
FBN2, PCDH8, TFAP2B & FLRT2	0.743	**<0.001**	75.0	65.9	86.0	48.5	68.6
FBN2, PCDH8, TAC1 & FLRT2	0.746	**<0.001**	56.5	84.6	81.9	61.1	76.1
FBN2, TFAP2B, TAC1 & FLRT2	0.717	**<0.001**	76.1	61.8	85.8	46.0	66.1
PCDH8, TFAP2B, TAC1 & FLRT2	0.716	**<0.001**	75.0	62.6	85.4	46.2	66.3
Panel of five biomarkers							
ZNF677, FBN2, PCDH8, TFAP2B & TAC1	0.748	**<0.001**	82.6	61.0	88.5	47.2	67.5
ZNF677, FBN2, PCDH8, TFAP2B & FLRT2	0.715	**<0.001**	81.5	65.0	89.1	50.0	70.0
ZNF677, FBN2, PCDH8,TAC1 & FLRT2	0.727	**<0.001**	79.4	66.7	88.3	50.5	70.5
ZNF677, FBN2, TFAP2B,TAC1 & FLRT2	0.761	**<0.001**	78.3	67.5	87.9	50.8	70.7
ZNF677, PCDH8, TFAP2B, TAC1 & FLRT2	0.743	**<0.001**	80.4	61.0	87.9	46.9	66.8
FBN2, PCDH8, TFAP2B,TAC1 & FLRT2	0.730	**<0.001**	77.2	61.8	86.3	46.4	66.4
Panel of all six biomarkers							
ZNF677, FBN2, PCDH8, TFAP2B, TAC1 & FLRT2	0.726	**<0.001**	79.4	66.7	88.3	50.5	70.5

AUC – area under the curve; PPV – positive predictive value; NPV – negative predictive value; ROC – Receiver Operating Characteristic. DSp – diagnostic specificity; DSe – diagnostic sensitivity; ACC – accuracy; Significant P-values are in bold.

Table S11. Associations of biomarkers methylation in ccRCC patients urine sediments samples with clinical-pathological patients' characteristics.

Continuous methylation data							
Variable		***ZNF677***	***FBN2***	***PCDH8***	***TFAP2B***	***TAC1***	***FLRT2***
Stage (pT3-4 vs. pT1)	**Zad**	0.31	0.62	0.84	-0.25	1.33	-0.10
	P-value	0.758	0.537	0.400	0.805	0.182	0.921
Tumor size, mm	**Rs**	-0.14	0.11	0.04	-0.04	0.18	-0.11
	P-value	0.186	0.318	0.721	0.687	0.089	0.311
WHO/ISUP grade (G≥3 vs. G≤2)	**Zad**	-1.01	1.12	-0.64	0.04	-0.80	-0.75
	P-value	0.311	0.264	0.523	0.964	0.423	0.456
Intravascular invasion (Yes vs. No)	**Zad**	0.25	1.48	1.49	0.07	1.52	-0.41
	P-value	0.801	0.139	0.136	0.947	0.129	0.681
Fat invasion (Yes *vs.* No)	**Zad**	0.44	0.19	0.78	0.40	1.82	-0.31
	P-value	0.659	0.850	0.437	0.689	0.069	0.757
Necrosis (Yes *vs.* No)	**Zad**	-1.06	0.01	-1.23	0.65	0.34	0.42
	P-value	0.289	0.996	0.218	0.519	0.731	0.676
Dichotomous methylation data							
Tumor size, mm	**Zad**	-0.19	1.40	1.18	0.14	1.57	-0.15
	P-value	0.852	0.160	0.239	0.886	0.117	0.877
WHO/ISUP grade	**G≥3**	34.8%	41.3%	69.6%	67.4%	71.8%	45.7%
	G≤2	49.4%	32.5%	66.2%	67.5%	71.4%	46.8%
	P-value	0.135	0.338	0.843	1.00	1.00	1.00
Intravascular invasion	**Yes**	42.5%	45.0%	75.0%	77.5%	75.0%	45.0%
	No	44.6%	31.3%	63.9%	62.7%	69.9%	47.0%
	P-value	0.849	0.162	0.304	0.107	0.671	0.850
Necrosis	**Yes**	41.4%	34.5%	69.0%	75.9%	72.4%	51.7%
	No	44.7%	36.2%	67.0%	64.9%	71.3%	44.7%
	P-value	0.832	1.00	1.00	0.365	1.00	0.530

WHO/ISUP – World Health Organisation/Internation Society of Urological Pathology; Zad – Mann-Whitney's Z adjusted parameter. Significant P-values are in bold.

Table S12. Univariate and multivariate Cox proportional hazard analysis of overall survival according to molecular and/or clinicopathologic variables in ccRCC patients urine sediments samples.

UNIVARIATE ANALYSIS			
Covariates	**HR [95% CI]**	**P-value**	**Model P-value**
Biomarkers			
FBN2 & PCDH8 (M *vs.* U)	4.16 [0.97 - 17.73]	0.055	**0.021**
ZNF677, FBN2 & PCDH8 (M *vs.* U)	3.34 [0.99 - 11.27]	0.053	**0.027**
FBN2, PCDH8 & FLRT2 (M *vs.* U)	4.18 [0.98 - 17.81]	0.055	**0.020**
FBN2, PCDH8, TAC1 & FLRT2 (M *vs.* U)	>1000	0.960	**0.004**
MULTIVARIATE ANALYSIS			
Biomarkers with clinical-pathological variables			
FBN2 & PCDH8 (M *vs.* U)	4.86 [0.98 - 23.96]	0.053	
Age, years (cont.)	1.10 [1.04 - 1.17]	**0.001**	
Gender (male *vs.* female)	3.01 [1.11 - 8.17]	**0.031**	
Stage (pT3-4 *vs.* pT1-2)	1.87 [0.54 - 6.42]	0.323	**< 0.001**
Tumor size (cont.)	1.02 [1.00 - 1.03]	**0.037**	
WHO/ISUP grade (G=3 *vs.* G≤2)	0.66 [0.21 - 2.09]	0.481	
Necrosis (yes *vs.* no)	4.31 [1.33 - 13.93]	**0.015**	
ZNF677, FBN2 & PCDH8 (M vs. U)	2.66 [0.72 - 9.83]	0.143	
Age, years (cont.)	1.11 [1.05 - 1.17]	**<0.001**	
Gender (male *vs.* female)	2.47 [0.92 - 6.67]	0.075	
Stage (pT3-4 *vs.* pT1-2)	2.35 [0.72 - 7.69]	0.160	**< 0.001**
Tumor size (cont.)	1.02 [1.00 - 1.03]	0.037	
WHO/ISUP grade (G=3 *vs.* G≤2)	0.76 [0.25 - 2.27]	0.621	
Necrosis (yes *vs.* no)	3.58 [1.25 - 10.28]	**0.018**	
FBN2, PCDH8 & FLRT2 (M vs. U)	2.94 [0.62 - 13.93]	0.177	
Age, years (cont.)	1.09 [1.03 - 1.15]	**0.002**	
Gender (male vs. female)	2.46 [0.90 - 6.69]	0.080	
Stage (pT3-4 vs. pT1-2)	2.97 [0.95 - 9.30]	0.063	**< 0.001**
Tumor size (cont.)	1.02 [1.00 - 1.03]	**0.033**	
WHO/ISUP grade (G=3 *vs.* G≤2)	0.77 [0.25 - 2.38]	0.648	
Necrosis (yes *vs.* no)	3.25 [1.09 - 9.69]	**0.036**	

M/U – methylated/unmethylated status; cont. – continuous variable; WHO/ISUP – World Health Organisation/Internation Society of Urological Pathology; pT – pathological tumor stage; G – grade; HR – hazard ratio; CI – confidence interval. Significant P-values are in bold.

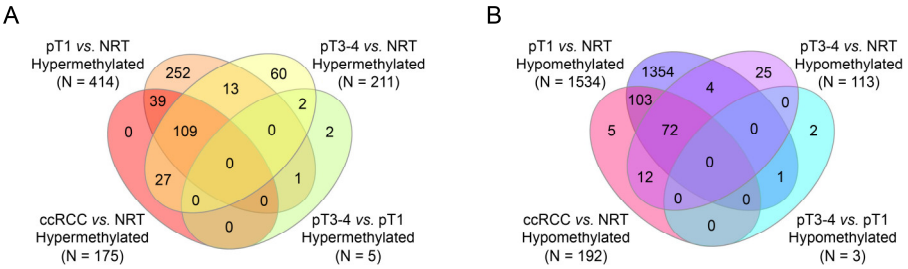

Fig S1. Venn diagrams of the genes with significantly different methylation levels according to renal tissue histology and tumor stages. A – hypermethylated genes; B – hypomethylated genes. pT – pathological stage.

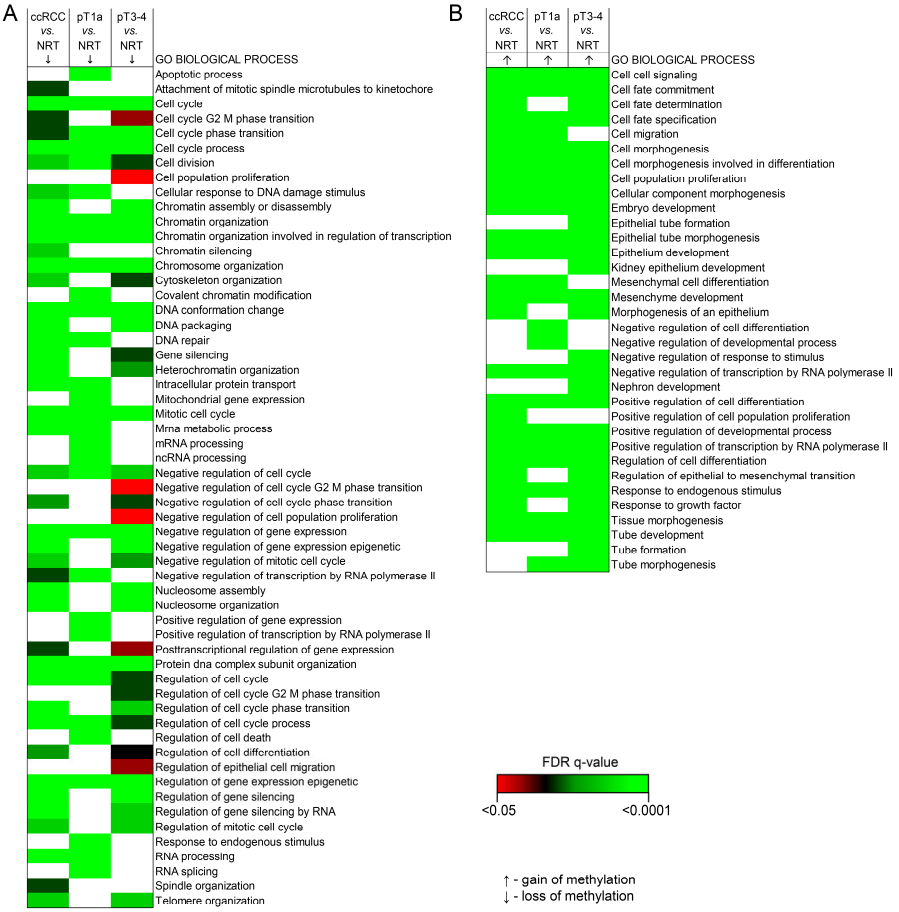

Fig. S2. Gene set enrichment analysis of differentially methylated genes identified in genome-wide methylation profiling. Gene ontology (biological process) analysis for A – hypomethylated and B – hypermethylated genes. Only genes with significant methylation differences with fold change values ≥1.5 were included. The color intensities indicate the level of false discovery rate (FDR) adjusted P-values (q-values). Abbreviations: ccRCC – clear cell renal cell carcinoma; NRT – non-cancerous renal tissues; pT – pathological tumor stage.

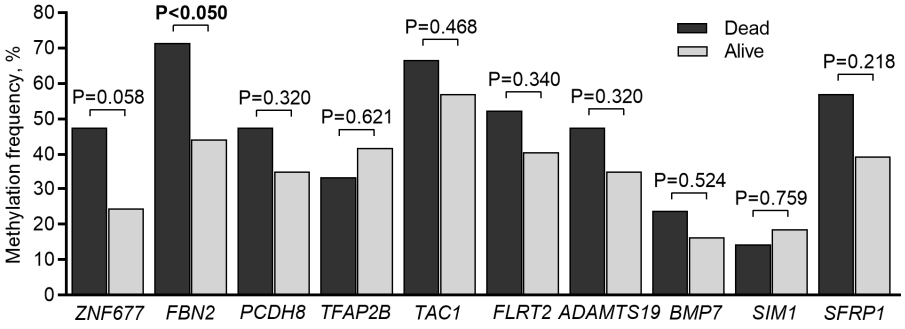

Fig S3. Methylation frequencies of the selected genes in the ccRCC tissue samples according to the patient's survival status. Significant P-values are in bold.

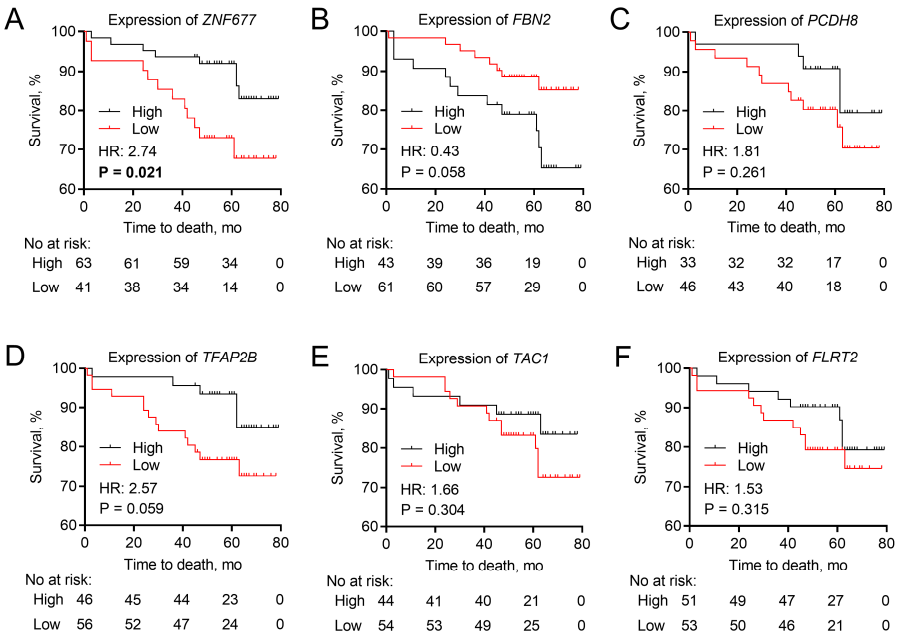

Fig S4. The relationship between expression of selected genes and patients' overall survival. Kaplan-Meier survival curves according to expression status (Low/High) of A – *ZNF677*, B – *FBN2*, C – *PCDH8*, D – *TFAP2B*, E – *TAC1*, F – *FLRT2*. Abbreviation: HR – hazard ratio. Significant P-values are in bold.

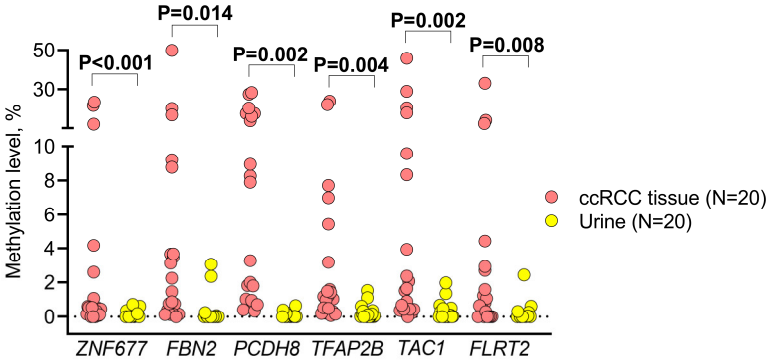

Fig. S5. The comparison of DNA methylation intensities in ccRCC patient's tissue and urine samples. The results were obtained by quantitative methylation-specific PCR. ccRCC – clear cell renal cell carcinoma. Significant P-values are in bold.

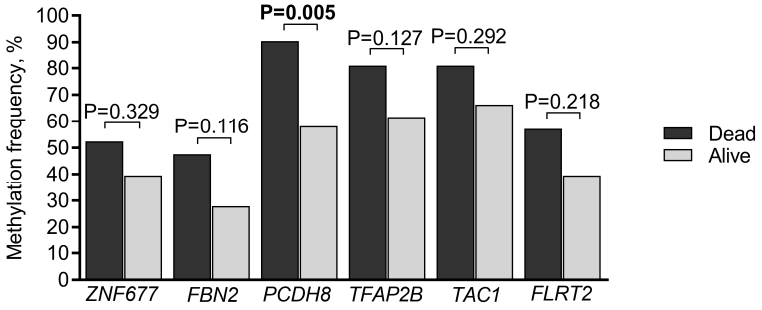

Fig S6. Methylation frequencies of the selected genes in the urine samples of ccRCC patients according to their survival status. Significant P-values are in bold.

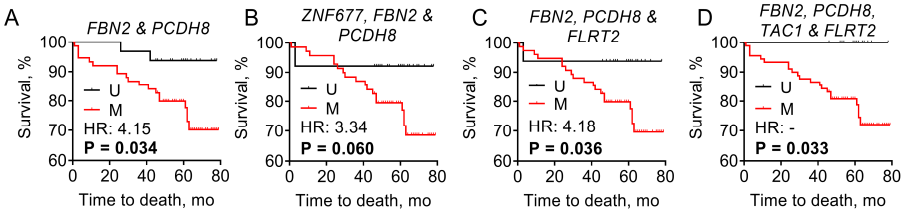

Fig. S7. The relationship between methylation status of investigated genes in urine sediments samples and patients' overall survival. (A-D) – Kaplan-Meier survival curves according to the methylation status of panels, consisting of two-four biomarkers. Abbreviations: M/U – methylated/unmethylated gene status, HR – hazard ratio (when the panel is methylated). Significant P-values are in bold.

CURRICULUM VITAE

General information

Name, Surname	Raimonda Kubiliūtė
Date of birth	26th May 1992
Main workplace	Genetic Diagnostics Laboratory, National Cancer Institute; Baublio st. 3b, LT-08406, Vilnius, Lithuania
Second workplace	ThermoPharma Baltic; Sauletekio ave. 7C, LT-10257 Vilnius, Lithuania
Personal contacts	Tel: +37064128534; E-mail: kubiliute.raimonda5@gmail.com

Education

2016-2020	Doctoral studies (Biology, 01 B); Institute of Biosciences, Life Sciences Center, Vilnius University, Vilnius, Lithuania.
2014-2016	Master of Genetics (*Magna Cum Laude*), Faculty of Natural Sciences, Vilnius University, Vilnius, Lithuania.
2010-2014	Bachelor of Biology, Faculty of Natural Sciences, Vytautas Magnus University, Kaunas Lithuania.

Training courses

2014	The course of Laboratory Animal Science at Vilnius University (FELASA C certificate); Vilnius, Lithuania

Work experience

2020-2021	Junior researcher at Institute of Biosciences, Life Sciences Center, Vilnius University.
Since 2019	Researcher at ThermoPharma Baltic.
Since 2019	Junior researcher at Genetic Diagnostics Laboratory, National Cancer Institute.
2016-2019	The biologist at Genetic Diagnostics Laboratory, National Cancer Institute.
2015-2017	Junior researcher at the Faculty of Natural Sciences, Vytautas Magnus University.

Research projects

Since 2015	Participation in 4 research projects, one ongoing

Scientific publications

Since 2016	Six articles published in journals with a citation index (IF) in the Clarivate Analytics Web of Science platform.

Scientific conferences

Since 2014	Scientific results presented at 11 international and national scientific conferences.

Membership

Since 2014	Lithuanian Biochemical Society
Since 2020	European Society for Medical Oncology (ESMO)

NOTES

NOTES

Vilniaus universiteto leidykla
Saulėtekio al. 9, III rūmai, LT-10222 Vilnius
El. p.: info@leidykla.vu.lt, www.leidykla.vu.lt
Tiražas 12 egz.